STUDIES OF THE CLASS A HIGH-MOLECULAR WEIGHT PENICILLIN-BINDING PROTEINS IN *BACILLUS SUBTILIS*

Derrell C. McPherson

Dissertation submitted to the Faculty of the
Virginia Polytechnic Institute and State University
in partial fulfillment of the requirements for the degree of

Doctorate of Philosophy
in
Biology

APPROVED

David L. Popham, Chairman

Joseph O. Falkinham, III
Ann M. Stevens
Timothy J. Larson
Richard A. Walker

April 16, 2003
Blacksburg, VA

Keywords: *Bacillus subtilis*, penicillin-binding proteins, peptidoglycan, glycosyl transferase, sporulation, cortex, germ cell wall

STUDIES OF THE CLASS A HIGH-MOLECULAR WEIGHT PENICILLIN-BINDING PROTEINS IN *BACILLUS SUBTILIS*

Derrell C. McPherson

David L. Popham, Chairman

Department of Biology

(ABSTRACT)

The survival of all organisms depends on their ability to perform certain enzymatic activities and the ability to construct certain structures. In prokaryotes, enzymes are required for the final reactions of peptidoglycan (PG) synthesis, the structural element of the bacterial cell wall. These proteins, known as penicillin-binding proteins (PBPs), are identified through the presence of conserved motifs within their functional domains. The Class A high-molecular weight PBPs are bifunctional, performing the penicillin-sensitive transpeptidase activity and the glycosyl transferase (GT) activity required for the polymerization of the glycan strands. The Class A PBPs in *Bacillus subtilis* are PBP1, PBP4, PBP2c, and PBP2d (YwheE) and they are encoded by *ponA, pbpD, pbpF,* and *pbpG* (*ywhE*), respectively. These proteins appear to be somewhat functionally redundant because removal of one or more does not cause any noticeable change in phenotype. However, the loss of PBP1 has previously been demonstrated in *B. subtilis* to cause a decreased growth rate and changes in morphology of vegetative cells, both of which are increased upon the additional loss of PBP4.

Furthermore, the loss of sporulation-expressed Class A PBPs, PBP2c and 2d, causes a 10,000-fold decrease in the production of heat resistant spores. This double mutant is shown to have changes in the structural parameters of cortex PG that appear minor when compared to other strains, but are coupled with a large defect on the deposition of cortex PG, apparently from the synthesis of an abnormal germ cell wall. The Class A PBPs are believed to be the only proteins capable of performing the GT activity and it is therefore believed that cell viability requires the presence of at least one functional Class A PBP. This requirement has been demonstrated in other organisms, but a *B. subtilis* strain lacking all Class A PBPs is viable. The phenotypical changes seen in the PBP1 mutant are exacerbated in this strain. The GT activity remaining in this strain is sensitive to the antibiotic moenomycin *in vitro* whereas it appears resistant *in vivo*. Identification of the protein(s) performing this novel GT activity will rely on the demonstration of the GT activity *in vitro*.

DEDICATION

I would like to dedicate this work to my entire family. Mom and Dad, your love and support through everything that I have done has given me the faith and encouragement to continue and accomplish my goals. I love you both. I would also like to thank my Blacksburg parents, Jesse and Peggy Arnold. I appreciate you always being there when needed and for telling me about Tech. Thank you for being such great friends of my parents - you are a model for how true friendships endure the test of time.

To my wife, Shannon. Your love, support, and encouragement has also provided me with the will to accomplish my goals. Thanks for the understanding you showed when I said that I needed to go into the lab when you had previously made plans for us. I love you and appreciate everything you do. Thanks for always being there and for being my sugar-momma.

To my daughter, Jordan. You have brought a joy to my life I didn't realize I missed. Everytime I hold you, my heart melts and I swell with pride. You are truly a gift.

ACKNOWLEDGEMENTS

I would like to start by thanking Dave and all the past and present members of the Popham lab. All of you have made this experience a little less daunting and a lot more fun. Dave - I can only hope that I can portray the knowledge and patience that you show me, each of your students in the lab, and everyone who comes to you for advice. You have certainly been a great mentor and I feel very fortunate to have been a member of your lab. Jennifer Meador-Parton – You and James (and the little Guys) have really become great friends over the past five years. Always stay in touch so that our daughters may grow to be good friends. Meghan Gilmore – you left too soon. You too are a great friend and it really was my yogurt. Jen and Meg, lab mates like you are hard to find, thanks for being my first.

To all the remaining, yet not forgotten, lab mates. Amanda Dean – we could always count on you to be happy. Thanks for letting Cleo be part of your family. Yuping Wei - we could always count on you to make us laugh, you are missed around here. Amy Weaver, Sarah Linnstaedt and others, thanks for your help. To everyone, sorry for all the teasing, but I had to put up with it from Jen and Meg, so I had to pass it on to someone. You were all good sports.

To all the other labs on the 4th floor. Dave O'Brien, John Varga, Mary Thorson, Marie Faini and the many others that have come and gone through the years - it's been a lot of fun, thanks for making it that way.

To my committee members. Ann Stevens, Joe Falkinham, Rich Walker, and Tim Larson - thanks for all the encouragement. It was a little rough at times, but I feel better and stronger for having gone through it all. I really appreciate the open doors and advice you all provided. You were a great committee.

LIST OF FIGURES

CHAPTER ONE

CHAPTER TWO

CHAPTER THREE

LIST OF TABLES

CHAPTER TWO

CHAPTER THREE

CHAPTER FOUR

TABLE OF CONTENTS

Chapter 1

Introduction and Review of Literature

The bacterial cell wall is essential for cell viability because its structural component, known as peptidoglycan, prevents cell rupture from the internal turgor pressure caused by osmotic stress. The importance of this structure is exemplified in the fact that the mode of action for numerous antibiotics is to target the enzymatic activities involved in its synthesis. Another role is demonstrated in the dormant endospore, where the cell wall is important in maintaining spore core dehydration and may play a role in attaining that dehydrated state. The cell wall is a huge mesh-like structure that surrounds the cell and the rigid nature of this structure also confers cell shape to both the vegetative cells and dormant endospores. The proper development of the bacterial cell wall to insure the construction of a stable structure as well as the typical morphological characteristics seen in the various eubacterial genera relies on the activity and putative interaction of the many proteins involved in its synthesis.

Bacillus subtilis and *Escherichia coli*, Gram-positive and Gram-negative organisms respectively, are the most well studied prokarotes thereby making them the models for the physiological and morphological characteristics of eubacteria. Peptidoglycan (PG) and the proteins involved in its synthesis are certainly areas that have recently come back to the mainstream of study because of their essential role in cell viability and the increase in antibiotic resistance among bacteria. These two organisms are models for the examination of PG synthesis and structure, and further study of the PG synthetic machinery may lead to the identification of target sites for new antibiotics. The research presented in this dissertation examines the roles and activity of a group of proteins thought to be essential for the synthesis of PG using *Bacillus subtilis* as the

model organism. These proteins are found throughout all eubacteria that synthesize PG and are known as the Class A high-molecular-weight penicillin-binding proteins (PBPs).

Through my study of these proteins, I have found that they play specific, although somewhat redundant roles throughout the life cycle of the cell. Furthermore, I have found that they are not essential to the synthesis of PG and therefore to the viability of the cell as was thought, at least not for *B. subtilis*. Because one of the PG synthesizing reactions performed by the Class A PBPs was believed to be unique to only those proteins, the viability of the strain lacking those proteins suggests this activity is being performed through a novel mechanism by another protein or group of proteins. Identification of the proteins responsible for performing this activity is the final focus of this research.

Bacillus subtilis and Sporulation

B. subtilis is a Gram-positive soil eubacterium and is a member of the Group II *Bacillus* species that also includes *B. anthracis, B. licheniformis,* and *B. popilliae* (96). This group is characterized as being primarily aerobic, but able to grow in the absence of oxygen, at least weakly. They also produce ellipsoidal spores that are sub-terminal and do not swell the mother cell. *B. subtilis* is naturally transformable making it easily genetically manipulated, thus allowing for this organism to be the most well studied Gram-positive eubacterium.

B. subtilis has two life cycles that allows for the study of differential gene expression as well as cellular differentiation (Figure 1.1). The vegetative life cycle of

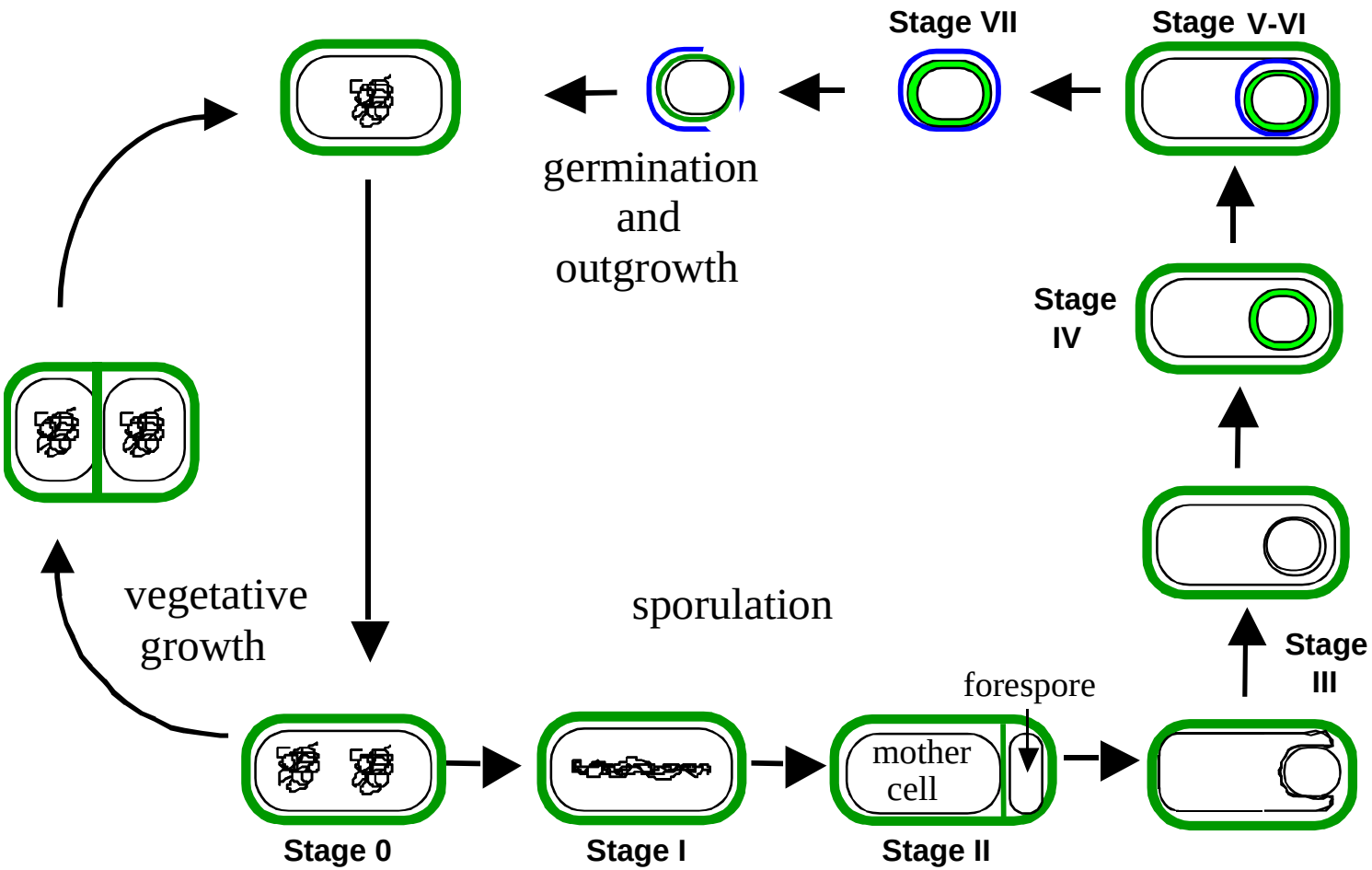

Figure 1.1. Stages of the *Bacillus subtilis* life cycle.

B. subtilis is used when nutrients are plentiful and the cells can grow and divide. However, when nutrients become depleted, the cells terminate vegetative growth and enter sporulation. During sporulation, the vegetative cell produces a forespore, which will mature into a metabolically inactive, or dormant, endospore that is released into the environment upon lysis of the mother cell. The endospore can remain dormant and viable for decades until it senses an increase in nutrients, at which time the cell initiates germination and enters back into the vegetative life cycle.

Sporulation is divided into seven stages and begins with termination of vegetative growth, followed by duplication and condensation of the genome into an axial filament during Stage I (Figure 1.1) (reviewed in (28)). During Stage II, asymmetric septation occurs producing two separate cell compartments; a large compartment known as the mother cell and a smaller compartment known as the forespore, each containing a complete genome. At this point, the small amount of PG synthesized within the asymmetric septa is degraded and the mother cell membrane begins to surround the forespore until the leading edges fuse. This process, known as engulfment, proceeds during the transition from Stage II to Stage III, and results in a free-floating forespore within the mother cell. Two membranes now surround the forespore and are known as the inner forespore membrane and the outer forespore membrane, in between which spore PG is synthesized beginning in Stage IV. Spore coat proteins are deposited around the forespore during Stage V along with the completion of spore PG synthesis. Spore maturation is completed to achieve the fully dormant and resistant spore properties during

Stage VI and finally, Stage VII involves lysis of the mother cell releasing the dormant endospore into the environment.

Throughout the process of sporulation, gene expression is controlled by various sigma factors that are activated both chronologically and compartmentally through a signal cascade (reviewed in (28, 55)). Prior to asymmetric septation, the first two sporulation-specific sigma factors, σ E and σ F, are expressed under the control of the regular housekeeping sigma factor, σ A, and the late stationary phase sigma factor, σ H. These sporulation-specific sigma factors are inactive because of an N-terminal pro-peptide on σ E and the association of σ F with an anti-sigma factor called SpoIIAB. Following asymmetric septation, SpoIIAB disassociates from σ F and forespore-specific genes are then expressed. Once these forespore genes are expressed, a signal is transduced across the double membranes separating the forespore and mother cell that causes SpoIIGA to begin processing pro-σ E thereby activating σ E within the mother cell to express mother cell-specific genes.

Another gene expressed by σ F is *spoIIIG*, which encodes σ G. Upon completion of engulfment, σ G is activated within the forespore following release of an anti-sigma factor, thought to be SpoIIAB. Transcription of the inactive form of the final sigma factor, pro-σ K, is controlled by σ E and takes place specifically within the mother cell. Pro-σ K is associated with the mother cell side of the outer forespore membrane where it interacts with other proteins. These proteins process pro-σ K in response to a signal from the forespore that requires SpoIVB. It has been proposed that SpoIVB interacts with the outer forespore membrane proteins and that this interaction transduces a signal across the

intermembrane space inducing pro-σ K processing, thereby activating this final sigma factor within the mother cell compartment. SpoIVB has a putative second activity that appears to be involved in spore PG synthesis (76). Loss of SpoIVB results in cells that do not synthesize germ cell wall (the inner layer of spore PG), though spore PG synthesis is not thought to be involved in the signal that induces pro-σ K processing (144).

One characteristic of the dormant endospore is that during its maturation, it develops properties that confer resistances to heat, ultraviolet irradiation, and chemical and enzymatic degradation (reviewed in (103)). The ability of the spore to resist several, if not all of these damaging conditions appears to be due in part to the level of dehydration within the spore core, which is achieved during spore maturation. The dehydrated core appears to reduce the production of hydrogen radicals, reduce the protein denaturing effects of heat, and also appears to at least slow the effects of damaging chemicals on both the chromosome and proteins within the spore core. The primary ability of the spore to resist chemical and enzymatic degradation is due to the coat proteins that surround the spore. These proteins are highly charged and cross-linked, a combination that severely impedes the passage of chemicals, such as chloroform, or enzymes, such as lysozyme, beyond the outer spore surface. Finally, resistance to UV irradiation is due to the accumulation of small acid-soluble proteins, or SASPs. These proteins accumulate in the spore core and bind the DNA to a saturating degree, changing the B-like helical configuration of the DNA to an A-like helical configuration. This change in DNA configuration causes a type of DNA damage incurred by UV light that is more efficiently and effectively repaired by the germinating cell.

Peptidoglycan Synthesis

The structure of PG consists of glycan strands that are cross-linked by peptide side-chains (Figure 1.2) (reviewed in (31)). The glycan strands consist of repeating residues of N-acetyl glucosamine (NAG) and N-acetyl muramic acid (NAM). The glycan strands vary in length depending on the organism and can range from 10 disaccharide subunits in *E. coli* to approximately 100 in *Bacillus subtilis*, but this is not necessarily dictated by whether the organism is Gram-positive or Gram-negative (136). The PG structure is also located on the outer surface of the cytoplasmic membrane in Gram-positives, but is located within the periplasmic space of Gram-negatives. The PG layer of the Gram-negative is also approximately 10 to 20-fold thinner than that of the Gram-positives. Furthermore, Gram-positive organisms contain a large number of highly charged anionic polymers called teichoic and/or teichuronic acids that are anchored to NAM residues (7, 8). These polymers may serve to inhibit the diffusion of some molecules towards the cytoplasmic membrane, a similar role to that seen of the outer membrane and periplasmic space of Gram-negative organisms.

The precursors for PG are synthesized within the cytoplasm of the cell as lipid-linked disaccharide-pentapeptides (reviewed in (31) and (41)). The steps in precursor synthesis begin by adding each amino acid stepwise to UDP-NAM, which produces the UDP-NAM-pentapeptide (Figure 1.3) (68). One difference in the PG composition between the various organisms is the amino acids used for the peptide side-chains (98, 101). The sequence of amino acids in *B. subtilis* PG is L-alanine, D-glutamate, and meso-diaminopimelic acid, followed by two D-alanines (8). The next reaction involves

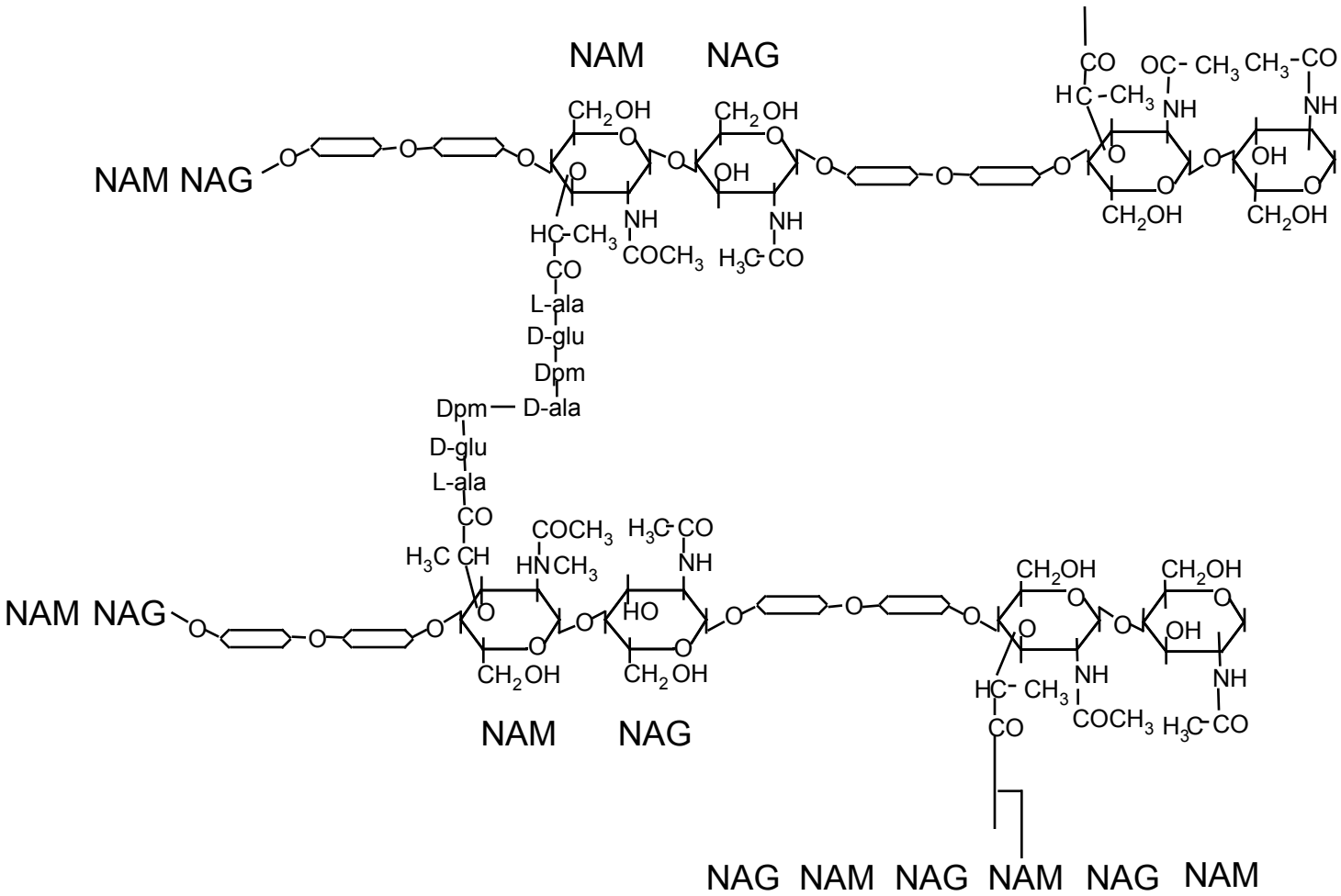

Figure 1.2. The structure of peptidoglycan. Peptidoglycan consists of glycan strands cross-linked by peptide side-chains. Abbreviations: NAG, N-acetylglucosamine; NAM, N-acetylmuramic acid

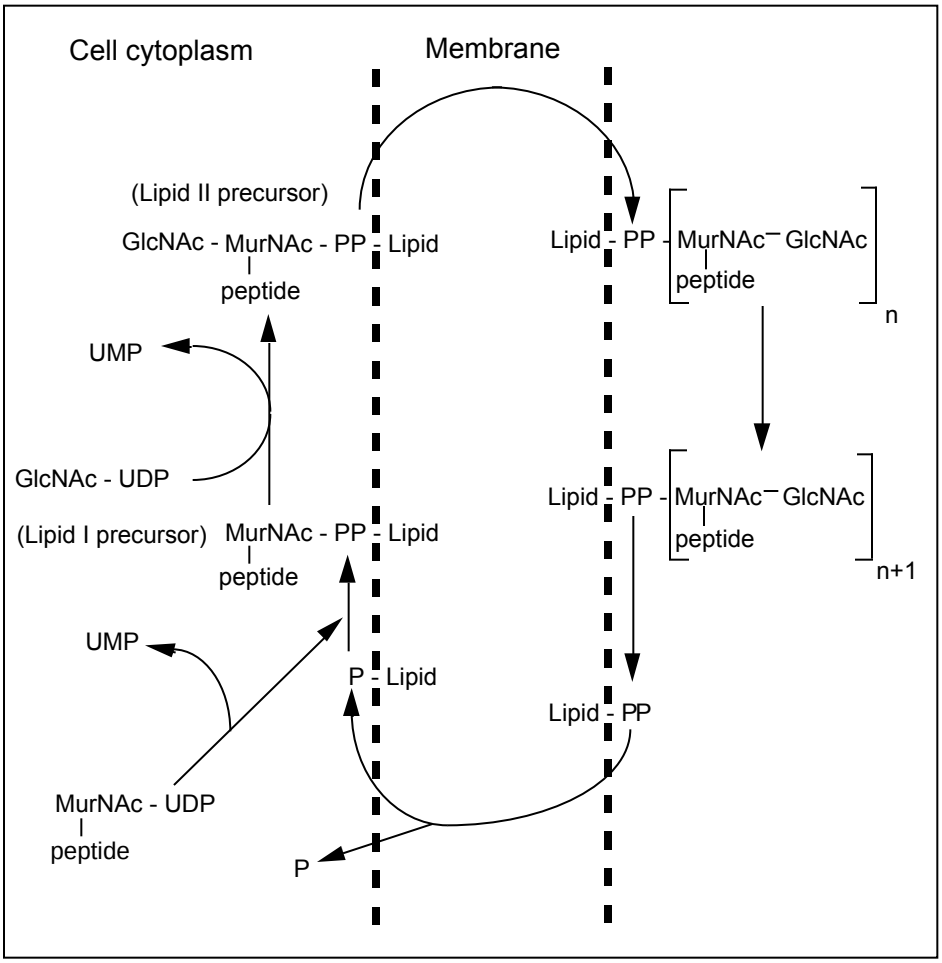

Figure 1.3. Synthesis of the Lipid II precursor to peptidoglycan. Abbreviations: UDP, Uridine diphosphate; UMP, uridine monophosphate; MurNAc, N-Acetylmuramic acid; GlcNAc, N-acetylglucosamine; PP, pyrophosphate; P, phosphate.

removal of the NAM-pentapeptide from the UDP-precursor and adding it to a C_{55}-undecaprenol lipid located in the cytoplasmic membrane (40). This lipid-linked monosaccharide-pentapeptide is known as Lipid I. Finally, NAG is added from its UDP-precursor to the lipid I moiety with a β−1-4 glycosidic linkage. This final precursor is known as Lipid II and is the basic subunit of PG (6).

Once synthesized, this Lipid II precursor is flipped outside the cell where it is utilized to polymerize glycan strands (Figure 1.4) (5, 8). The glycan strands are polymerized by a glycosyl transferase activity that catalyzes either the 4-hydroxyl group of NAG from Lipid II to displace the pyrophosphate on the glycan strand or the 4-hydroxyl group of the terminal NAG on the glycan strand to displace the pyrophosphate of Lipid II (5, 34, 64). The peptide side-chains are then utilized either concurrently with glycosyl transferase activity or shortly after by a transpeptidase to cross-link adjacent glycan strands. They can also be cleaved to tetra- or tri-peptides thereby regulating the number of side-chains available for cross-linking. The proteins involved in these final reactions of PG synthesis are known as penicillin-binding proteins (PBPs).

Vegetative PG is a dynamic structure that is synthesized on the outer surface of the cytoplasmic membrane of *B. subtilis* (reviewed in (31)). As the cell grows and newglycan strands are synthesized, old strands slowly migrate outward until they are degraded and shed into the medium. This process is called inside-to-outside growth and allows for the expansion of the PG structure as the cell grows. It is believed that when nascent strands are synthesized and added to the innermost structural layer, the new cross-links used to connect those strands to the existing structure are loose. As the

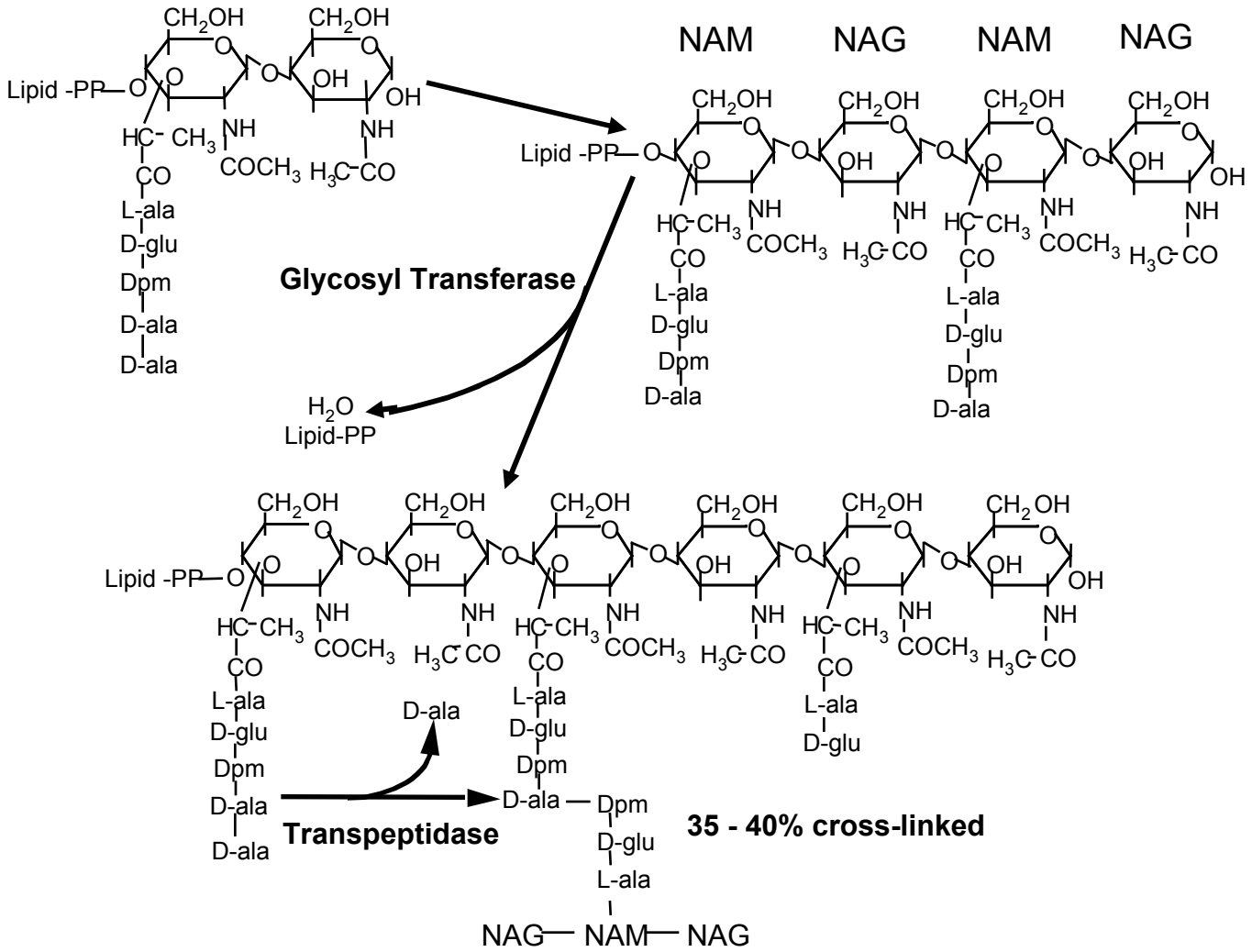

Figure 1.4. The structure and final reactions of vegetative peptidoglycan. The glycosyl transferase reaction polymerizes the glycan strands whereas the transpeptidase reaction cross-links adjacent glycan strands. Abbreviations: NAG, N-acetylglucosamine; NAM, N-acetylmuramic acid.

strands move outward, the cross-links tighten so that the majority of stress is placed upon the outer layers until these stressed cross-links are cleaved and the strands are degraded and shed into the medium.

The synthesis of vegetative PG is continuous with cell growth and therefore must be coordinated in a fashion that allows for the structure to elongate during growth then switch to invaginate the structure at the appropriate location for cell division. Proper coordination of elongation versus invagination is postulated to require the presence of specific enzymes interacting to form a multi-enzyme complex to synthesize the correct form of PG, either cylindrical or septal (41). Specific enzymes have been shown to be required for proper elongation and septation, but how these proteins interact and the localization of these proteins to the proper cellular location is presently unknown. The idea of a multi-enzyme complex is supported by demonstration of protein interaction using affinity chromatography with immobilized PG lytic transglycosylases or hydrolases to bind other membrane-associated enzymes (99, 134). Using this method, researchers were able to identify proteins from each class of PBPs. In a model proposed by Holtje (41), a complex of at least one glycosyl transferase and transpeptidase is required to synthesize and attach each strand and the addition of the other enzymes (lytic transglycosylases, hydrolases, and endopeptidases) would allow for modifications to the network of glycan strands. The involvement of specific mono-functional transpeptidases (Class B PBPs) appears to specify the complex for synthesis of either the cylindrical wall or the invagination needed for cell division (24, 69, 71-73, 108, 111, 140). Specific cell wall synthesizing proteins (PBPs) might also interact with cell division proteins and other

proteins involved in providing a helical framework (51) that may be used to define the morphological structure of PG. How all of these proteins interact and in what specific ratios they are used to create a multi-enzyme, PG synthesizing complex is unknown at this time. But their interaction and the interaction of them with other cell morphology related proteins is certainly inferred in order to maintain a proper cell elongation/division relationship.

The Structure of Vegetative and Spore Peptidoglycan

The structure of vegetative PG in *B. subtilis* is cross-linked at 29-33% of the NAM residues and the majority of peptide side-chains are either tetra-peptides or tri-peptides ((9, 138) and reviewed in (31)). Most free carboxyl groups on the diaminopimelic acid are amidated and glycine has been identified on the number 5 position in low numbers of the peptide side-chains. Furthermore, NAM residues are generally found at the reducing ends of the glycan strands although anhydro-muropeptides are also found.

Spore PG is synthesized between the inner and outer forespore membranes during Stages IV and V of sporulation. Although spore PG is synthesized using the same enzymatic reactions as vegetative PG, it has some structural characteristics that make it quite distinguishable. Spore PG is divided into two layers that can be distinguished both structurally and functionally (Figure 1.5). The layer adjacent to the inner forespore membrane is known as the germ cell wall and it makes up the innermost 10 – 20% of spore PG. The germ cell wall has a structure very similar to vegetative PG and acts as the

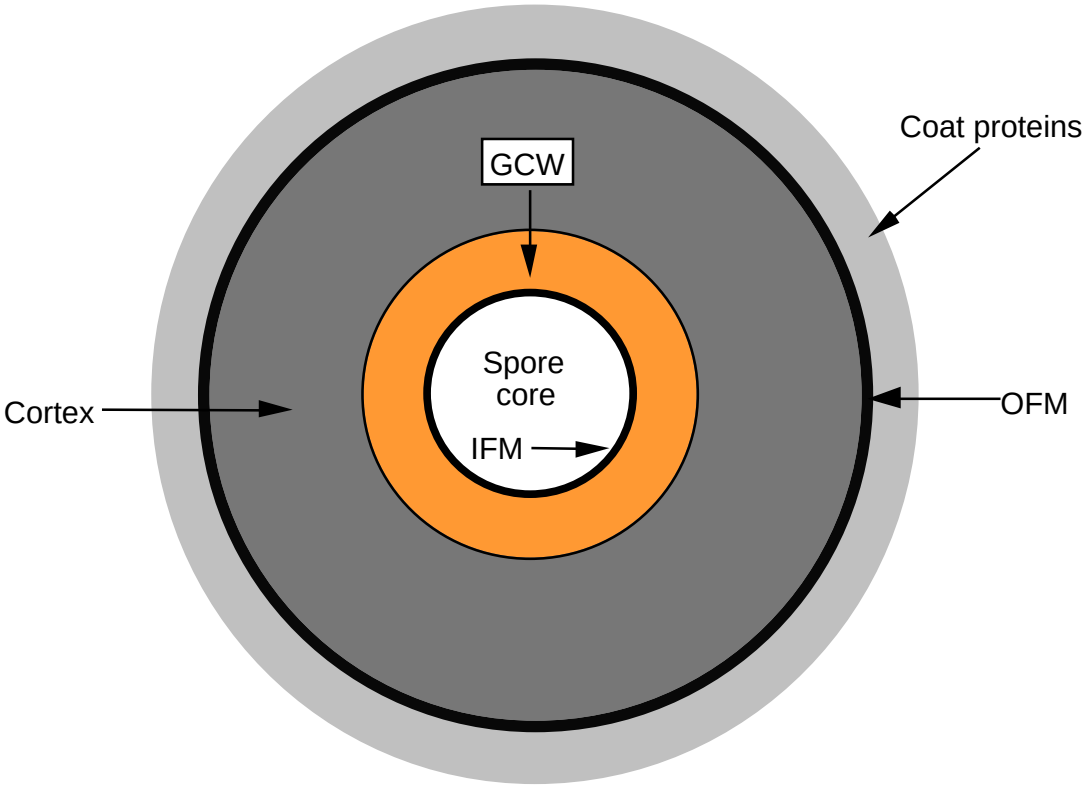

Figure 1.5. Model of the mature spore. The germ cell wall (GCW) is adjacent to the inner forespore membrane (IFM) and the cortex is adjacent to the outer forespore membrane (OFM).

initial wall during spore outgrowth (10, 11, 67, 123, 124). The outer 70 – 90% of spore PG, known as the cortex, has a structure very different from vegetative PG (Figure 1.6) (10, 67, 87, 137, 139). While the peptide side-chains of vegetative PG are primarily tripeptides and tetrapeptides (9), tetrapeptides and single alanines each make up 24% and tripeptides only make up 2% of the side-chains in cortex PG. Furthermore, 50% of the remaining side-chains from spore PG are removed and the muramic acid residues are converted to muramic-δ-lactam. Part of this transformation of N-acetylmuramic acid-pentapeptide into muramic-δ-lactam occurs through the activity of a protein named CwlD (cell wall lysis) (10, 87). Cells lacking CwlD do not produce muramic-δ-lactam and are deficient in cortex lysis (10, 87, 102), therefore muramic-δ−lactam appears to act as a specificity marker for the degradation of cortex PG during the initial stages of germination (87, 102). By analyzing spore PG from various stages of synthesis, it was determined that there is a gradient of cross-linking throughout spore PG ranging from 6% in the germ cell wall to an average of 3.5% throughout the cortex (67). Finally, spore PG does not contain any of the anionic polymers found in vegetative PG (10, 87).

The synthesis of PG in both the vegetative cell and developing forespore occurs through the same basic reactions. However, instead of synthesizing in an inside-to-outside manner as during synthesis of vegetative PG, spore PG synthesis is initiated adjacent to the inner forespore membrane (germ cell wall), while the addition of cortex layers are believed to be synthesized by enzymes present within the outer forespore membrane (67, 124). Changes in the spore PG structural parameters of strains lacking proteins that are expressed specifically during sporulation, suggests the requirement for a

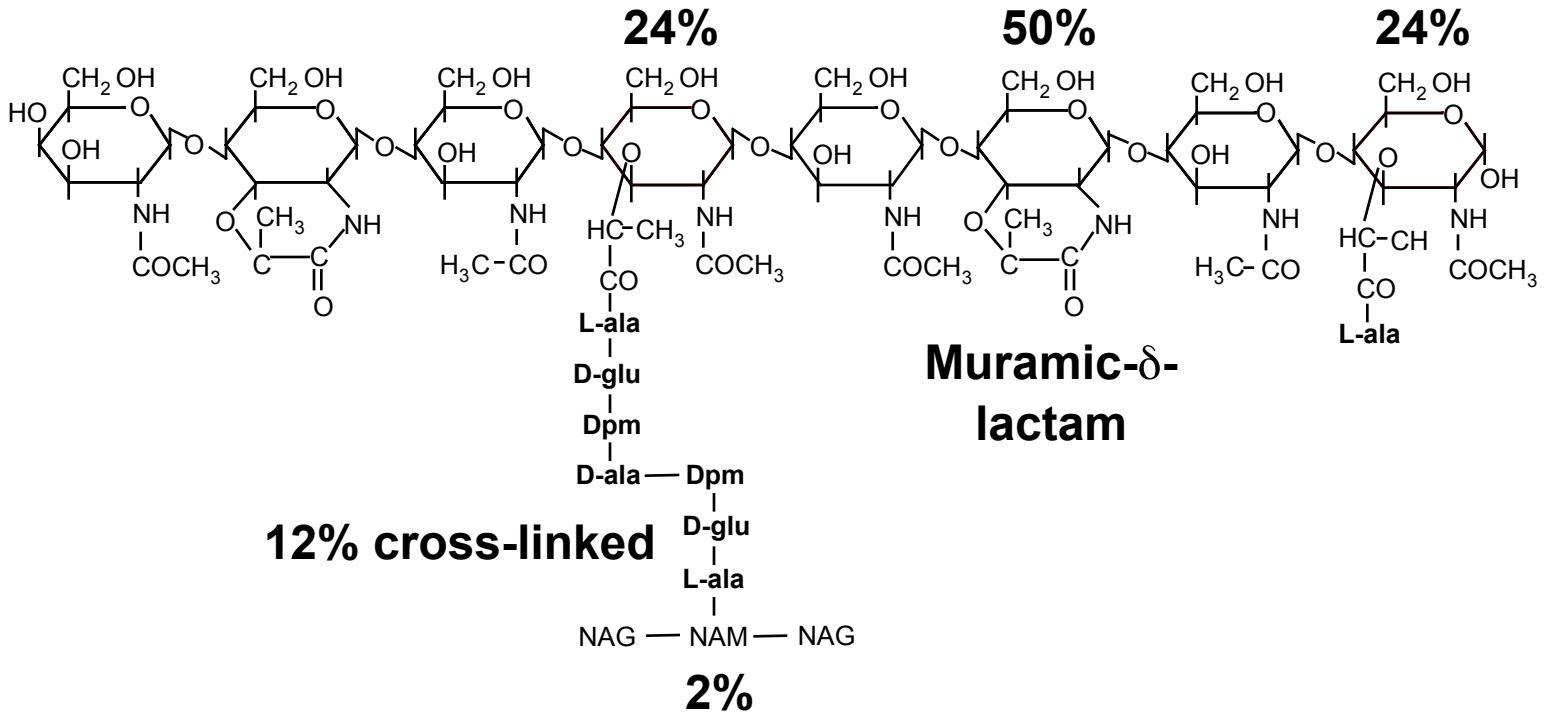

Figure 1.6. The structure of spore cortex peptidoglycan

specialized set of proteins (PBPs) that are involved in the production of structurally accurate spore PG. Where these proteins are expressed appears to be a determinant to how involved they are in spore PG synthesis. For instance, proteins expressed within the mother cell are presumed to be present in the outer forespore membrane and could be involved in synthesis of the entire spore PG structure. However, those proteins expressed specifically in the forespore might only be involved in the initial stages of germ cell wall synthesis, unless they were released from the inner forespore membrane to remain active throughout the spore PG synthesis process. However, it has not been demonstrated that any of these proteins are cleaved. Therefore, in order for that activity to remain throughout production of new spore PG layers, either they or enzymes with similar roles must be expressed within the mother cell (34, 85). Proteins expressed within the mother cell and present within the outer forespore membrane must, then, play primary roles in the synthesis of cortex PG (85).

Penicillin-Binding Proteins

Penicillin-binding proteins (PBPs) are divided into three classes based on their molecular weight and the presence of conserved amino acid motifs (Figure 1.7) (32, 34). One characteristic of these proteins is that they are all membrane associated due to an non-cleavable signal sequence located at the N-terminus, which acts as a membrane anchor. All three classes of PBPs contain a peptidase activity that is located in the C-terminal domain, also known as the penicillin-binding domain (32, 34). The low-molecular weight PBPs (generally ≤ 60 kDa) consist of only a single domain and they

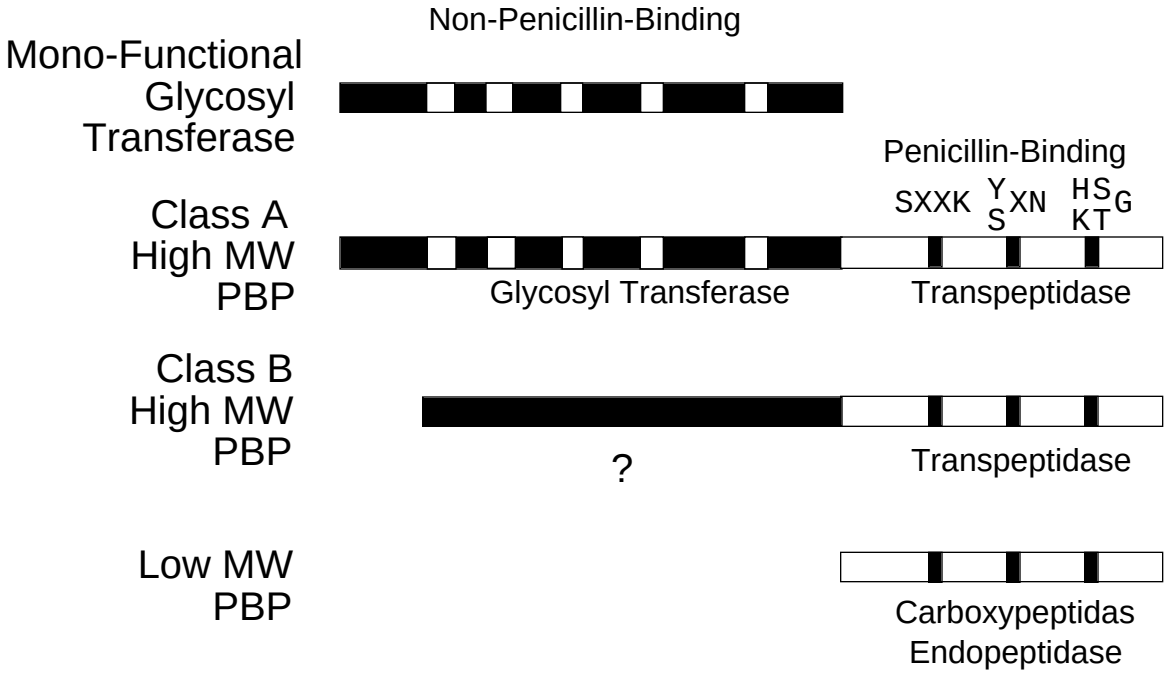

Figure 1.7. Classes, domains, and conserved motifs of the penicillin-binding proteins. White boxes within the non-penicillin-binding domains of the mono-functional glycosyl transferase and Class A PBP models represent the conserved amino acid sequence motifs of the glycosyl transferase activity. Black boxes within the penicillin-binding domain in each class of PBPs represent the conserved amino acid sequence motifs of peptidase activity.

perform either the D,D-carboxypeptidase or endopeptidase activity used to cleave the peptide side-chains, thereby regulating the number of side-chains involved in cross-linking. The Class A and Class B high molecular-weight PBPs (generally ≥ 60 kDa) have two domains and contain the transpeptidase activity in the penicillin-binding domain. The Class A PBPs are the only PBPs that have demonstrated a second activity required for the polymerization of the glycan strands, that being the glycosyl transferase (GT) activity located in the N-terminal, non-penicillin-binding domain. The Class B PBPs also have an N-terminal domain that contains homologous regions to other Class B PBPs, but not to the N-terminus of the Class A PBPs. Although the N-terminus is required for proper folding and activity of the Class B PBPs, these proteins are believed to be mono-functional transpeptidase enzymes.

Using either radio- or fluorescent-labeled penicillin, which becomes covalently bound to PBPs, these proteins can be identified through visualization of labeled proteins using SDS-PAGE (58, 111). The PBP migration pattern presents a method of naming each protein from the highest molecular weight to the lowest. The grouping of PBPs into the three different classes based on the presence of conserved motifs suggests their inherent role in PG synthesis (34) and several of these proteins show great homology to other PBPs from the same class, but in different organisms. Furthermore, phenotypic analyses of various PBP mutant strains suggest these proteins are orthologs. However, the migration pattern that is used for the identification and nomenclature does not suggest any relationship between these orthologs, nor does the class grouping indicate the specific role each protein may play in PG structural development.

Every eubacterium studied to date that synthesizes PG contains several proteins in each of the three classes of PBPs (34). For example, B. subtilis contains four Class A PBPs and six of each of the Class B and low molecular weight PBPs ((17, 18, 20, 72, 73, 82, 89, 91-94, 125, 126, 141, 142) and reviewed in (31)). There are two reasons why there would be multiple proteins in each class. First, because the PG structure is essential to cell viability, the enzymatic reactions required for its synthesis are targets for many antibiotics, such as β-lactams (32). Because of this, some proteins within the same class have evolved to become less susceptible to certain antibiotics. This allows for one protein to compensate for the inactivation of another because of the partial redundancy in function performed within each class of PBPs. An example of this susceptibility is seen in *B. subtilis*, where PBP2a and PbpH have demonstrated a redundancy in function but yet have different sensitivities to various antibiotics (140). Another reason for having multiple proteins for a single class is that each protein may play specific roles throughout the development of the cell. Examples of this are PBPs 2 and 3 of *E. coli*, where PBP2 has been shown to be required for elongation of the cylindrical wall (108, 111) and PBP3 is essential for septation (16, 108). Furthermore, some *B. subtilis* proteins from each class are expressed either during vegetative growth or during sporulation, suggesting specific roles during those stages of the organism's life cycle (18, 20, 72, 73, 82, 89, 91-93, 125, 142). Although these proteins may certainly play specific roles, within those roles there often does appear to be some partial redundancy (34).

Conserved Motifs within the Active Sites of PBPs

The identification of PBPs is accomplished through the demonstration that each protein covalently binds the β-lactam antibiotic, penicillin (32). The active site of PBPs consists of three conserved amino acid motifs (Figure 1.8) where the serine in the motif SxxK of the penicillin-binding domain is essential in formation of the serine ester-linked peptidyl enzyme and causes the release of the terminal D-alanine from the peptide side-chain (32, 34). This can be followed by the transpeptidase activity, which transfers the peptidyl moiety to the free amino group of the diaminopimelic acid located on the peptide side-chain on adjacent glycan strand (32, 34). Similar reactions occur to produce the endo- and carboxy-peptidase activities of the low molecular weight PBPs, which result in cleaved, uncross-linked side-chains. β-lactam antibiotics, such as penicillin, contain a β-lactam ring structure that resembles the terminal D-alanine-D-alanine linkage of the peptide side-chains. Recognition of this β-lactam ring causes the PBPs to bind and initiate hydrolysis of the ring. However, this reaction does not go to completion because the active site is not accessible to nucleophilic attack by a water molecule resulting in a metabolically inert enzyme/substrate complex. Another group of proteins, called β-lactamases, contain the same conserved motifs found in PBPs, but have evolved in such a way that allows access to the water molecule resulting in completion of the reaction process.

Identification of the bifunctional Class A PBPs relies on the presence of conserved amino acid sequence motifs found within both the C-terminal, penicillin-binding domain that performs a transpeptidase activity and the N-terminal,

Class A PBPs

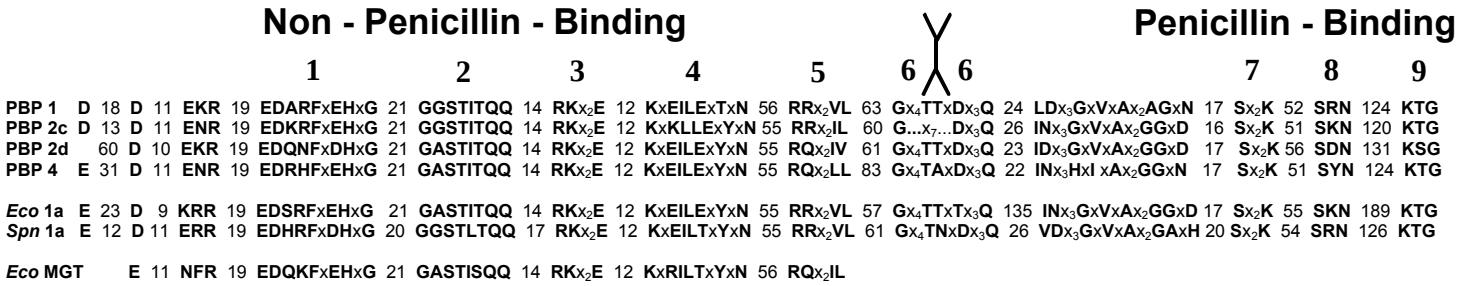

Class B PBPs

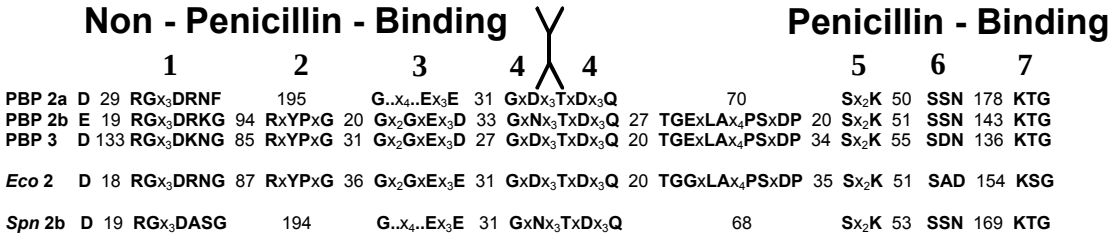

Figure 1.8. Conserved sequence motifs of the Class A and Class B high-molecular weight PBPs. PBPs1, 2c, 2d, and 4 of the Class A PBPs and PBPs 2a, 2b, and 3 of the Class B PBPs are *Bacillus subtilis* PBPs. Other strains are *Eco, E. coli* and *Spn, S. pneumoniae*. The numbers above the alignments indicate the conserved motifs for each PBP class and the intermodule junctions are noted within motif 6 of the Class A PBPs and motif 4 of the Class B PBPs. Figure adapted from (33).

non-penicillin-binding domain that performs the glycosyl transferase (GT) activity (Figure 1.8) (34). These motifs are found in all Class A PBPs of all eubacteria that synthesize PG. Proteins containing these motifs are the only enzymes that reproducibly catalyze the polymerization of glycan strands. These motifs are also contained in mono-functional GT (MGT) proteins found in some organisms such as *E. coli* (27, 112) and *Staphylococcus aureus* (135). There are six conserved motifs found in the non-penicillin binding domain of the Class A PBPs and MGTs, with the most highly conserved sequence, **G A**/G **S**/T **T I**/L **T**/D/E **Q**/M **Q**, (Motif 2) located approximately between positions 100 - 120 (Figure 1.8) (34).

Class A PBPs

The Class A PBPs and MGTs are the only enzymes that have demonstrated the GT activity required for the polymerization of the glycan strands (46, 49, 74, 97, 118, 121). The fact that most organisms contain multiple Class A PBPs suggests that the individual proteins play specific roles in the development of the cell. It is further suggested that these proteins have at least some partial redundancy of function because they perform the same basic enzymatic activities. This redundancy has been demonstrated in several organisms where the removal of one or more PBPs from any class is not lethal to the cell (26, 32, 34, 42, 78, 95, 143). In *E. coli* and *Streptococcus pneumoniae*, there are three Class A PBPs and one MGT. Removal of any one or specific combinations of the Class A PBPs by mutation confers little or no growth phenotype to these cells. However, removal of both PBPs 1a and 1b from *E. coli* (26, 143) and PBPs 1a and 2a from *S.*

pneumoniae (42, 78) is lethal. This indicates that some activity of these Class A PBPs is essential for cell viability. This essential activity is presumably the GT activity, because only these and MGT proteins have reproducibly demonstrated the activity *in vitro*.

B. subtilis contains four Class A PBPs. The genes encoding three of them were identified through cloning and sequencing (91, 93, 94). The fourth Class A PBP was identified through sequence analysis of the *B. subtilis* genome (56, 82). These proteins are named PBP 1(13, 14, 91), PBP 2c (93), PBP 4 (94), and YwhE (82) and these are encoded by their respective genes, *ponA*, *pbpF*, *pbpD*, and *ywhE*. According to the genome sequence, *B. subtilis* does not contain any mono-functional GT enzymes (56), therefore, the Class A PBPs should be the only enzymes capable of performing the GT activity that is essential for cell viability (34).

PBP1 was one of the first PBPs identified using biochemical methods (13, 14). Researchers initially identified this protein as a doublet and labeled them PBPs 1a and 1b. It was later determined that both protein products were encoded by the same gene and the difference in mass was due to processing of a carboxy terminal tail (91). The gene encoding PBP1 was named *ponA* to maintain consistency among PBP identification between organisms because the genes encoding PBPs 1a and 1b in *E. coli* were previously named *ponA* and *ponB*, respectively (108, 110). PBP1 is 914 amino acids in length with a molecular mass of 99,362 Da. The *ponA* gene is calculated to map to the 199.9˚ position on the chromosome (91). PBP1 contains all the conserved motifs found in Class A PBPs and displays 37% and 30% amino acid sequence identity with PBP1a of *S. pneumoniae* and *E. coli*, respectively. This gene, *ponA*, is most highly expressed

during log phase and decreases through stationary phase until there is little or no expression during sporulation. Expression begins to increase again approximately fifteen minutes after a spore enters germination.

Initial morphological studies of *B. subtilis* mutants showed that strains with a narrower diameter contained an altered PBP1, thus suggesting this protein to be involved in cell morphology (53). It was not until *ponA* was cloned and sequenced that specific mutational analyses were performed. Colonies of *ponA* mutants have raised edges whereas wild type colonies have raised centers. *ponA* mutants also have a reduced growth rate in rich, liquid medium along with a 16% decrease in diameter of the individual cells (91), as suspected in the previous study (53). A small population of individual cells in strains lacking PBP1 are also found to be elongated (80).

PBP1 has also been shown to localize at the division septa. Along with this data, the Z-ring, a structure constructed early at the division site by the polymerization of FtsZ, develops an aberrant structure and is localized improperly in the majority of cells lacking PBP1 (80). These data suggest that PBP1 plays at least a minimal role in placement and proper development of the division septa and that there must be other proteins that interact with PBP1 to relay information on Z-ring placement and PG synthesis.

One protein that may interact with PBP1 could be the cytoplasmic protein called penicillin-binding protein-related factor, or PrfA. This protein is encoded by *prfA*, which is the first gene transcribed in an operon with *ponA* (91). Mutants lacking PrfA show problems with chromosomal partitioning (83) and double mutants also lacking PBP1 are non-viable (91). Because these are expressed from the same operon and at least one is

essential, this suggests the possibility of interaction between them or at least other proteins involved in cell division.

PBP4 is the shortest and least complex of the Class A PBPs in *B. subtilis*. This 70,447 Da, 624 amino acid protein is encoded by *pbpD*, which is calculated to map to the 276.1° position on the chromosome. Its expression increases during log phase, decreases as the culture enters sporulation and begins again approximately 45 minutes following germination (94). Although null mutations in *pbpD* produce no obvious changes in phenotype, the combination of *pbpD* and *ponA* mutations produce a greater reduction in growth rate as well as increased cell lengths than what is seen in the single *ponA* mutant strain (95).

A third Class A PBP, PBP2c, is encoded by *pbpF*. This protein is 714 amino acids in length, has a molecular mass of 79,095 Da, and its gene is calculated to map to the 92.5° position on the chromosome (93). Low expression of *pbpF* occurs during vegetative growth under control of σ A and this expression decreases as the culture enters sporulation. However, *pbpF* is induced within the forespore during late sporulation under the control of σ G. Analysis of single *pbpF* mutants does not show any obvious phenotypic changes and the combination of this mutation with either *pbpD* or *ponA* mutations does not appear to exacerbate any of the previously mentioned single mutant phenotypes for those genes. However, the addition of the *pbpF* mutation into the *ponA pbpD* double mutant does cause an even greater decrease in growth rate as well as increased cell length in the individual cells (95). These results demonstrate that a *B.*

subtilis strain lacking three Class A PBPs is viable and suggests the presence of either a fourth Class A PBP or an MGT.

Upon completion of the *B. subtilis* genome, the fourth and final Class A PBP was identified. This protein (YwhE) contains all nine conserved motifs of the Class A PBPs (56). The *ywhE* gene is predicted to encode a 647 amino acid protein with a molecular mass of 71,660 Da. The gene is calculated to map to the 328.8° position on the chromosome. Expression of *ywhE* does not appear to occur during vegetative growth, but is induced approximately two hours into sporulation under control of σ F and to a lesser extent σ G within the forespore (82). Analysis of the *ywhE* single mutant did not reveal any phenotypic change either during vegetative growth, sporulation, or germination.

Class B PBPs

The non-penicillin-binding domain (n-PB) of the Class B PBPs also contains conserved motifs, but a second enzymatic activity has not been associated with this domain (Figure 1.8) (34). In 1981, Ishino and Matsuhashi (45) suggested that PBP3, a Class B PBP of *E. coli,* could catalyze the polymerization of glycan strands. However, this has been refuted by Adam, et al. (2) and more recently by van Heijenoort, et al. (128). The Class B PBPs play important roles in proper PG development (72, 108, 111, 142) and although the non-PB domain has not demonstrated any enzymatic activity, it does appear to be required for proper activity of the enzyme. This may be accomplished either through coordinating the proper protein folding or through the interactions with other proteins, such as Class A PBPs, or both.

B. subtilis contains six Class B PBPs, two of which are expressed during sporulation and the other four during vegetative growth. The Class B PBPs are as follows: PBP2a encoded by *pbpA* (72), PBP2b encoded by *pbpB* (142), PBP3 encoded by *pbpC* (73), PBPH encoded by *pbpH* (previously known as *ykuA*) (140), PBP4b encoded by *pbpI* (previously known as *yrrR*) (Wei and Popham, Unpublished Data), and SpoVD encoded by *spoVD* (23). As mentioned earlier, some Class B PBPs have demonstrated specific roles in *E. coli* cell development, and the same is true for *B. subtilis* (23, 71, 72, 142). PBP2a apparently plays a role in cell wall elongation as germinating cells are unable to elongate effectively and are delayed in spore outgrowth (71, 72).

The *E. coli* homolog of PBP2b (142) is PBP3, encoded by *ftsI* (also named *pbpB*) (16, 108). Both are encoded by genes that are located in a cluster of genes involved in cell division and cell wall metabolism suggesting a role for each of these proteins (25, 130, 142). PBP2b of *B. subtilis* and PBP3 of *E. coli* certainly play a role in cell division because the lack of these homologs in either organism produces filamentous cells and is lethal (24, 108, 142). Furthermore, a carboxy-terminal extension on PBP2b that is partially required to maintain the wild type cellular phenotype (142) suggests the possibility that this extension may interact with either proteins involved in cell division or cell wall synthesis, such as PBP1, or even structures, such as PG .

PBP3, encoded by *pbpC* is a protein predominately expressed during vegetative growth. Removal of this protein alone or in combination with other PBPs produces no observable changes in phenotype (73).

PBPH has not been identified through penicillin labeling and therefore retains its gene nomenclature. Mutational analysis of this gene shows no observable phenotypic changes in single mutants but is lethal when combined with a mutation in *pbpA* (140). This lethal combination indicates a redundancy of function even though *pbpH* is expressed at extremely low levels during vegetative growth. Expression of *pbpH* under control of an inducible promoter enables growth and study of this *pbpA pbpH* double mutant.

PBP4b is encoded by *pbpI* and is expressed during sporulation. Mutational analyses of single or multiple genes including *pbpI* has presented no observable phenotypic changes (Wei and Popham, Unpublished Data).

The Class B PBP SpoVD, encoded by the gene with the same name, is expressed specifically in the mother cell during sporulation. Although cells of strains lacking this protein appear to synthesize some germ cell wall, they lack cortex PG (23).

Low Molecular-Weight PBPs

The activity of low molecular-weight (low-MW) PBPs is primarily involved in regulating the number of cross-links through cleaving free peptide side-chains (DD-carboxypeptidase) or cleaving side-chains already involved in cross-links (endopeptidase). There are six low-MW PBPs in *B. subtilis*, but only three have demonstrated effects on any PG structural alterations or cellular phenotypes. The genes encoding the low-MW PBPs are as follows: *dacA* (126), *dacB* (18), *dacC* (81), *dacF* (141), *pbpE* (92), and *pbpX* (http://genolist.pasteur.fr/SubtiList/). Strains lacking low-

MW PBPs might be expected to have changes in the lengths of side chains as well as an increase in the percentage of cross-linking. For instance, a *dacA* mutant demonstrates an increase in the number of pentapeptide side-chains from approximately 3% in wild type to approximately 82%, but the amount of muropeptides involved in cross-linking does not differ significantly (9). Also, strains containing mutations in one of two low-MW PBPs expressed during sporulation has demonstrated spore PG structural alterations, which are increased when both are combined in the same strain. In cells lacking DacB, the amount of cross-linking throughout the spore PG is largely increased (10, 86, 87, 89) whereas no changes are seen in the single *dacF* mutant (86). However, the amount of cross-linking is increased even more in the *dacB dacF* double mutant. These structural changes also lead to an increase in water content of the spore core and a subsequent decrease in spore heat resistance (86).

Bacterial antibiotic resistance is on the rise, particularly for β-lactam antibiotics. Therefore, studies on the structure of PG and the enzymatic activities required for its synthesis need to be performed in order to determine potential target sites for new antibiotics. The GT activity performed by Class A PBPs and mono-functional GTs is an attractive prospect in this search as there are very few antibiotics that specifically target this reaction and the activity is thought to be highly conserved. Because of these reasons, the possibility of having resistance genes present in the environment might be extremely low. One antibiotic that is specific for the GT activity of Class A PBPs is called moenomycin, produced by *Streptomyces bambergiensis* (43, 127, 129). Use of this

antibiotic is limited to being an additive to livestock feed and is not used for medical purposes on humans due to potential negative side-effects. This antibiotic mimics the Lipid II precursor (57) recognized by Class A PBPs and must bind to the active site of these proteins (114, 132, 133) suggesting conservation of the GT mechanism of these enzymes. The purpose of this composition of studies is to examine the Class A PBPs in *B. subtilis* in an attempt to identify specific roles for each and also to examine the GT activity of these proteins.

Chapter 2

Two Class A High-Molecular-Weight Penicillin-Binding Proteins of *Bacillus subtilis* Play Redundant Roles in Sporulation

McPherson, Derrell C., Adam Driks, and David L. Popham. 2001. J. Bacteriol. **183**(20):6046-6053.

ABSTRACT

The four class A PBPs of *Bacillus subtilis* appear to play functionally redundant roles in polymerizing the peptidoglycan (PG) strands of the vegetative cell and spore walls. The *ywhE* product was shown to bind penicillin, so the gene and gene product were renamed *pbpG* and PBP2d, respectively. Construction of mutant strains lacking multiple Class A PBPs revealed that while PBP2d plays no obvious role in vegetative wall synthesis it does play a role in spore PG synthesis. A *pbpG* null mutant produced spore PG structurally similar to that of the wild type, however, electron microscopy revealed that in a significant number of these spores the PG did not completely surround the spore core. In a *pbpF pbpG* double mutant this spore PG defect was apparent in every spore produced, indicating that these two gene products play partially redundant roles. A normal amount of spore PG was produced in the double mutant, but it was frequently produced in large masses on either side of the forespore. The double mutant spore PG had structural alterations indicative of improper cortex PG synthesis, including 2-fold decreases in production of muramic-δ-lactam and L-alanine side chains and a slight increase in cross-linking. Sporulation gene expression was normal in the *pbpF pbpG* double mutant, but the double mutant spores failed to reach dormancy and subsequently degraded their spore PG. We suggest that these two forespore-synthesized PBPs are required for synthesis of the spore germ cell wall, the first layer of spore PG synthesized on the surface of the inner forespore membrane, and that in the absence of the germ cell wall the cells lack a template needed for proper synthesis of the spore cortex, the outer layers of spore PG, by proteins on the outer forespore membrane.

INTRODUCTION

Peptidoglycan (PG) is the essential structural element that provides shape and stability to most bacterial cells. In the dormant endospore PG is required for the maintenance of spore core dehydration and therefore for spore heat resistance. Both vegetative cell and spore PG are composed of glycan strands of repeating N-acetyl glucosamine (NAG) and N-acetyl muramic acid (NAM) residues cross-linked by peptide side chains (reviewed in (8)). Polymerization of PG involves the addition of disaccharide pentapeptide subunits onto a growing glycan strand by a glycosyl transferase. The peptide side-chains are then utilized by a transpeptidase to cross-link the glycan strands. Side-chains that are not utilized for cross-linking are cleaved to tripeptides or tetrapeptides.

Spore PG consists of two layers that can be distinguished structurally and functionally. The germ cell wall is adjacent to the inner forespore membrane and serves as the initial cell wall during spore germination and outgrowth. It is surrounded by the cortex, which comprises the outer 70-90% of the spore PG (67) and which is rapidly degraded during spore germination (11, 30). Cortex PG is more loosely cross-linked than vegetative PG and 50% of the NAM residues have had their peptides side chains removed and have been converted to muramic-δ-lactam (10, 87, 137, 139). The structure of the germ cell wall appears to be more similar to that of vegetative PG in that most of the peptide side chains are tripeptides and there is little or no muramic-δ-lactam (11, 67, 124). Despite the differences between the spore and vegetative PG structure, the mechanism of PG polymerization appears to be similar in the two situations.

The glycosyl transferase and transpeptidase activities required for PG synthesis are found in the penicillin-binding proteins (PBPs) (32). The PBPs can be placed into three classes based on amino acid sequence similarities (32, 34). Class A high-molecular weight PBPs are bifunctional PBPs that contain an N-terminal glycosyl transferase domain and a C-terminal transpeptidase domain. Class B high-molecular weight PBPs are only known to have transpeptidase activity and are, in some cases, required for cell septation and maintenance of cell shape (71, 108, 109, 142). Low-molecular weight PBPs generally have D,D-carboxypeptidase activity and, in some cases, are involved in regulating the number of cross-links between the glycan strands (86, 89, 104).

Redundancy in the functions of multiple Class A PBPs has been previously demonstrated in vegetative cells of *B. subtilis* (95), *E. coli* (26, 119, 143), and *S. pneumoniae* (42, 78). Sequence analysis of the *B. subtilis* genome (56) revealed genes encoding four Class A PBPs (82, 95). Loss of three (PBP1, PBP2c, and PBP4) of the four slows the vegetative growth rate, mostly due to the loss of PBP1, and decreases the production of spores ten-fold (95). Recent studies have indicated that YwhE, the fourth Class A PBP, has no effect on vegetative PG synthesis and demonstrated that *ywhE* is expressed only in the forespore under the control of σ^F and, to a lesser degree, σ^G (82). Another Class A PBP, PBP2c, is expressed vegetatively but is also induced in the forespore under control of σ^G (93) suggesting potential roles for both PBP2c and YwhE in spore PG synthesis or spore germination. In this communication we present studies examining the phenotypes of double and triple Class A PBP mutants lacking *ywhE*. We

demonstrate that loss of both PBP2c and YwhE has no effect on vegetative growth but that this double mutant is unable to complete sporulation.

METHODS AND MATERIALS

Bacterial growth, transformation, and sporulation. All strains of *B. subtilis* listed in Table 2.1 were derivatives of strain 168. Transformation was performed as previously described (3). Transformants were selected and maintained using appropriate antibiotics: chloramphenicol (3 μg/ml), spectinomycin (100 μg/ml), kanamycin (10 μg/ml), tetracycline (10μg/ml) and erythromycin (0.5 μg/ml) plus lincomycin (12.5 μg/ml) (MLS resistance). Antibiotics were omitted in cultures grown for determination of growth rates, sporulation efficiencies, and spore PG structure.

Growth rates were determined in 2xSG medium (59) at 37˚C with shaking. Cultures were allowed to sporulate following nutrient exhaustion for 24 hours, at which time spore heat resistance and chloroform resistance were measured as previously described (75). β-galactosidase activity, glucose dehydrogenase activity, and dipicolinic acid contents of sporulating cultures were assayed as previously described (75). Sporulating cells were prepared for electron microscopy as previously described, except that grids were stained with uranyl acetate as well as Reynolds lead (19). The amount and structure of spore peptidoglycan produced within cultures was analyzed as previously described (67).

Class A PBP mutant construction. Plasmid pDPC145 (94) was digested with *Eco*RI and *Eco*RV to produce an 800 bp fragment containing the first 147 bp of *pbpD*

TABLE 2.1. *B. subtilis* strains used

Strain	Genotype[a]	Transformation		Source or reference
		Donor	Recipient	
1A626	*hisA*82::Tn917			Bacillus Genetic Stock Center
AD51	*gerE-lacZ*			(22)
AD52	*cotD-lacZ*			(144)
AD799	*sspB-lacZ*			(62)
DPVB29	Double Δ*pbpD*::Cm	pDPC271	PS832	This work
DPVB30	Δ*pbpD* (Spo$^-$)			This work
DPVB40	Δ*pbpD hisA*82::Tn917 (Spo$^+$)	1A626	DPVB30	This work
DPVB42	Δ*pbpD* (Spo$^+$)	DPVB30	DPVB40	This work
DPVB45	Δ*pbpG*::Kn	pDPV35	PS832	This work
DPVB46	Δ*pbpD* Δ*pbpF*::Erm	PS1869	DPVB42	This work
DPVB49	Δ*pbpD* Δ*pbpG*::Kn Δ*pbpF*::Erm	DPVB45	DPVB46	This work
DPVB56	Δ*pbpG*::Kn Δ*pbpF*::Erm	DPVB45	PS1869	This work
DPVB57	Δ*pbpD* Δ*pbpG*::Kn	DPVB45	DPVB42	This work
DPVB61	Δ*ponA*::Sp Δ*pbpG*::Kn	PS2062	DPVB45	This work
DPVB62	Δ*ponA*::Sp Δ*pbpD* Δ*pbpG*::Kn	PS2062	DPVB57	This work
DPVB63	Δ*ponA*::Sp Δ*pbpG*::Kn Δ*pbpF*::Erm	PS2062	DPVB56	This work
DPVB68	Δ*ponA*::Sp Δ*pbpD*	PS2062	DPVB42	This work
DPVB69	Δ*ponA*::Sp Δ*pbpD* Δ*pbpF*::Erm	PS2062	DPVB46	This work
DPVB84	*sspB-lacZ*	AD799	PS832	This work
DPVB85	*sspB-lacZ* Δ*pbpF*::Erm	AD799	PS1869	This work
DPVB86	*sspB-lacZ* Δ*pbpG*::Kn	AD799	DPVB45	This work
DPVB89	*sspB-lacZ* Δ*pbpG*::Kn Δ*pbpF*::Erm	DPVB84	DPVB56	This work
DPVB90	*gerE-lacZ*	AD51	PS832	This work

DPVB91	*gerE-lacZ* Δ*pbpF*::Erm	AD51	PS1869	This work
DPVB92	*gerE-lacZ* Δ*pbpG*::Kn	AD51	DPVB45	This work
DPVB93	*gerE-lacZ* Δ*pbpG*::Kn Δ*pbpF*::Erm	AD51	DPVB56	This work
DPVB94	*cotD-lacZ*	AD52	PS832	This work
DPVB95	*cotD-lacZ* Δ*pbpF*::Erm	AD52	PS1869	This work
DPVB96	*cotD-lacZ* Δ*pbpG*::Kn	AD52	DPVB45	This work
DPVB97	*cotD-lacZ* Δ*pbpG*::Kn Δ*pbpF*::Erm	AD52	DPVB56	This work
DPVB141	Δ*pbpG*::Kn *cwlD*::Cm	PS2307	DPVB45	This work
DPVB142	Δ*pbpF*::Erm *cwlD*::Cm	PS2307	PS1869	This work
DPVB143	Δ*pbpG*::Kn Δ*pbpF*::Erm *cwlD*::Cm	PS2307	DPVB56	This work
DPVB157	Δ*pbpF*::Erm *sleB*::Sp *cwlJ*::Tet	FB111, FB112	PS1869	This work
DPVB158	Δ*pbpG*::Kn *sleB*::Sp *cwlJ*::Tet	FB111, FB112	DPVB45	This work
DPVB159	Δ*pbpG*::Kn Δ*pbpF*::Erm *sleB*::Sp *cwlJ*::Tet	FB111, FB112	DPVB56	This work
FB111	*cwlJ*::Tet			(77)
FB112	*sleB*::Sp			(77)
FB113	*cwlJ*::Tet *sleB*::Sp			(77)
PS832	Prototrophic revertant of strain 168			Laboratory stock
PS1869	Δ*pbpF*::Erm	pDPC89	PS832	(93)
PS2062	Δ*ponA*::Sp	pDPC197	PS832	(91)
PS2251	Δ*ponA*::Sp Δ*pbpF*::Erm	PS2062	PS1869	(95)
PS2307	*cwlD*::Cm	ADD1	PS832	(102)

[a] Abbreviations: Erm, resistance to erythromycin and lincomycin; Sp, resistance to spectinomycin; Cm, resistance to chloramphenicol; Kn, resistance to kanamycin; Tet, resistance to tetracycline.

plus upstream sequences. This fragment was ligated into *Eco*RI, *Pvu*II-digested pDPC179 (94), which contains the last 243 bp of *pbpD*, to create an in-frame deletion of codons 50-543 (out of 624). The plasmid containing the deletion, pDPC271, was used to transform PS832 with selection for chloramphenicol resistance. Insertion of pDPC271 into the chromosome via a single crossover results in copies of *pbpD* on both sides of the vector sequence. Transformants were screened by PCR to identify a strain in which a recombination event caused both copies of *pbpD* to contain the in-frame deletion (DPVB29) (data not shown). This strain was grown for 50 generations in non-selective liquid media, allowing for recombination of the plasmid out of the chromosome to leave a single Δ*pbpD*. The culture was plated for single colonies on non-selective media and replica plated to identify a chloramphenicol sensitive isolate (DPVB30). The single Δ*pbpD* in this strain was verified using PCR and Southern blot analysis (data not shown). DPVB30 was found to have a Spo^- phenotype that was not present in DPVB29 and was believed to result from a spontaneous mutation in an unrelated locus. DPVB30 was transformed with chromosomal DNA of strain 1A626 with selection for MLS resistance. The resulting colonies were screened for cotransformation to a Spo^+ phenotype and one Spo^+ isolate was saved as DPVB40. This strain was then transformed with limiting chromosomal DNA from DPVB30 with selection for His^+. Most transformants retained the Spo^+ phenotype and one (DPVB42) was verified using PCR to contain Δ*pbpD*.

A PCR product containing sequence from 417 bp upstream of the *ywhE* start codon to 212 bp downstream of the *ywhE* stop codon (56, 82) was ligated into the pGEM-T vector (Stratagene) to produce pDPV24. This plasmid was digested with *Pvu*II

and *Sal*I to obtain a 524 bp fragment containing the first 90 bp of *ywhE* and with *Pvu*II and *Sph*I to obtain a 485 bp fragment containing the final 251 bp of *ywhE*. These two fragments were ligated with *Sph*I- and *Sal*I-digested pJH101 to obtain pDPV33, in which bases 91-1691 of *ywhE* are deleted. Plasmid pDG780 (37) was digested with *Sma*I and *Hinc*II to obtain a kanamycin resistance cassette that was inserted into pDPV33 at the *Pvu*II site at the point of the *ywhE* deletion to create pDPV35. pDPV35 was linearized with *Sca*I and used to transform PS832, with selection for kanamycin resistance, to create DPVB45 (Δ*ywhE*::Kn). Strains containing multiple mutations were made by transformation using limiting chromosomal DNA and selection with the appropriate antibiotics.

PBP detection. Penicillin X was synthesized and labeled with ^{125}I as previously described (50, 63). Membranes were prepared from *B. subtilis* cells at the 4th hour of sporulation in 2xSG medium as previously described (91). Membrane samples containing 40 µg of protein were incubated for 30 min at 30°C with 3 µCi of labeled-penicillin X in a total volume of 20 µl of 50 mM tris HCl pH 8.0, 1 mM β-mercaptoethanol, and 0.1 mM phenylmethylsulfonyl fluoride. Proteins were separated using SDS-PAGE on a 7.5% polyacrylamide gel. PBPs were detected and signal intensities were integrated using a STORM 860 phosphoimager and ImageQuant software (Molecular Dynamics).

RESULTS

Construction of Class A PBP mutant strains. Previous genetic analysis of the Class A PBPs in *B. subtilis* utilized some Campbell-type plasmid insertion mutations that have the ability to revert. The appearance of revertants produced significant problems in strains with reduced growth rates due to the loss of multiple Class A PBPs. To avoid this problem we utilized non-revertible mutations, such as deletions or deletion/antibiotic resistance insertions, in each of the four genes. Each of the mutations removed ≥79% of the genes' coding sequence. Deletion/ insertion mutations in *ponA* (91), *pbpF* (93), and *ywhE* terminated the coding sequences at or before codon 30 (out of ≥647) so that any resulting protein product would be missing all nine highly conserved motifs found within Class A PBPs (34). The in-frame deletion in *pbpD* removed 79% of the coding sequence, including conserved motifs 1-8 (34).

PCR was used to verify the presence of the expected alleles in each mutant strain (data not shown). Southern blot analysis (107) was then used to verify that all of the expected mutations were present as well as the fact that none of the genes were present in a form undetectable by our PCR assay (undetectable due to some undefined non-homologous recombination event). Two probes were used for each gene. One probe contained a region of the gene outside the deletion to verify the existence of either the wild type or mutant allele in each strain and a second probe interior to the deleted region to verify the complete absence of this region in each mutant. The expected wild type and mutant genes are present in each of the triple mutants (data not shown).

We used radioactively-labeled penicillin to visualize the PBPs present in our wild type and mutant strains. We identified a PBP that appeared to be the product of *ywhE* in membranes prepared from cells in the fourth hour of sporulation. This PBP migrated on SDS-PAGE in nearly the same place as PBP2c and could only be clearly seen in a *pbpF* mutant (Fig. 2.1, panels A and B). This result is consistent with the predicted molecular masses of PBP2c (93) and the *ywhE* product (82), 79 and 77 kDa, respectively. We will from this point on refer to *ywhE* as *pbpG* and to the gene product as PBP2d.

Growth and sporulation of Class A PBP mutants. The growth rates and sporulation efficiencies of *ponA, pbpD,* and *pbpF* single and multiple mutant strains were consistent with those previously reported (Table 2.2 and (95)). Deletion of *pbpG*, alone and in multiple mutants, had no effect on growth rate (Table 2.2 and (82)). Sporulation efficiency of each strain was determined by the number of heat resistant cfu compared to the number of viable cfu after 24 hours of sporulation. Small decreases in production of heat- and chloroform-resistant spores were observed in strains lacking PBP1 and PBP4 (Table 2.2), as observed previously (95). These decreases were attributed to poor initiation of sporulation as a result of decreased growth rate rather than to a specific block in the sporulation process (95). In contrast, the *pbpF pbpG* strain exhibited a growth rate equal to that of the wild type but a >10,000-fold decrease in spore production (Table 2.2, strain DPVB56). The cells in this *pbpF pbpG* double mutant culture appear to initiate and proceed through sporulation as demonstrated by glucose dehydrogenase (GDH) and dipicolinic acid (DPA) assays (Fig. 2.2). However, the amount of DPA extracted from the double mutant decreases compared to wild type and single mutants after about 7

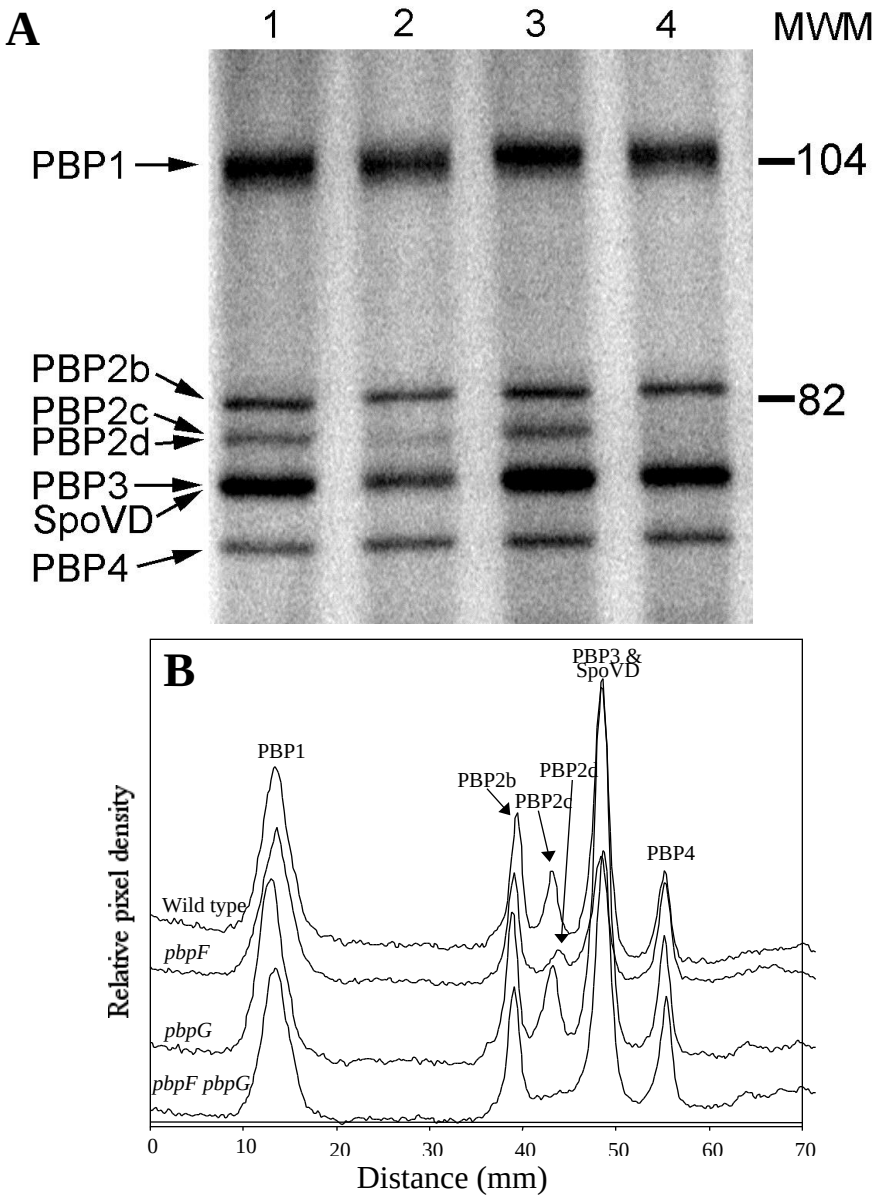

Figure 2.1. PBP profiles of wild type, *pbpF* mutant, and *pbpG* mutant, and *pbpF pbpG* double mutant strains. Membranes were purified from cultures at the 4th hour of sporulation. (A) Membranes were incubated with ^{125}I-labeled penicillin X, proteins were separated on a 7.5 % SDS-PAGE gel, and PBPs were detected using a phosphoimager. Lane 1, wild type; lane 2, *pbpF*; lane 3, *pbpG*; lane 4, *pbpF pbpG*. Molecular weight standards (MWM) were Bio-Rad low range prestained SDS-PAGE standards, and calibrated molecular weights are indicated in kDa. PBP2a decreases dramatically during sporulation (17) and is not visible on this gel. (B) A histogram of PBP band intensities was produced by integrating signal strength within columns that covered 90% of each lanes' width. PBPs are numbered as previously described (13, 52).

TABLE 2.2. Growth and sporulation of Class A PBP mutant strains[a]

Strain	PBP Phenotype	Doubling time[b] (min)	Cell counts[c] (cfu/ml)		
			Viable	Heat-resistant spores	Chloroform-resistant spores
PS832	Wild type	20	2×10^9	2×10^9	2×10^9
PS1869	PBP2c$^-$	20	1×10^9	2×10^9	2×10^9
DPVB45	PBP2d$^-$	20	4×10^9	2×10^9	2×10^9
DPVB42	PBP4$^-$	20	3×10^9	2×10^9	1×10^9
PS2062	PBP1$^-$	25	2×10^9	3×10^9	2×10^9
DPVB57	PBP4$^-$, PBP2d$^-$	20	1×10^9	7×10^8	9×10^8
DPVB56	PBP2c$^-$, PBP2d$^-$	20	2×10^8	4×10^4	2×10^4
DPVB46	PBP2c$^-$, PBP4$^-$	20	2×10^9	4×10^8	7×10^8
DPVB61	PBP1$^-$, PBP2d$^-$	26	2×10^9	2×10^9	2×10^9
PS2251	PBP1$^-$, PBP2c$^-$	26	7×10^8	1×10^9	7×10^8
DPVB68	PBP1$^-$, PBP4$^-$	31	5×10^8	3×10^7	4×10^7
DPVB49	PBP2c$^-$, PBP4$^-$, PBP2d$^-$	21	8×10^8	7×10^3	3×10^2
DPVB63	PBP1$^-$, PBP2c$^-$, PBP2d$^-$	28	4×10^8	8×10^3	5×10^3
DPVB69	PBP1$^-$, PBP2c$^-$, PBP4$^-$	28	4×10^8	9×10^6	5×10^7
DPVB62	PBP1$^-$, PBP4$^-$, PBP2d$^-$	31	4×10^8	2×10^7	$1.x 10^7$

[a] Doubling times and cell counts are averages from at least three separate experiments.

[b] Growth was in liquid 2xSG medium at 37˚C.

[c] Cell counts determined 24 h after initiation of sporulation.

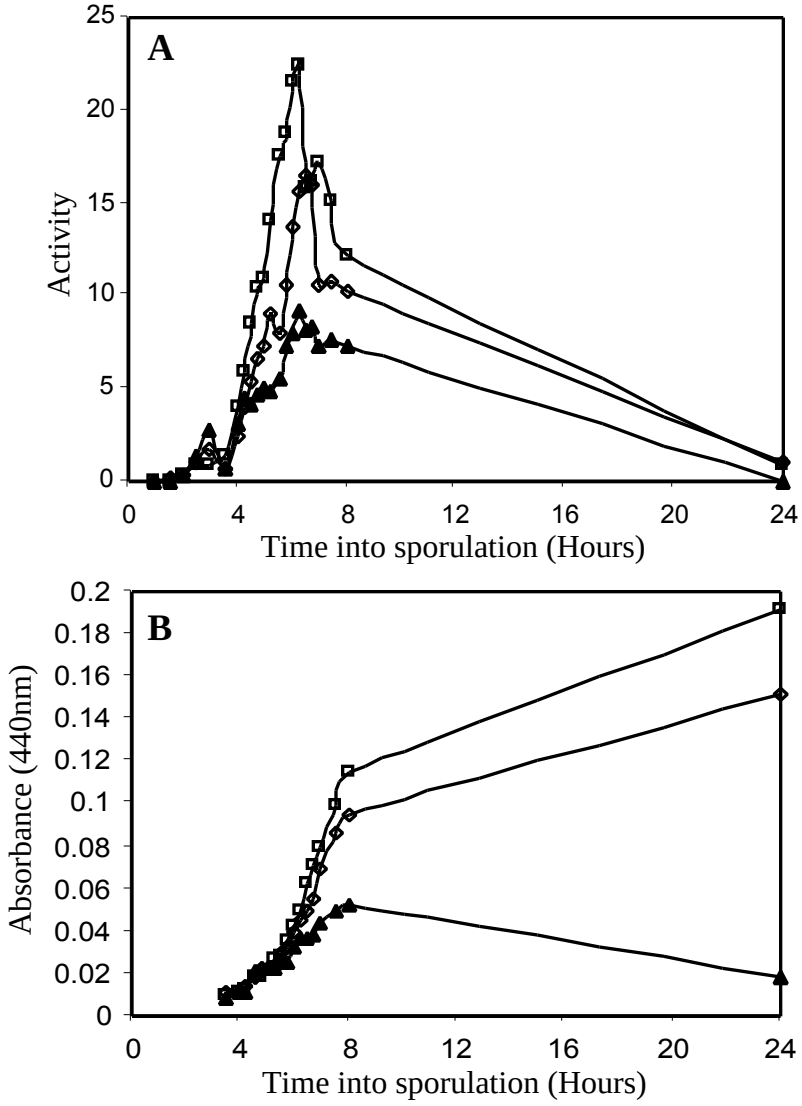

Figure 2.2. Glucose dehydrogenase (GDH) (A) and dipicolinic acid (DPA) (B) assays of *pbpF* and *pbpG* mutant strains. Cultures of *pbpF* (◇) and *pbpG* (□) single and *pbpF pbpG* (▲) double mutant strains were induced to sporulate using nutrient exhaustion and samples for GDH and DPA were obtained throughout sporulation and assayed as previously described (74). Both single mutants produced results similar to wild type (66).

hours of sporulation. A similar sporulation block was observed in triple mutants that lacked *pbpF* and *pbpG* (Table 2.2, strains DPVB49 and DPVB63).

Regulation of sporulation gene expression in the *pbpF pbpG* double mutant. Following engulfment, activation of σ^G leads to expression of a set of sporulation genes in the forespore, some of which, in turn, are required for activation of σ^K in the mother cell (Reviewed in (117)). It has been theorized that spore PG synthesis could be one component of the signal needed for the activation of σ^K (144). We theorized that loss of expression of two PBPs within the forespore might disrupt spore PG synthesis, in turn blocking σ^K activation and completion of sporulation. Studies were performed in the wild type, *pbpF*, *pbpG*, and *pbpF pbpG* strains to determine if gene expression during late sporulation was altered. A σ^G-dependent gene, *ssp* (Fig. 2.3A), and two σ^K-dependent genes, *cotD* (Fig. 2.3B) and *gerE* (Fig. 2.3C), were expressed at or above wild type levels in all three mutant strains, indicating that there was no block in the signal cascade between the forespore and mother cell.

Spore PG synthesis in *pbpF* and *pbpG* mutants. The amount and structure of spore PG synthesized in mutant strains was determined. Culture samples were collected every 30 minutes for eight hours following the initiation of sporulation. The muramic acid content (67) of the wild type and *pbpF* and *pbpG* single and double mutant cultures increased similarly throughout sporulation (Fig. 2.4). This muramic acid was present in peptidoglycan strands because similar amounts of spore PG could be purified in a muramidase-sensitive form from all the sporulating cultures. PG was purified from developing forespores (67) collected throughout sporulation of each culture. Structural

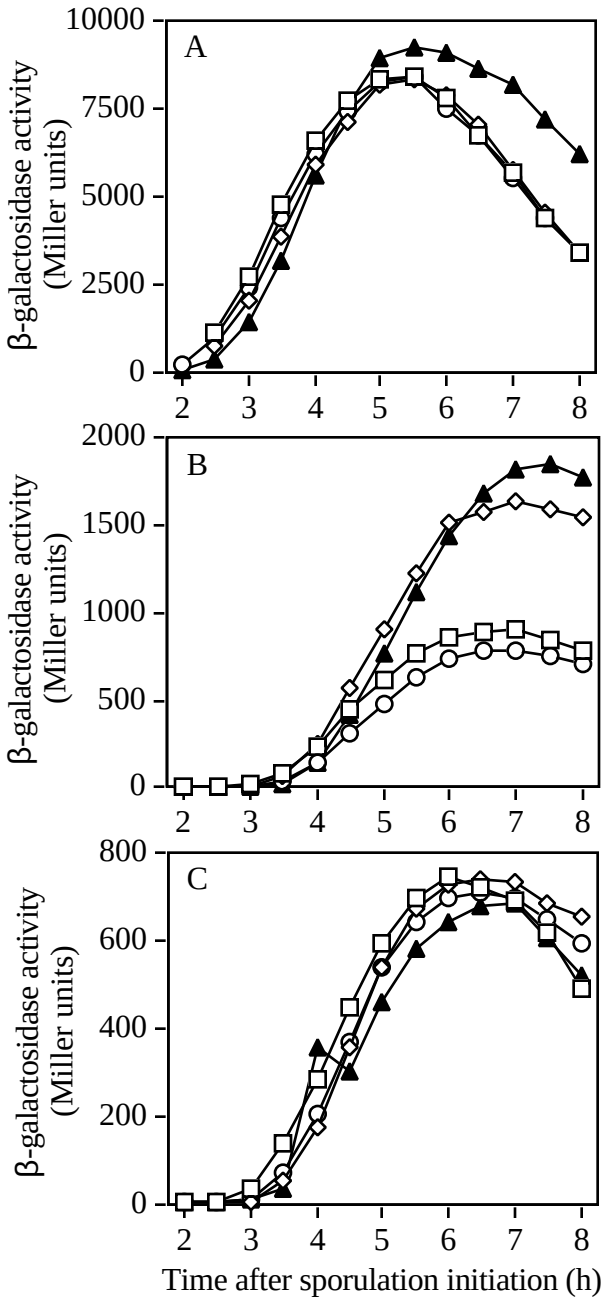

Figure 2.3. Expression of late sporulation genes in *pbpF* and *pbpG* mutant strains. Cultures of wild type (□), *pbpF* (◇) and *pbpG* (○) single mutant, and *pbpG pbpF* double mutant (▲) strains carrying fusions of *lacZ* to late sporulation genes were sampled following initiation of sporulation in 2xSG medium at 37°C. β-galactosidase expression from *sspB-lacZ* under regulatory control of σ^G (A) or from *cotD-lacZ* (B) and *gerE-lacZ* (C) under regulatory control of σ^K was assayed using *o*-nitrophenyl-β-D-galactopyranoside as previously described (74). The cause of *cotD* overexpression in the *pbpF* mutants is unknown.

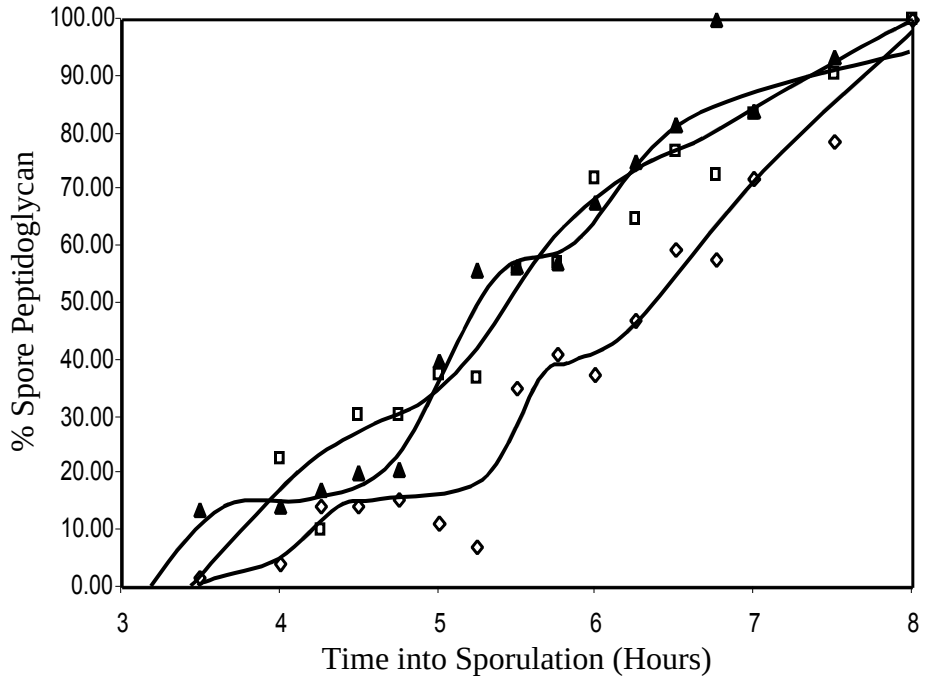

Figure 2.4. Hexosamine data from the *pbpF* and *pbpG* mutant strains. Hexosamine of the *pbpF* (◇) and *pbpG* (□) single and *pbpF pbpG* (▲) double mutants is used to determine the total amount of spore PG synthesized at various time points throughout sporulation as previously described (66).

analysis of this forespore PG using reverse-phase HPLC (67) demonstrated that, throughout sporulation, the *pbpF* and *pbpG* strains produced spore PG with structural parameters similar to that found in the wild type (Table 2.3 and (67)). The *pbpF pbpG* strain produced spore PG with altered structural parameters including a two-fold reduction in the percentage of muramic acid side-chains that have been cleaved to form muramic-δ-lactam and a three-fold reduction in the number of side chains cleaved to single L-alanine residues (Table 2.3). An increase in the number of both tripeptide and tetrapeptide side-chains was also observed. The amount of muramic acid involved in cross-linking was slightly higher throughout the spore PG in the double mutant relative to the single mutants. Although normal amounts of spore PG could be recovered from the double mutant until at least the eighth hour of sporulation, all spore PG was apparently degraded by 24 hours after sporulation initiation.

Microscopic examination of mutant cells. Examination of the *pbpF pbpG* cells under phase contrast microscopy six hours into sporulation revealed that >80% of the cells visible phase-dark forespores (data not shown). Twenty-four hours following the initiation of sporulation, very few phase-bright endospores were visible. To characterize the status of the spore peptidoglycan in more detail, we performed thin section electron microscopic analysis of mutant cells. In cultures of *pbpG* cells approximately 7 hours after the initiation of sporulation, we observed two morphologically distinct populations. The majority of cells resembled those of a wild type population (Fig. 2.5, panel A). In particular, the cortex was clearly visible. In a subset (approximately 35%) of the cells that had clearly completed engulfment, we observed a severe and novel defect in

TABLE 2.3. Structural parameters of forespore PG produced by *pbpF* and *pbpG* mutant strains[a]

Genotype	Time in sporulation (h)	% spore PG made[b]	% muramic acid with:				
			side chain of:[c]				cross-linked side chain
			Lactam	L-Ala	TriP	TP	
pbpF	3.5	2	4.6	7.9	72.1	15.4	14.8
	4	4.5	30.3	33.3	27.5	8.9	6.3
	4.5	13.5	41.4	44.2	9.5	4.9	2.7
	5	22.5	43.5	38.6	7.7	10.2	2.6
	5.5	33	44.5	30.9	5.2	19.3	2.9
	6	46.5	45.6	29.3	3.7	21.3	3.0
	6.5	59.5	45.5	26.5	3.3	24.7	3.2
	7	75	46.1	26.6	2.7	24.6	3.0
	7.5	89	46.4	24.8	2.4	26.4	3.1
	8	100	46.5	22.8	2.3	28.4	3.4
	24	100	48.5	21.6	1.5	28.4	3.4
pbpG	3.5	9.5	13.2	17.1	56.8	12.9	11.1
	4	18.5	32.4	34.3	26.2	7.2	5.5
	4.5	27.5	37.3	35.6	17.7	9.4	4.1
	5	37.5	39.8	29.7	12.0	18.5	4.0
	5.5	52	41.0	27.4	9.5	22.0	3.8
	6	71	42.7	26.0	7.0	24.2	3.9
	6.5	78.5	43.4	24.7	6.1	25.7	3.8
	7	86	44.4	24.6	5.4	25.6	3.7
	7.5	93.5	45.1	23.6	4.9	26.4	3.9
	8	100	46.1	23.7	4.2	26.0	3.6
	24	100	47.7	18.1	3.2	31.0	4.1
pbpF pbpG	3.5	5	0.0	0.0	80.9	19.1	14.0
	4	11	10.9	11.5	53.4	24.2	12.1
	4.5	17.5	18.8	14.9	29.6	27.7	9.7
	5	36	16.7	7.3	21.0	55.0	7.2
	5.5	57	14.3	5.4	11.1	69.3	6.5
	6	70	15.6	5.6	8.2	70.6	6.4
	6.5	81	16.4	5.5	7.2	70.9	6.5
	7	89.5	17.7	5.7	6.6	70.0	6.3
	7.5	95	18.7	6.1	6.1	69.2	6.1
	8	100	19.3	6.0	5.8	68.9	6.0
	24	0	-	-	-	-	-

[a] Forespore PG was purified from culture samples taken every 15 min between t_4 and t_7, but only data for samples taken every 30 min are shown.

[b] These values are derived from the interpolation of culture muramic acid contents as determined by amino acid analyses (67).

[c] Lactam, muramic-δ-lactam; L-Ala, single alanine; TriP, tripeptide; TP, tetrapeptide.

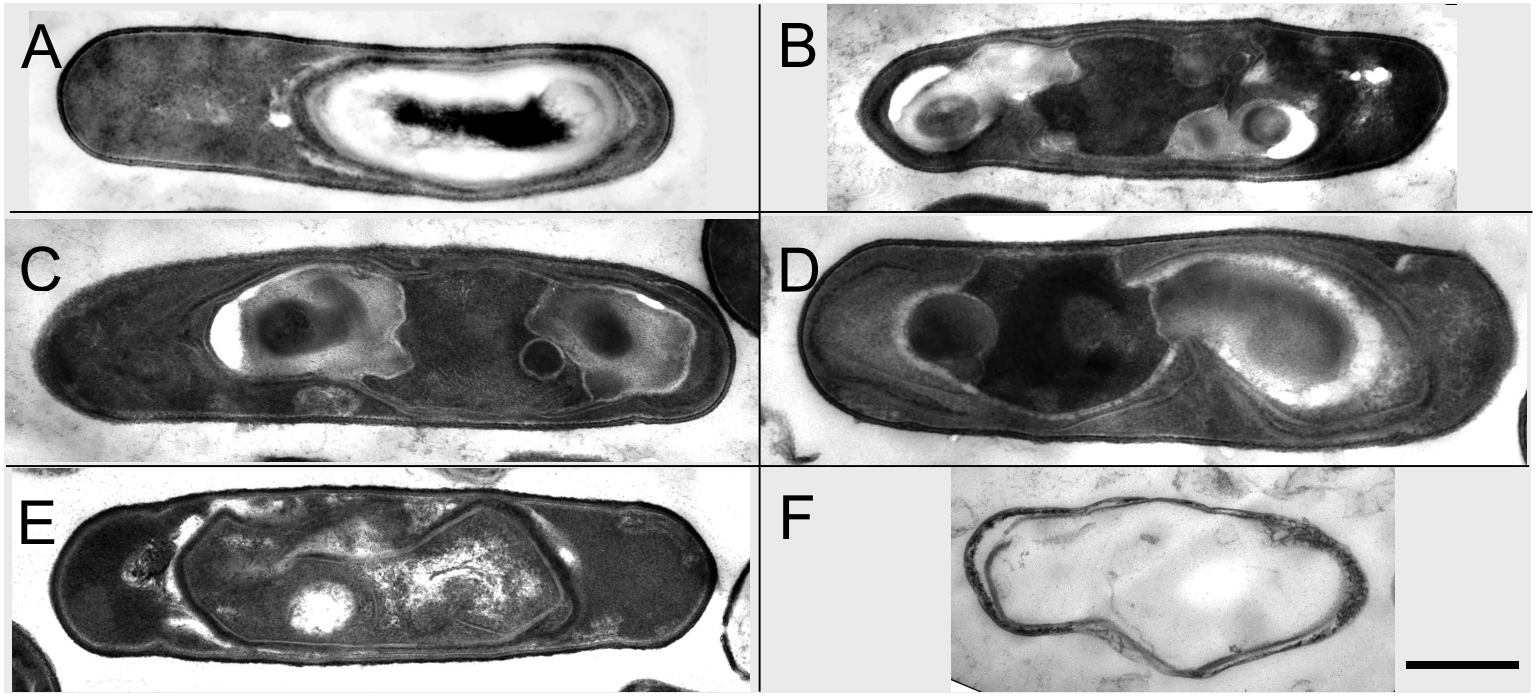

Figure 2.5. Thin-section electron microscopy of sporulating mutant cells. Cells of *pbpG* (panels A-C) or *pbpG pbpF* (panels D-F) strains were sporulated, harvested at hour 7 (panels A-D) or hour 24 (panels E and F), and prepared for electron microscopy. (A) The majority of *pbpG* cells had this appearance, similar to the wild type. (B-D) A minority of the *pbpG* cells had this appearance in which masses, presumed to be spore PG, do not completely surround the forespore. The majority of these *pbpF pbpG* cells had this appearance. (E) A *pbpF pbpG* double mutant cell at the 24th hour of sporulation in which the masses on either side of the forespore have disappeared. (F) Empty spore coat structure released by lysis of a *pbpF pbpG* double mutant cell at the 24th hour of sporulation. CX, cortex; fs, forespore cytoplasm. Arrowheads indicate spore coat structures. Size bar in panel F indicates 500 nm; all images are at the same magnification.

development (Fig. 2.5, panels B and C). These cells possess what appears to be a highly disorganized forespore. The central regions of these cells resemble a forespore cytoplasm in electron density and granularity. However, instead of being surrounded by a lightly staining region clearly corresponding to the cortex, one or two lightly staining masses were present adjacent to the apparent forespore cytoplasm, generally at opposite ends of the forespore. The regions of the section containing these masses frequently sustained tears during electron microscopy, suggesting they tended to infiltrate poorly with the embedding resin. Spore coat material surrounded these regions. These coats possessed inner and outer layers but tended not to form a contiguous shell and to be thinner than wild type spore coats. Those cells lacking a normal spore PG layer are not expected to achieve normal heat resistance. We believe that the proportion of defective spores in *pbpG* cultures is low enough (and possibly highly variable) that it was not detectable in our assays of heat resistant spore production (Table 2.2).

pbpF pbpG cells harvested at hour 7 differed from *pbpG* cells in that the defect was present in all the cells (Fig. 2.5, panel D). At hour 24 the majority of spore structures within double mutant sporangia no longer contained the masses (Fig. 2.5, panel E), and mother cells that had lysed released what appeared to be simply shells of spore coat without any interior PG or cytoplasm (Fig. 2.5, panel F). One interpretation of these data is that in the absence of *pbpG* a significant percentage of cells form a defective cortex, resulting in the accumulation of incorrectly assembled peptidoglycan in pockets near the forespore. This defect is magnified with the addition of a mutation in *pbpF*, such that none of the cells form functional cortexes. As a consequence of the resulting failure in

dehydration, when the mother cell lyses the spore interior lyses as well, producing a spore that is fragment of coat without a core. Several lines of evidence suggest that the masses seen in the *pbpF pbpG* developing spores consist of disorganized spore PG. The masses are positioned between the inner forespore membrane and the spore coats, as is normal spore PG. The masses disappear by hour 24 of sporulation, and we were unable to recover any spore PG from culture samples at that time (Table 2.3 and Fig. 2.4). Two types of mutations result in stabilization of spore PG in *B. subtilis*: mutations in *cwlJ* and *sleB* which encode germination lytic enzymes (15, 44, 70), and a mutation in *cwlD* (102) which is required for the production of muramic-δ-lactam in the spore PG (10, 88), a recognition determinant for germination lytic enzymes. When *cwlJ* and *sleB* mutations (77) or a *cwlD* mutation (102) were introduced into the *pbpF pbpG* strain, the masses contained within the spore coats were still clearly visible under phase contrast microscopy at the 24th hour of sporulation (data not shown) and the spore PG that was produced remained stable. Spore PG was isolated from the *cwlJ sleB*, *cwlJ pbpF sleB*, *cwlJ pbpG sleB*, and *cwlJ pbpF pbpG sleB* strains at both the 8th and the 24th hour of sporulation. The presence of the *cwlJ* and *sleB* mutations had no effect on the spore PG structure produced by these strains (data not shown). However, the presence of these mutations allowed us to isolate spore PG from the *cwlJ pbpF pbpG sleB* strain at the 24th hour of sporulation, and we found it to have a structure similar to that produced by the *pbpF pbpG* strain at the 8th hour of sporulation (Table 2.3 and data not shown). Similarly, the introduction of a *cwlD* mutation into each *pbp* mutant strain resulted only

in the loss of all muramic-δ-lactam from the spore PG but spore PG could still be recovered from the *cwlD pbpF pbpG* strain at the 24th hour of sporulation.

DISCUSSION

Previous studies performed on three Class A PBPs of *B. subtilis* indicated that they have redundant functions in vegetative PG polymerization but revealed no clear role in spore PG synthesis (95). Pedersen, et al. (82) found that *pbpG*, which encodes a fourth Class A PBP, is expressed only during sporulation and that a *pbpG* mutation had no effect on vegetative growth. We have now shown that loss of *pbpG* in multiple mutants lacking other Class A PBPs reveals no redundant role for PBP2d in vegetative growth. This suggests that in a mutant strain lacking PBPs 1 and 4, which has a greatly reduced growth rate, *pbpG* is not being induced to take on a significant role in vegetative wall synthesis.

A *pbpF pbpG* double mutant strain has a severe sporulation defect in the absence of any vegetative growth deficiency. Electron microscopy and biochemical assays of glucose dehydrogenase, dipicolinic acid (data not shown), and spore PG production revealed that this double mutant initiated and progressed through stage four of sporulation at a rate equivalent to the wild type and both single mutants. Consistent with a block at this stage, mutant cells never achieved full resistance properties, and the spore was degraded during the next 24 hours. The fact that expression of both *pbpF* and *pbpG* is induced specifically within the forespore compartment (82, 93) suggests that these proteins might be involved in synthesis of spore PG from the surface of the inner

forespore membrane. This is the site of the germ cell wall in the dormant spore, and this structure appears to be synthesized first, prior to synthesis of the cortex PG (67). However, the initial 10-20% of the spore PG produced by the double mutant appeared normal, having the structure expected in the germ cell wall (11, 67). The structure of the cortex PG was greatly altered in the double mutant. One major change was a two-fold decrease in the amount of muramic-δ-lactam, a structural marker used to differentiate cortex from germ cell wall (10, 11, 67, 87, 88). This was surprising since several lines of evidence indicate that the cortex PG is synthesized from the mother cell side. The spore PG defects revealed by electron microscopy in a minority of *pbpG* mutant sporangia must not reflect a major alteration of spore PG structural parameters or must have been present in too small a percentage of the cells to produce a large change in the spore PG structural parameters determined for the population.

The particular spore PG structural alterations present in the *pbpF pbpG* strain would not be expected to result in failure to achieve dormancy. Previous studies have shown that mutant strains that produce spore PG containing either no muramic-δ-lactam (*cwlD*) (10, 88), high cross-linking (*dacB*) (87, 89), or both (*cwlD dacB*) (90) are able to achieve normal spore dehydration and dormancy. The spore PG produced by a *dacB* strain also has a three-fold decrease in the amount of single L-alanine side-chains, similar to that seen in the *pbpF pbpG* double mutant, but normal spore dormancy. Failure of the *pbpF pbpG* spores to achieve dormancy is almost certainly due to the large change in the three dimensional PG architecture we observed in electron micrographs.

We consider several possibilities for the mechanism by which loss of *pbpF* and *pbpG* results in altered synthesis of spore cortex PG. One possibility is that cortex PG is not actually produced from the mother cell side and that PBP2c and PBP2d are required on the inner forespore membrane to synthesize this structure. While there is no direct evidence for cortex synthesis from the mother cell side, there are a variety of lines of evidence that suggest this, including: the production of spore PG-specific precursors in the mother cell (124), mother cell-specific synthesis of two PBPs that have significant effects on cortex PG synthesis (18, 23, 105), and the fact that the cortex PG appears to be synthesized after the germ cell wall PG (67). A second possibility is that altered synthesis of the first layers of spore PG (alterations of a type undetectable with our current methods of analysis) could disrupt the cell-cell communication carried out by the forespore and mother cell. This communication is necessary for activation of σ^K in the mother cell and σ^K activity is required for completion of spore PG synthesis (21). It is possible that spore PG synthesis could be one component of a signal transduced from the forespore to the mother cell (144). Although previous studies have indicated that expression of *spoIVB* is the only function of the forespore-specific transcription factor σ^G required for activation of σ^K (35) and that σ^G was required for initiation of spore PG synthesis (52, 76), we felt that previous electron microscopic examinations could have missed production of a very small amount of spore PG in a *sigG* mutant. However, expression of genes dependent on both σ^G and σ^K were normal in the *pbpF pbpG* strain. It is interesting to note that the failure of *pbpF pbpG* double mutant spores to reach dormancy is similar to the phenotype produced by certain *spoIVB* point mutants which

allow σ^K activation but which are deficient in an undefined second role required for spore maturation (76). We plan to examine if similar spore PG defects are present in this type of *spoIVB* mutant which might suggest that this second role of *spoIVB* is exerted through the spore PG synthetic machinery.

A third explanation for defective cortex synthesis in the *pbpF pbpG* strain is that the requirement for the *pbpF* and *pbpG* products is actually on the outer forespore membrane. These particular Class A PBPs may be required for the coordination of other activities required for production of muramic-δ-lactam and L-Ala side chains. Such a model would require both of these gene products to be present and functional on the outer forespore membrane in order to result in the functional redundancy seen in our genetic analysis. The *pbpF* gene is expressed at relatively low levels during vegetative growth, and during the process of engulfment its product, PBP2c, could be distributed to both the inner and outer forespore membranes. Previous studies of *pbpG* expression identified only forespore-specific transcription (82). We would have to theorize that either: a) extremely low-level mother cell expression of *pbpG*, below the detection limit of previous assays, was sufficient to satisfy a requirement for cortex synthesis on the surface of the outer forespore membrane, or b) PBP2d is produced within the forespore and crosses the inner forespore membrane but, unlike other Class A PBPs (34, 95), does not remain associated with this membrane and is free to move to the surface of the outer forespore membrane. Our detection of PBP2d in membrane preparations of sporulating cells argues against this idea.

Finally, the model we prefer is that alteration of the germ cell wall PG structure presents an improper "template" for synthesis of the cortex PG by proteins on the outer forespore membrane. We propose that either PBP2c or PBP2d can carry out synthesis of germ cell wall PG in a uniform shell surrounding the entire forespore. In the absence of both of these PBPs an incomplete germ cell wall is produced (potentially by Class A PBPs 1 and/or 4). Cortex PG polymerization is carried out by PBPs associated with the outer forespore membrane, potentially using the germ cell wall PG as a template. In the absence of a proper template we suggest that the cortex is synthesized in disorganized masses, often on either side of the forespore. If this synthesis of cortex PG is specifically targeted to the forespore poles, it could possibly be due to remnants of septum PG synthetic machinery. The last known sites of PG synthesis on the membranes surrounding the forespore were at the centers of a vegetative division septum and the asymmetric sporulation septum. An alternative explanation is that the cortex PG masses are not actually synthesized at the forespore poles but that a major elongation of the spore in one direction, due to the odd PG synthesis at any single site on the forespore surface, causes the forespore to turn within the cell so that the PG extension appears to be at a pole. Finally, PG synthesis at the apparent poles of the forespore may simply be due to the fact that this is where there is available space within the sporangium. The fact that a fraction of *pbpG* cells produce disorganized cortex PG may be due to the fact that PBP2d expression in the forespore, directed by σ^F, takes place before forespore expression of PBP2c, directed by σ^G. In some *pbpG* cells, cortex synthesis may advance too far in an altered way before PBP2c is produced in large enough amounts to produce a normal germ

cell wall. Investigation of the requirements for *pbpF* and *pbpG* expression in the mother cell and forespore compartments in order to complete spore formation will be a step towards eliminating some of these alternate theories.

ACKNOWLEDGEMENTS

This work was supported by grants GM56695 (D.L.P) and GM53989 (A.D.) from the National Institutes of Health. We thank Madan Paidhungat, Peter and Barbara Setlow, and Patrick Stragier for providing strains, David Nelson and Kevin Young for advice on the use of ^{125}I-penicillin X, Jennifer Meador-Parton and Amy Weaver for technical assistance, and Marita Seppanen Popham for editing of the manuscript.

Chapter 3

Peptidoglycan Synthesis in the Absence of Class A Penicillin-Binding Proteins in *Bacillus subtilis*

McPherson, Derrell C. and David L. Popham. 2003. J. Bacteriol. **185** (4):1423-1431.

ABSTRACT

Penicillin-binding proteins (PBPs) catalyze the final, essential reactions of peptidoglycan synthesis. Three classes of PBPs catalyze either trans-, endo-, or carboxy-peptidase activities on the peptidoglycan peptide side chains. Only the Class A high-molecular weight PBPs have clearly demonstrated glycosyl transferase activities that polymerize the glycan strands, and in some species these proteins have been shown to be essential. The *Bacillus subtilis* genome sequence contains four genes encoding Class A PBPs and no other genes with similarity to their glycosyl transferase domain. A strain lacking all four Class A PBPs has been constructed and produces a peptidoglycan wall with only small structural differences from that of the wild type. The growth rate of the quadruple mutant is much slower than those of strains lacking only three of the Class A PBPs, and increases in cell length and frequencies of wall abnormalities were noticeable. The viability and wall production of the quadruple mutant strain indicates that a novel enzyme can perform the glycosyl transferase activity required for peptidoglycan synthesis. This activity was demonstrated *in vitro* and shown to be sensitive to the glycosyl transferase inhibitor moenomycin. In contrast, the quadruple mutant strain was resistant to moenomycin *in vivo*. Exposure of the wild type strain to moenomycin resulted in production of a phenotype similar to that of the quadruple mutant.

INTRODUCTION

The structural element of the bacterial cell wall is peptidoglycan (PG), and the importance of this structure is apparent in the number of antimicrobial agents targeting its components and the enzymatic reactions leading to its synthesis. The glycosyl transferase (GT) activity carrying out one of the final enzymatic reactions in PG synthesis is an attractive target because the enzymes performing that activity are highly conserved and believed to be essential (32, 34). PG is composed of glycan strands cross-linked by peptide side-chains. The glycan strands are synthesized by a GT that adds lipid-linked disaccharide pentapeptide subunits to nascent glycan strands. The pentapeptides are then utilized by a transpeptidase to cross-link adjacent glycan strands (reviewed in (8). Most of the proteins involved in these final enzymatic reactions are penicillin-binding proteins (PBPs), which are divided into three classes based on the presence of conserved functional domains (32, 34). Only the Class A PBPs have an N-terminal domain that contains the conserved amino acid sequences found in all GTs clearly demonstrated to polymerize PG. Class B PBPs have a different N-terminal domain; and although some researchers have associated GT activity with Class B PBPs (45), others have been unable to reproduce those results (2). Both classes have C-terminal penicillin-binding domains containing the transpeptidase activity that cross-links peptide side-chains. Some species also have mono-functional glycosyl transferases (MGTs) that contain the conserved amino acid sequences found in the Class A PBP GT domain but which lack a penicillin-binding domain (27, 112, 135).

The fact that many species contain multiple Class A PBPs (34) and that removal of one or more of those proteins results in little or no effect on PG polymerization or cell viability demonstrates their functional redundancies (26, 65, 95). However, a function of Class A PBPs has been demonstrated to be essential in both *Escherichia coli* and *Streptococcus pneumoniae*. Although loss of either PBP 1a or 1b from *E. coli* was tolerated, loss of both was lethal, even in the presence of PBP1c and an MGT (26, 143). A similar result was seen in *S. pneumoniae* where removal of PBPs 1a and 2a was lethal despite the presence of PBP1b and an MGT (42, 78). *Bacillus subtilis* has four Class A PBPs and no MGTs, as determined from sequence analysis of the *B. subtilis* genome (56). The genes *ponA*, *pbpD*, *pbpF*, and *pbpG* encode the Class A PBPs 1, 4, 2c, and 2d, respectively (65, 91, 93, 94). Construction of null mutations in each Class A PBP-encoding gene revealed that only loss of PBP1 resulted in phenotypic changes: a decrease in growth rate along with changes in cell morphology (65, 80, 95) and PG structure (9). The growth rate and morphological changes were more pronounced in strains lacking PBPs 1 and 4 (95), and a strain lacking PBPs 2c and 2d was unable to properly construct spore PG (65). However, strains lacking any three of the four Class A PBPs were viable (65).

In this communication, we demonstrate that a *B. subtilis* strain lacking all four Class A PBPs is viable and produces PG of relatively normal structure. Phenotypic and morphological changes in the quadruple mutant are greater than those noted in the single PBP1 and triple mutants. The glycosyl transferase activity present in the quadruple mutant is demonstrated *in vitro* and shown to be sensitive to moenomycin. Finally, we

show that the quadruple mutant is resistant to high concentrations of moenomycin *in vivo* while exposure of the wild type strain causes phenotypic changes similar to those of the quadruple mutant.

METHODS AND MATERIALS

Bacterial growth and transformation. All strains of *B. subtilis* listed in Table 3.1 were derivatives of strain 168. Natural transformation was performed as previously described (3). Transformants were selected and maintained using appropriate antibiotics: spectinomycin (100 µg/ml), kanamycin (10 µg/ml), and erythromycin (0.5 µg/ml) plus lincomycin (12.5 µg/ml, macrolide-lincosamide-streptogramin B resistance). Cultures were grown with shaking at 37˚C in 2xSG medium (59) without antibiotics except where noted. Membranes were prepared from vegetative *B. subtilis* cultures at OD_{600} of 0.5 as previously described (91). PBPs were labeled using ^{125}I-penicillin-X and detected as previously described (65).

Plasmid construction. A 1,189 bp *Hinc*II – *Eco*RV fragment containing the downstream end of *ponA* and an inversely oriented gene, *ypoC*, was cloned into the *Hinc*II site of pUC19 to create pDPC254. This plasmid was then digested with *Cla*I, treated with the Klenow fragment of DNA polymerase to blunt the ends, and ligated with a 1,193 bp *Eco*RV – *Hinc*II fragment from pDG1726 (37) containing a spectinomycin resistance gene. This ligation resulted in two plasmids, pDPV43 and pDPV44, in which the spectinomycin gene was inserted in opposite directions. pDPV43 and pDPV44 were used to transform PS832 with selection for spectinomycin resistance to construct

Table 3.1. *B. subtilis* strains used

Strain	Genotype[a]	Transformation		Source of reference
		Donor	Recipient	
DPVB42	Δ*pbpD*	DPVB30	DPVB40	(65)
DPVB45	Δ*pbpG*::Kn	pDPV35	PS832	(65)
DPVB46	Δ*pbpD* Δ*pbpF*::Erm^r	PS1869	DPVB42	(65)
DPVB49	Δ*pbpD* Δ*pbpG*::Kn Δ*pbpF*::Erm^r	DPVB45	DPVB46	(65)
DPVB56	Δ*pbpG*::Kn Δ*pbpF*::Erm^r	DPVB45	PS1869	(65)
DPVB57	Δ*pbpD* Δ*pbpG*::Kn	DPVB45	DPVB42	(65)
DPVB61	Δ*ponA*::Sp Δ*pbpG*::Kn	PS2062	DPVB45	(65)
DPVB62	Δ*ponA*::Sp Δ*pbpD* Δ*pbpG*::Kn	PS2062	DPVB57	(65)
DPVB63	Δ*ponA*::Sp Δ*pbpG*::Kn Δ*pbpF*::Erm^r	PS2062	DPVB56	(65)
DPVB66	Sp downstream of and opposing *ponA*	pDPV43	PS832	This work
DPVB67	Sp downstream of *ponA* and opposing *ypoC*	pDPV44	PS832	This work
DPVB68	Δ*ponA*::Sp Δ*pbpD*	PS2062	DPVB42	(65)
DPVB69	Δ*ponA*::Sp Δ*pbpD* Δ*pbpF*::Erm^r	PS2062	DPVB46	(65)
DPVB87	Δ*ponA*::Sp Δ*pbpD* Δ*pbpF*::Erm^r Δ*pbpG*::Kn	PS2062	DPVB49	This work
DPVB88	Δ*ponA*::Sp Δ*pbpD* Δ*pbpF*::Erm^r Δ*pbpG*::Kn	PS2062	DPVB49	This work
PS832	Prototrophic revertant of strain 168			Laboratory stock
PS1869	Δ*pbpF*::Erm^r	pDPC89	PS832	(93)
PS2062	Δ*ponA*::Sp	pDPC197	PS832	(91)
PS2061	Δ*prfA*::Sp	pDPC195	PS832	(91)
PS2251	Δ*ponA*::Sp Δ*pbpF*::Erm^r	PS2062	PS1869	(95)

[a] Abbreviations: Erm^r, resistance to erythromycin and lincomycin; Sp, resistance to spectinomycin; Kn, resistance to kanamycin.

DPVB66 and DPVB67, respectively, in which the plasmids inserted into the chromosome via a single cross-over. This placed the spectinomycin resistance marker downstream of *ponA*, which had no effect on growth (data not shown).

PCR and Southern blot analysis. PCR was used to demonstrate the presence of wild type and mutant alleles of Class A PBP-encoding genes. All nucleotide positions correspond to the coding sequences reported in the *B. subtilis* genome sequence (56) and on the SubtiList web site (http://genolist.pasteur.fr/SubtiList/). Primers located from 645 – 621 bp upstream of *ponA* and from 2,725 bp within *ponA* to 6 bp downstream produced PCR products of 3,396 bp from wild type *ponA* and 2,970 bp from Δ*ponA*::Sp. Primers located from 53-75 bp within *pbpD* and from 1,855 bp within *pbpD* to 7 bp downstream produced PCR products of 1,824 bp from wild type *pbpD* and 342 bp from Δ*pbpD*. Primers located from 11 bp upstream to 9 bp within *pbpF* and 2,136 bp within *pbpF* to 10 bp downstream produced PCR products that were subsequently digested using *Pvu*II. Digestion resulted in fragment sizes of 1,068 and 1,098 bp from wild type *pbp*F and an uncut fragment size of 2,169 bp from the Δ*pbpF*::Erm. Primers located from 416 – 396 bp upstream of *pbpG* and from 191 – 210 bp downstream of *pbpG* produced PCR products that were subsequently digested using *Pvu*II. Digestion resulted in fragment sizes of 463, 498, and 1,600 bp from wild type *pbpG* and an uncut fragment size of 2,461 bp from the Δ*pbpG*::Kn.

Two probes were used to verify the presence of each wild type and mutant allele by Southern blotting (Figure 3.1). For each gene, one probe was complementary to a sequence within the deleted region and the other probe was complementary to a sequence

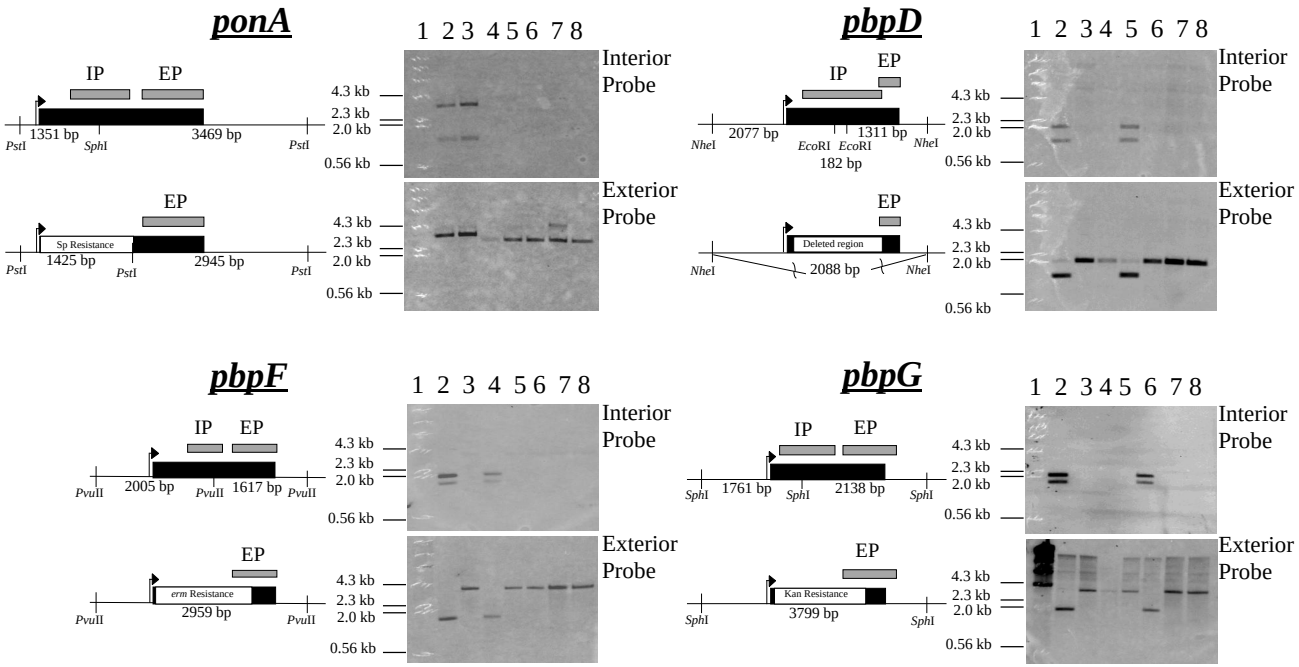

Figure 3.1. Southern blots of Class A PBP-encoding genes. Lanes contain digested chromosomal DNA from the following strains: 2, wild type; 3, *pbpD pbpF pbpG*; 4, *ponA pbpD pbpG*; 5, *ponA pbpF pbpG*; 6, *ponA pbpD pbpF*; 7, *ponA pbpD pbpF pbpG* (DPVB87); 8, *ponA pbpD pbpF pbpG* (DPVB88); or 1, *Hind*III digested Lambda DNA. Drawings are made to scale and show both wild type and mutant genes with black boxes indicating the coding regions and white boxes indicating antibiotic resistance cassette insertions and/or deleted regions. Relevant restriction sites and fragment sizes are indicated below the diagrams. Shaded boxes indicate the positions where the interior (IP) and exterior (EP) probes are expected to hybridize to each allele. The light band visualized at approximately 4.3 kb in lane 7 of the *ponA* Southern using the exterior probe is apparently due to incomplete digestion resulting in a fragment size of 4,370 bp.

at the 3' end of the gene. For *ponA*, the interior probe was complementary to bases 535 – 1,449 and the exterior probe was complementary to bases 1,769 – 2,745 of the coding sequence. For *pbpD*, the interior probe was complementary to bases 270 – 1,621 and the exterior probe was complementary to bases 1,591 within *pbpD* to 6 bp downstream of the coding sequence. For *pbpF*, the interior probe was complementary to bases 629 – 1,237 and the exterior probe was complementary to bases 1,447 within *pbpF* to 10 bp downstream of the coding sequence. For *pbpG*, the interior probe was complementary to bases 164 – 1,105 and the exterior probe was complementary to bases 1,251 within *pbpG* to 210 bp downstream of the coding sequence. Probes were prepared by restriction digestion of PCR products obtained from either wild type chromosomal DNA (*ponA*, *pbpF*, and *pbpG*) or plasmid DNA (pDPC142, *pbpD* (94)) using the primers described above followed by isolation of the desired fragments from agarose gels. Probes were labeled and detected using the ECF Random Prime Labeling and Signal Amplification System (Amersham Pharmacia Biotech) and a STORM 860 phosphorimager and ImageQuant software (Molecular Dynamics).

Microscopy. For electron microscopy, 10 ml samples from *B. subtilis* cultures grown to an OD_{600} of 0.5 were centrifuged at 5000 x g for 5 min. at 4˚C. Cell pellets were suspended in 840 µl of 0.5 M $NaPO_4$ (pH 7.0) plus 50 µl of 25% EM grade glutaraldehyde (Sigma) and held at 4˚C overnight. Cells were washed 4 times in cold 0.1 M $NaPO_4$ (pH 6.7), suspended in 1% osmium in phosphate buffer, and held at 4˚C overnight. Cells were washed in 0.5 M NH_4Cl and then suspended and pelleted in 2% agar. Dehydration was performed at 30%, 50%, 70%, 95% and 100% ethanol, then in a

1:1 solution of ethanol and Spurr's resin overnight. Samples were then suspended in 100% Spurr's resin overnight before being cured. Samples were sectioned, placed on 200 mesh copper grids, and stained with 1% uranyl acetate for 12 min and Reynold's lead for 5 min. Samples were viewed using a JEOL 100 CX-II Transmission Electron Microscope at an accelerating voltage of 80 kV.

Samples for fluorescence and phase-contrast microscopy were prepared by growing cultures to an OD_{600} of 0.5 for vegetative cultures or for 2.5 and 24 hours following exposure to 80 µg/ml moenomycin. For fluorescence microscopy, cells were pelleted from 0.5 ml of culture, resuspended in 200 µl TE buffer (10 mM Tris HCl, pH 7.5 and 1 mM EDTA), and applied to a poly-L-lysine-coated coverslip. Staining was performed as described (84). The coverslip was placed on a slide spotted with 10 µg/ml FM4-64 [*N*-(3-triethylammoniumpropyl)-4-(6-(4-(diethylamino)phenyl)hexatrienyl)pyridinium dibromide] and 2 µg/ml DAPI (4',6-diamidino-2-phenylindole, dihydrochloride) in either TE buffer or Slow Fade® (all stains and Slow Fade® Antifade Kit were obtained from Molecular Probes). Cells were visualized using a Nikon Microphot-SA microscope equipped with a UV-1B cube (DAPI) and a G-ZA cube (FM4-64) using a Nikon Fluor 100X/1.30 objective. Images were collected with a DAGE-MTI CCD100 video camera and DAGE InstaGater and pseudocolored using ISEE software (Inovision Inc.) on a Silicon Graphics O2 computer. For phase-contrast microscopy, cells were pelleted from 0.5 ml of culture and fixed in 0.5 ml 4.4% paraformaldehyde and 0.01% glutaraldehyde in 28 mM $NaPO_4$ (pH 7.0) for 15 min at room temperature and 30 min on ice. Cells were washed twice in 0.5 ml TE buffer

and resuspended in 50 µl TE buffer. Cells were visualized using an Olympus Provis AX70 microscope equipped with an Olympus UPlanF1 100X/1.30 Oil Ph3 objective. Images were collected using a Colorview 12 video camera and Olympus MicroSuite ™-B3 software. Fluorescence and phase-contrast images were transferred to a Macintosh G4 computer and processed for publication using Adobe Photoshop version 4.0.1.

Determination of *in vivo* moenomycin sensitivity. Samples from cultures grown to an OD_{600} of 0.5 were diluted 100-fold in 2xSG and plated in the presence of various concentrations of moenomycin (Intervet, Inc.). Colony number and morphology were examined after incubation at 37°C for 24 hours. The effects of moenomycin exposure to cells grown in liquid culture were examined by growing each strain to an OD_{600} of 0.5 prior to adding moenomycin. Incubation was continued and, at various time points, samples were diluted in 2xSG and plated on LB agar lacking moenomycin.

Peptidoglycan analysis. Cultures (100 ml) were grown to an OD_{600} of 0.5, chilled by swirling in ice water for 5 min, and centrifuged at 15,000 x g for 10 min at 4˚C. Pellets were suspended in 2 ml of 4˚C water, added drop wise to 50 ml of boiling 4% SDS, and boiled for 30 min. Suspensions were allowed to cool, centrifuged at 12,000 x g for 10 min at room temperature, and washed with water until free of SDS. Pellets were suspended in 1 ml of 100 mM Tris HCl (pH 7.5) and incubated with 100 µg of α-amylase (Sigma) at 37˚C for 2 hours. DNase I (10 µg), RNase A (50 µg), and $MgSO_4$ (20 mM) were added and incubation was continued at 37˚C for 2 hours. Trypsin (100 µg) and $CaCl_2$ (10 mM) were added and incubation was at 37˚C overnight. SDS was added to 1% and the solution was boiled for 15 min, diluted into 7 ml of water, and then

centrifuged at 12,000 x g for 10 min at 20˚C. The pellet was suspended and washed twice in 8 ml of water, once in 8 M LiCl, and twice more in water. The pellet was then lyophilized, suspended in 1 ml of 49% hydrofluoric acid, and rocked for 48 hours at 4˚C to remove teichoic acids. The peptidoglycan was collected by centrifugation at 13,000 x g for 5 min and washed 3 times with water. The pellet was then suspended in 1 ml of 100 mM NH_4HCO_3, and incubated with 5 units of calf intestinal alkaline phosphatase (Promega) at 37˚C overnight. The sample was boiled for 5 min, centrifuged at 13,000 x g for 15 min, and washed three times with water. Muramidase digestion of the peptidoglycan, reduction of the soluble muropeptides, and high-pressure liquid chromatography (HPLC) separation of muropeptides was performed as previously described (9). Muropeptide identification was performed by amino acid analysis (36) and matrix-assisted laser desorption ionization time-of-flight mass spectrometry (MALDI-TOF MS) using a Kratos Analytical Kompact SEQ instrument and software.

Glycosyl transferase activity. Cultures were grown to an OD_{600} of 0.5 in 1% tryptone, 0.5% yeast extract, 0.25% K_2HPO_4 (pH 7.3) with glucose added to a final concentration of 0.1% just before use (97). Cultures were centrifuged at 9,000 x g for 10 min at room temperature. Protoplasts were produced essentially as described by Taku and Fan (120). Briefly, the pellet was suspended in 20 ml of Buffer A (50 mM Tris HCl (pH 7.5), 20 mM $MgCl_2$, 15% sucrose) plus 1.25 mg/ml lysozyme and incubated at 37˚C for 1 hour. Protoplasts were pelleted at 9,000 x g for 10 min at 4˚C then washed twice more with 10 ml of Buffer A. The final protoplast pellet was then suspended in 2.5 ml of

Buffer B (50 mM Tris HCl (pH 7.5), 20 mM $MgCl_2$, 13% sucrose) and the protein content was determined using the Lowry assay (60).

Protoplasts containing 18 µg protein were incubated for 2 hours at 37˚C with 3 nmol UDP-N-acetyl-muramic acid-pentapeptide and 5.64 nmol UDP-N-acetyl-D-[U-^{14}C]glucosamine (266 mCi/mmol, Amersham Pharmacia Biotech) in a total volume of 40 µl of 50 mM Tris HCl (pH 7.5),10 mM $MgCl_2$, 6.5% sucrose. UDP-N-acetyl-muramic acid-pentapeptide was prepared from *B. subtilis* cultures as previously described (61, 79). Reactions were stopped by heating at 95˚C for 5 min. When used, lysozyme (2 mg/ml) or moenomycin (16 µg/ml) was added at the start of the reaction. Reactions were spotted on thick chromatography paper (Fisher Scientific) and separated using ascending paper chromatography with isobutyric acid and 1 M NH_4OH (5:3) for 12 hours (100). During solvent migration, polymerized PG remained at the origin while the free precursors migrated away from the origin. Chromatogram signal intensities were integrated using a STORM 860 phosphorimager and ImageQuant software (Molecular Dynamics).

RESULTS

Construction and verification of a *ponA pbpD pbpF pbpG* mutant. Each mutation in a Class A PBP-encoding gene was a deletion that removed ≥ 57% of the coding sequence, including the five most highly conserved motifs of the N-terminal GT domains (34). The deleted regions in the *ponA*, *pbpF*, and *pbpG* alleles were replaced by antibiotic resistance cassettes, insuring that the C-terminal domains were not expressed. The *pbpD* mutation was an in-frame deletion removing 79% of the coding sequence,

which also included the penicillin-binding active site serine (65). Construction of the quadruple mutant was performed by transforming a *pbpD pbpF pbpG* triple mutant (DPVB49) (65) with limiting chromosomal DNA from a *ponA* mutant (PS2062). As controls, DPVB49 was transformed separately with limiting chromosomal DNA from PS2061 (Δ*prfA*::Sp^R), DPVB66 (Sp^R downstream of *ponA*), and DPVB67 (Sp^R downstream of *ponA*), and DPVB56 (*pbpF, pbpG*) was transformed with chromosomal DNA from PS2062. All the chromosomal DNA preparations used for the transformations were equal in concentration, and quadruple mutant transformants were obtained at approximately the same frequency as the strains produced in the control transformations. This indicates that the viability of the quadruple mutant was not dependent on the presence of any type of suppressor mutation. Two independent isolates (DPVB87 and DPVB88) of the quadruple mutant were selected for further analysis.

Due to the unexpected result that the quadruple mutant was viable, the presence of each mutation was verified using both PCR and Southern blot analysis (Fig. 3.1). For the Southern blot analysis, two probes were utilized for each gene. One probe was complementary to a sequence interior to the deletion whereas the second probe was complementary to a sequence exterior to the deleted region. The probes complementary to a sequence exterior to a deleted region verified the presence of each wild type or mutant allele. The probe interior to the deleted region of each gene verified the presence or absence of that complementary sequence, indicating that the wild type sequence had not appeared elsewhere in the chromosome via some non-homologous recombination event. We demonstrated the absence of Class A PBPs 1, 2c, and 4 from the respective

strains using ^{125}I-labeled penicillin X (Fig. 3.2). PBP2d is not highly expressed during vegetative growth (82) and is therefore not visualized in the PBP profile of vegetative cultures. We found that the band intensities of PBPs 2c, 3, and 4 did not change relative to each other in any strain; however, the band intensities of two Class B PBPs, 2a and 2b, did change in relation to each other and to PBP3. Quantitative analysis indicated that, relative to PBP3, expression of PBPs 2a and 2b increased 51% (±17%, n=3) and 22% (±12%, n=3), respectively, in strains lacking PBP1, and more so in strains lacking PBPs 1 and 4, 87% (±31%, n=9) and 52% (±19%, n=9), respectively. We can not formally exclude the possibility that PBPs 2c, 3, and 4 are all decreasing under these conditions. However, we feel that their relative stability and the differential changes in the PBPs 2a and 2b are suggestive of increases in the latter two. This is consistent with a previous observation that PBP2a expression appeared to be elevated in strains lacking PBP1 and either PBP2c or PBP4 (95).

Growth and morphology of the *ponA pbpD pbpF pbpG* mutant strains. Doubling times of the quadruple mutant strains were 62 and 63 min (Table 3.2). This is three-fold slower than the doubling times of the wild type strain and the triple mutant lacking PBPs 2c, 2d, and 4 and two-fold slower than the triple mutants lacking PBP1 (65, 95)]. The fact that the quadruple mutant grows slower than the triple mutant lacking PBPs 1, 2c, and 4, suggests that, unlike the situation in the wild type (82), in this triple mutant PBP2d may be expressed during vegetative growth. When samples of quadruple mutant cultures were plated, colonies of various sizes arose. However, subsequent streaking of those various-sized colonies resulted in uniform colony sizes from all, and

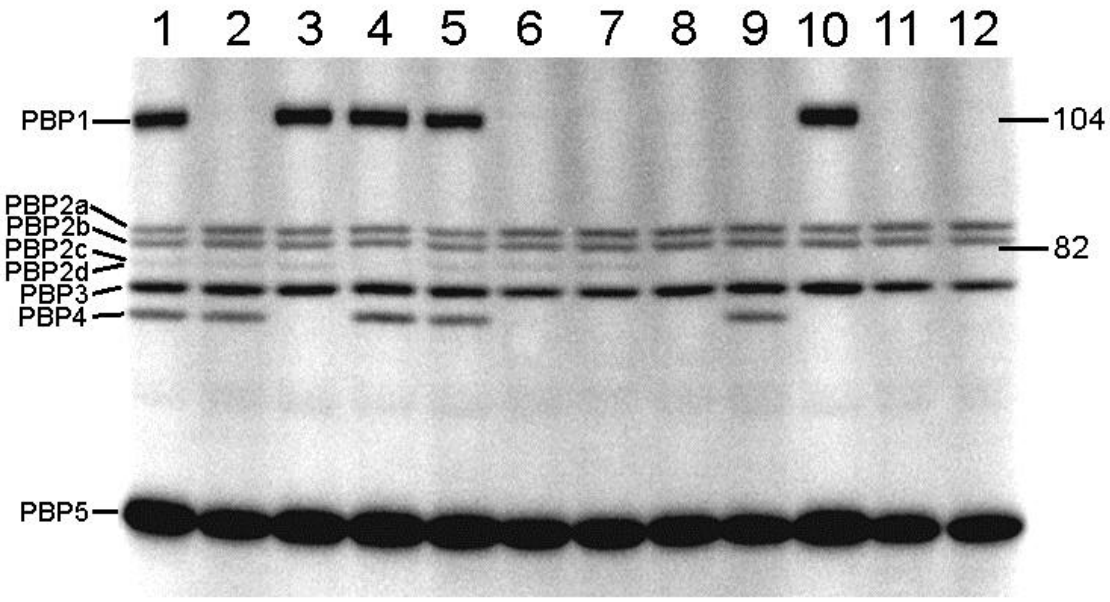

Figure 3.2. PBP profiles of various Class A PBP mutant strains of *B. subtilis*. Membranes were purified from exponentially growing cultures at an OD_{600} of 0.5 and incubated with ^{125}I-labeled penicillin X. Proteins were separated on a SDS-7.5% PAGE gel and PBPs were detected using a phosphoimager. Strains and PBPs expected to be lacking: Lane 1, PS832, wild-type; lane 2, PS2062, PBP1; lane 3, DPVB42, PBP4; lane 4, PS1869, PBP2c; lane 5, DPVB45, PBP2d; lane 6, DPVB68, PBPs 1 and 4; lane 7, DPVB62, PBPs 1, 2d, and 4; lane 8, DPVB69, PBPs 1, 2c, and 4; lane 9, DPVB63, PBPs 1, 2c, and 2d; lane 10, DPVB49, PBPs 2c, 2d, and 4; lane 11, DPVB87, PBPs 1, 2c, 2d and 4; lane 12, DPVB88, PBPs 1, 2c, 2d, and 4. The positions of molecular mass standards (Bio-Rad) are indicated on the right in kilodaltons.

Table 3.2. Growth rates of Class A PBP mutant strains[a]

Strain	PBP Phenotype	Doubling time[b] (min)
PS832	Wild type	20
PS1869	PBP2c$^-$	20
DPVB42	PBP4$^-$	20
DPVB45	PBP2d$^-$	20
PS2062	PBP1$^-$	25
DPVB49	PDP2c$^-$, PBP2d$^-$, PBP4$^-$	21
DPVB63	PBP1$^-$, PBP2c$^-$, PBP2d$^-$	28
DPVB69	PBP1$^-$, PBP2c$^-$, PBP4$^-$	28
DPVB62	PBP1$^-$, PBP2d$^-$, PBP4$^-$	31
DPVB87	PBP1$^-$, PBP2c$^-$, PBP2d$^-$, PBP4$^-$	62
DPVB88	PBP1$^-$, PBP2c$^-$, PBP2d$^-$, PBP4$^-$	63

[a] Growth was in liquid 2xSG medium at 37˚C.
[b] Doubling times are averages from at least three separate experiments.

growth in liquid medium revealed uniform growth rates (data not shown). These results suggest that suppressor mutations were not appearing at a high frequency in these quadruple mutant strains. We believe that the variations in colony size resulted from a wide variation in cell size (see below) in the liquid cultures. A filamentous cell with >5 times the mass of a cell of wild type dimensions could rapidly divide under the slower growing conditions on a plate. A colony resulting from a large cell could therefore be significantly larger than that derived from a smaller cell. Size variation was less pronounced among the slower-growing cells within a colony, resulting in more uniform colony size upon re-streaking.

As previously described (54, 80, 95), *B. subtilis* strains lacking PBP1 grew slowly, had a smaller cell radius, and their cultures contained a population of cells that were slightly longer, bent, and multi-nucleoid. The cell length and bending was more pronounced in a larger number of PBP1$^-$, 4$^-$ cells, and were even more pronounced in the PBP1$^-$, 2c$^-$, 4$^-$ strain (95). Using phase-contrast microscopy, we noted a large variation in cell length among the populations of the quadruple mutant strains and many individual cells appeared even longer and more bent than any produced by the triple mutant strains (Fig. 3.3). Quantitative analysis of the cell lengths revealed that while many of the quadruple mutant cells were of normal length, 30% of the cells were significantly longer than the entire wild type population (Fig 3.4). Upon entry into stationary phase, the filamentous cells underwent division to produce a population of relatively homogenous length (Fig. 3.3E). Electron micrographs of the quadruple mutants also show long, bent, multi-nucleoid cells (Fig. 3.5). Measurements of laterally cross-sectioned cells indicate

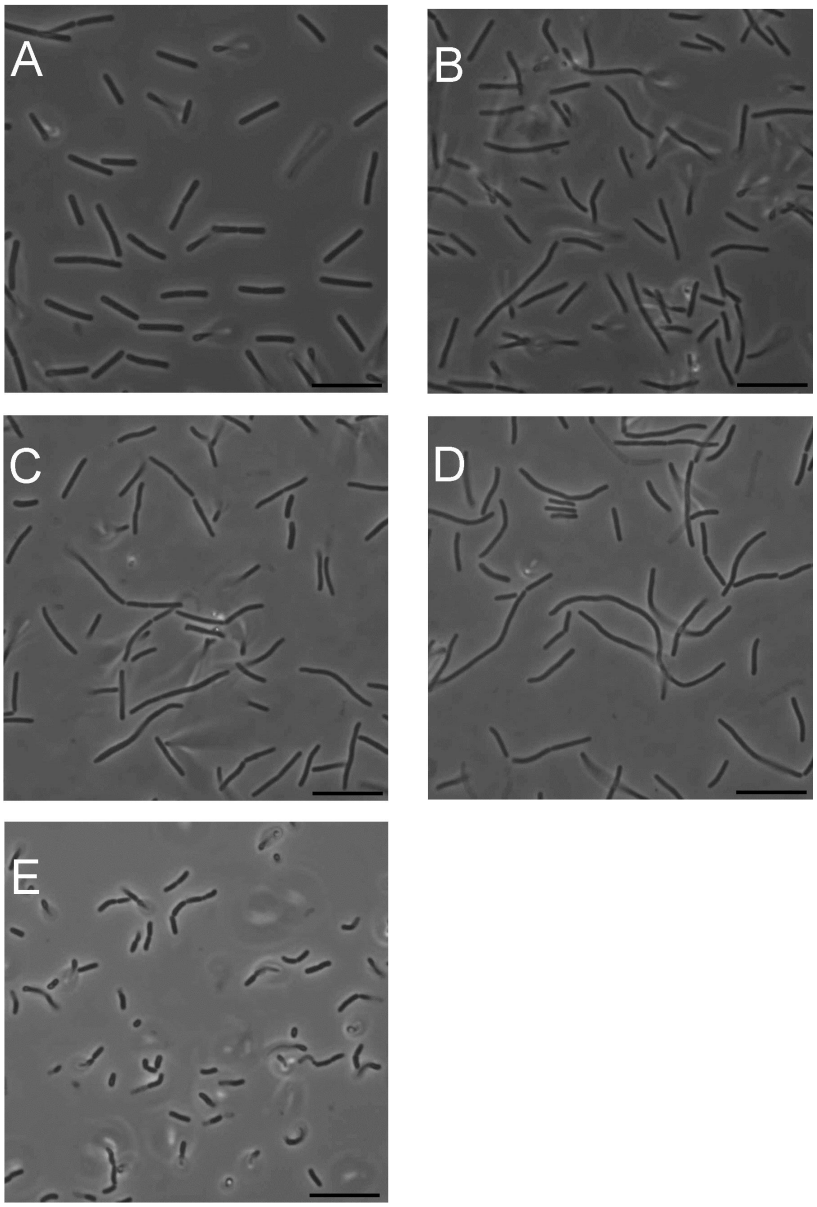

Figure 3.3. Phase-contrast microscopy of Class A PBP mutants. Cells were photographed from exponentially growing (A - D) and 24 hour (E) cultures of PS832 (wild type, A), PS2062 (PBP1$^-$, B), DPVB69 (PBP1$^-$, 2c$^-$, 4$^-$, C) and DPVB87 (PBP1$^-$, 2c$^-$, 2d$^-$, 4$^-$, D and E). Bars, 10 μm.

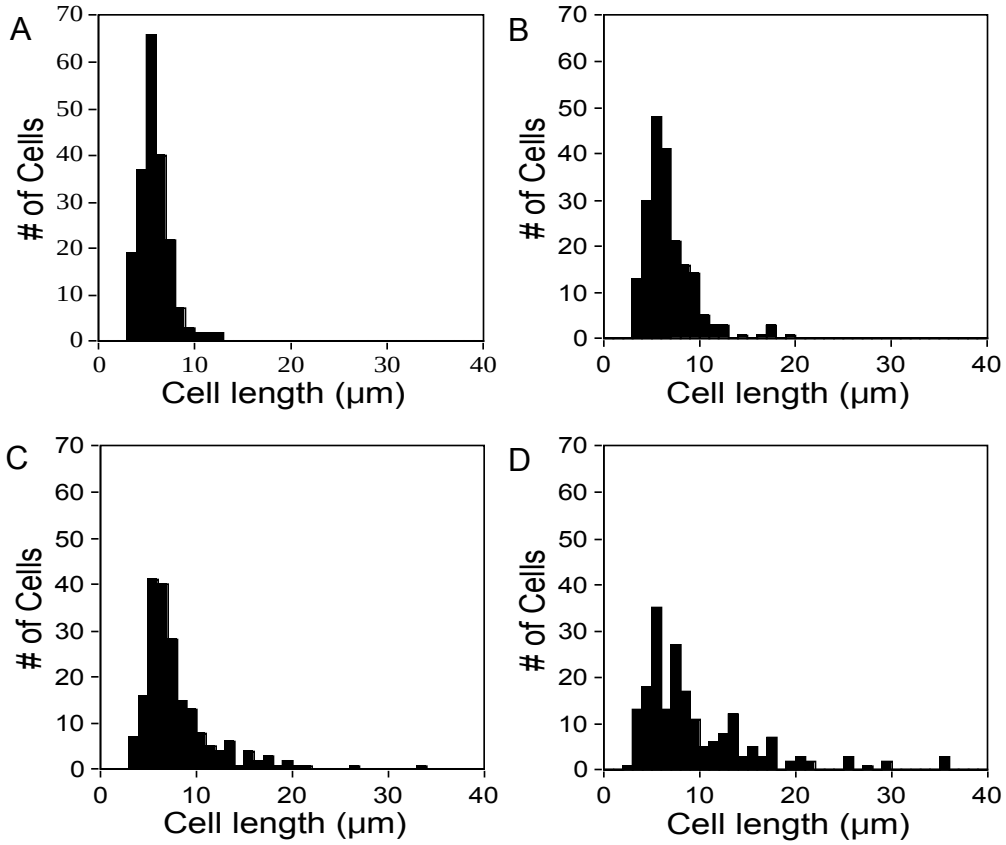

Figure 3.4. Cell length distributions of Class A PBP mutants. Cells were harvested from exponentially growing cultures and examined under phase-contrast microscopy. Cell lengths (n = 200 for each strain) were determined from digital images. (A) PS832 (wild type); (B) PS2062 (PBP1$^-$); (C) DPVB69 (PBP1, 2c, 4$^-$); (D) DPVB87 (PBP1, 2c, 2d, 4$^-$). In the wild type culture 3% of the cells were ≥10 μm. This increased to 9% in the PBP1$^-$ culture, 20% in the PBP1, 2c, 4$^-$ culture, and 33% in PBP1, 2c, 2d, 4$^-$ cultures.

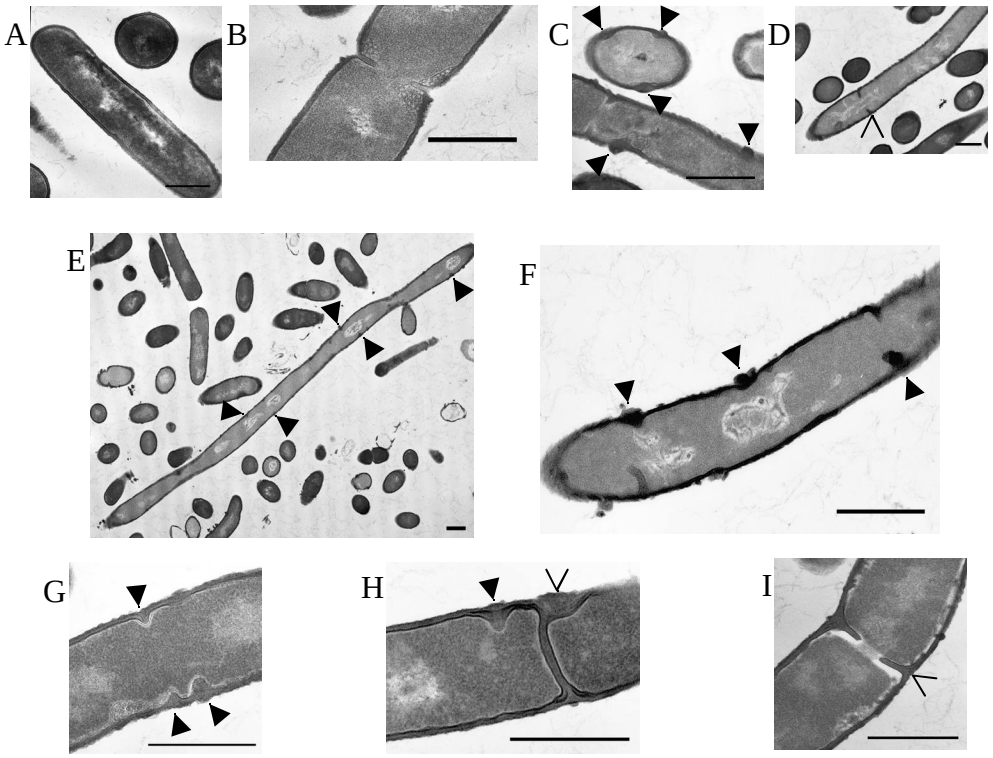

Figure 3.5. Electron microscopy of Class A PBP mutants. Cells obtained from exponentially growing cultures of PS832 (wild type, A and B), PS2062 (PBP1$^-$, C and D), and DPVB87 (PBP1$^-$, 2c$^-$, 2d$^-$, 4$^-$, E-I) were fixed, sectioned, and stained for transmission electron microscopy. Solid arrowheads in C, E, F, G, and H indicate abnormal cell wall material. Open arrowheads in H indicate irregularly formed septa and in D and I indicate septa impinging upon the chromosome. Bars, 0.5 μm.

that these cells had a reduced diameter, similar to that previously observed in a PBP1$^-$ strain (95). Relative to the wild type, the cell diameter decreased by 25% (±15%, n=384) in the PBP1$^-$ strain, by 21% (±11%, n=685) in the PBP1$^-$ 4$^-$ strain, and by 20% (±10%, n=527) in the quadruple mutant strains. This is consistent with earlier observations of narrow cell diameter in. It was previously noted that the PBP1$^-$ strain had wall material synthesized in aberrant masses along the cylindrical wall (80). We also noticed these formations (Fig. 3.5C and E through H), which appeared to occur more often in the PBP1$^-$, 2c$^-$, 2d$^-$, 4$^-$ strains, and some of these masses protruded into the cytoplasm (Fig. 3.5F through H). In some cases the positioning of these protrusions suggested that they are incomplete septa. Previously, strains lacking PBP1 were shown to have a defect in septation (80). Although the PBP1 and quadruple mutants contained some defects in septum formation (Fig. 3.5H), there were also many apparently normal septa. However, we observed a number of septa that appeared to impinge upon a chromosome (Fig. 3.5D and I).

Strains were prepared for fluorescence microscopy to further examine potential division septa irregularities upon loss of multiple Class A PBPs (Fig. 3.6). Staining with FM4-64, a membrane stain, showed irregular placement of what appeared to be division septa in all strains lacking at least PBP1 and was exacerbated in the quadruple mutant strains (Fig. 3.6Bi and Ci). In most cases, the chromosomes were segregated throughout the cell (Fig. 3.6Bii and Cii). However, many areas were visualized in which division septa appeared to be synthesized into an area of the cytoplasm containing DNA

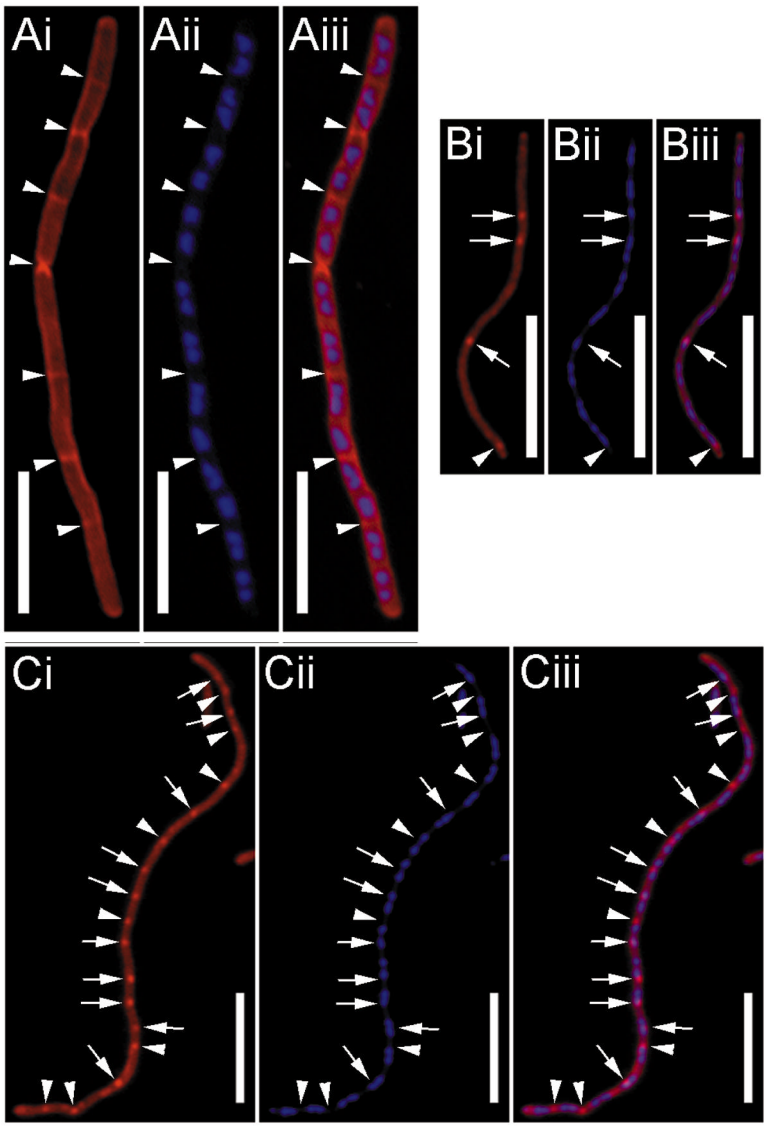

Figure 3.6. Fluorescent micrographs of wild type and Class A PBP null mutant strains. PS832 (wild type, A) and DPVB87 and DPVB88 (PBP1$^-$, 2c$^-$, 2d$^-$, 4$^-$, B and C) cells were obtained from exponentially growing cultures. A relatively rare filament within the wild type culture was chosen to demonstrate the regular placement of septa. For each set of pictures: i, FM4-64 staining; ii, DAPI staining; and iii, merged images of FM4-64 and DAPI staining. Arrowheads indicate potential division sites that are clear of chromosomal DNA and arrows are potential division sites that appear to be impinging upon the chromosome.

(Fig. 3.6B and C). Due to resolution restrictions, we were unable to differentiate division septa and those protrusions of cell wall material seen in the electron micrographs.

Growth and morphology in the presence of moenomycin. Moenomycin has previously been shown to specifically inhibit the GT activity performed by Class A PBPs (127) due to its structural similarity to the lipid II precursor (57). We tried to determine the minimal concentration needed to inhibit growth of *B. subtilis* strains by plating 10^5 bacteria in the presence of 1-16 µg/ml moenomycin (data not shown). For all strains containing PBP1 the number of colonies decreased approximately 100-fold as moenomycin increased from 0 to 16 µg/ml. As moenomycin increased from 0-8 µg/ml, the colony sized decreased, but on each plate the colonies were of uniform size. At 16 µg/ml moenomycin, approximately 1% of the colonies grew significantly faster than the others. Strains lacking PBP1 displayed a different phenotype. While colony number decreased with increasing moenomycin concentration, approximately 1000-fold from 0-16 µg/ml moenomycin, colony size did not change as much. At 16 µg/ml moenomycin, all the colonies were of uniform size and were as large as those on the 4 and 8 µg/ml plates. Comparison of the PBP1$^-$ strain to multiple mutants lacking additional Class A PBPs revealed that the multiple mutants displayed progressively fewer effects from exposure to the moenomycin. The quadruple mutant had only a 10-fold decrease in colony number between 0 and 16 µg/ml moenomycin and all the colonies on all the plates were of uniform size.

To determine the viability of cells grown in liquid medium containing moenomycin, cultures were grown to an OD_{600} of 0.5, at which time moenomycin was

added at concentrations of 16, 40, and 80 μg/ml. At various time points, samples were plated in the absence of moenomycin to determine viable counts. Wild type cultures entered a lag phase where the number of CFU remained constant for up to 4 hours depending on the concentration of moenomycin (Fig. 3.7A). The optical density of the culture exposed to 80 μg/ml moenomycin doubled during the first 30 min, but only increased 25% during the next 2 hours, and another 20% during the next 3 hours, suggesting that not only cell division but growth of the cells was impeded. Similar results were seen for Class A PBP mutant strains that contained PBP1 (data not shown). Growth of a quadruple mutant culture exposed to the same moenomycin concentrations was not affected (Fig. 3.7B). This also correlated with the optical density of the culture, which continued to increase at the same rate as that of the culture not exposed to the antibiotic. Again in this experiment, Class A PBP mutant strains lacking PBP1 exhibited a phenotype similar to that of the quadruple mutant (data not shown).

Cells exposed to 80 μg/ml moenomycin for 2.5 hours were observed using both phase-contrast and fluorescence microscopy. Phase-contrast microscopy showed that wild types cells became more filamentous and bent (Fig. 3.8A), a phenotype similar to what was seen in the quadruple mutant under normal growth conditions (Fig. 3.3D). These cells elongated by 2- to 8-fold, indicating that the increase in optical density corresponded to the increase in cell mass, but not cell division, which is consistent with the small change in CFU observed over that time period. Furthermore, irregularly spaced septa were visualized using fluorescence microscopy (data not shown). The quadruple mutant was largely unaffected by the presence of moenomycin. Figure 3.8C shows the

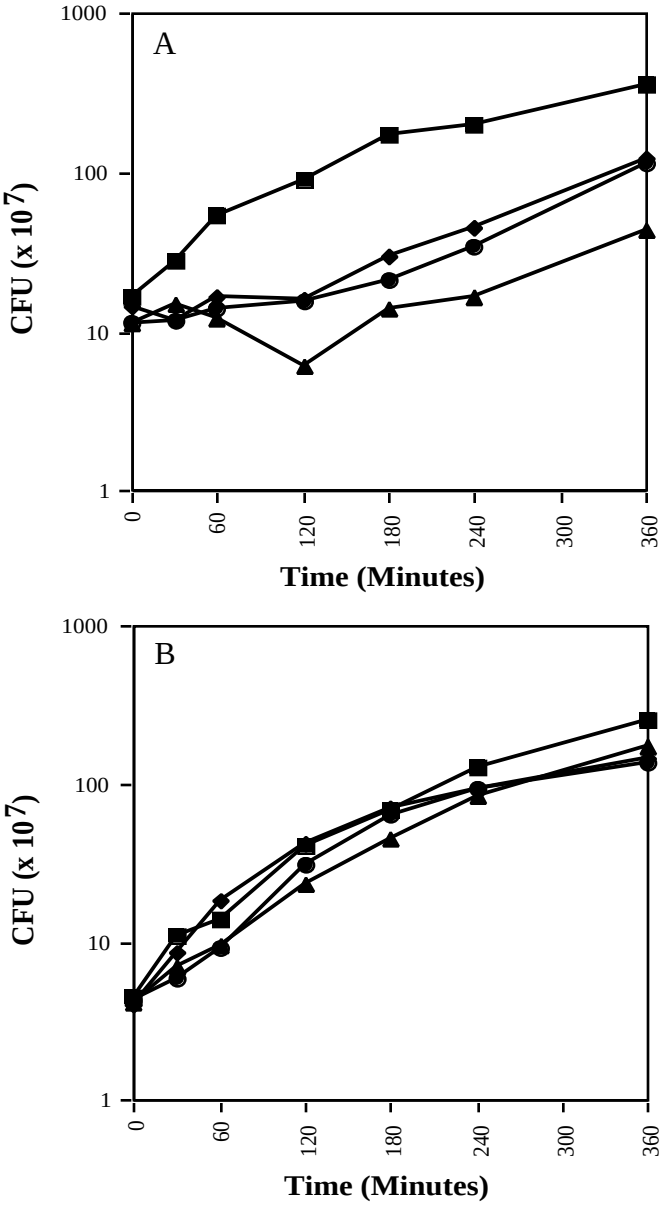

Figure 3.7. Effect of moenomycin on growth of *B. subtilis*. Cultures of PS832 (wild type, A) and DPVB87 (PBP1$^-$, 2c$^-$, 2d$^-$, 4$^-$, B) were exposed to either 0 (■), 16 (●), 40 (◆), or 80 (▲) µg/ml moenomycin. CFU values are averages from three separate experiments. Moenomycin was added when the OD reached 0.5. At this culture density, growth of the wild type strain had begun to slow, reducing the difference between the growth rates of the wild type and quadruple mutant strains.

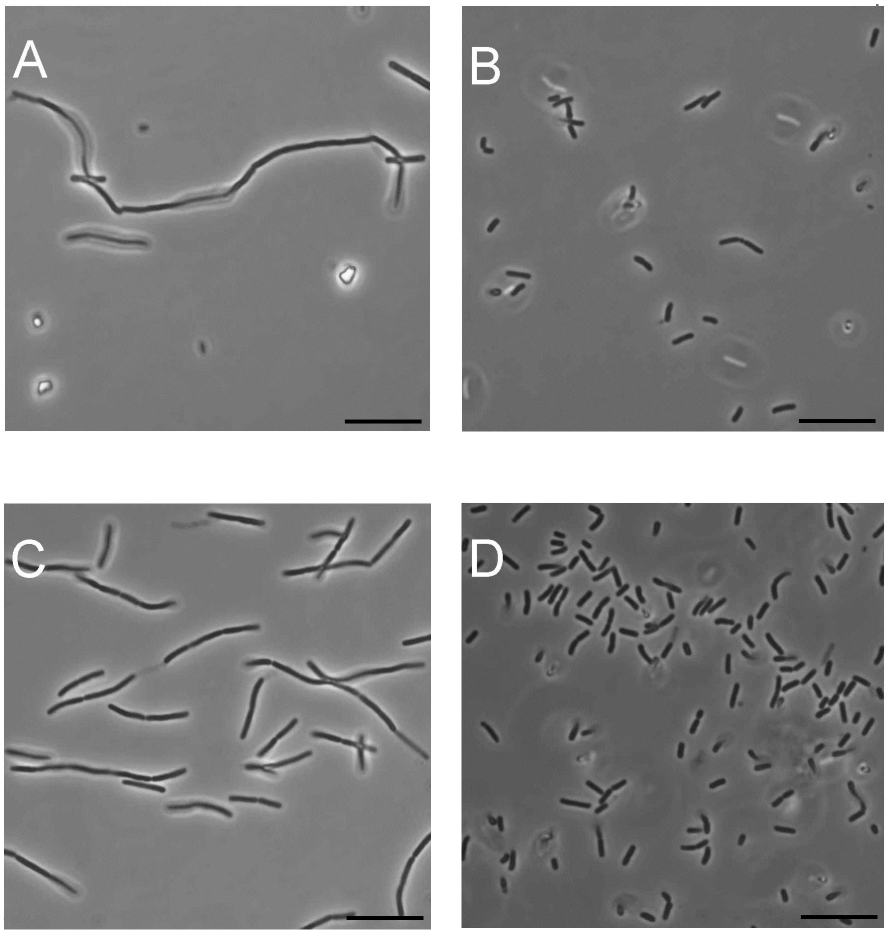

Figure 3.8. Effect of moenomycin on morphology of *B. subtilis.* PS832 (wild type, A and B) and DPVB87 (PBP1^{-}, 2c^{-}, 2d^{-}, 4^{-}, C and D) cells were exposed to 80 µg/ml moenomycin for 2.5 hours (A and C) and 24 hours (B and D) and examined by phase-contrast microscopy. Bars, 10 µm.

general population of the quadruple mutant cells may be slightly more filamentous than when grown in the absence of moenomycin (Fig. 3.3D). After exposure to moenomycin for 4-6 hours, cells from both the wild type and the quadruple mutant cultures began to shorten (data not shown). At 24 hours following exposure to moenomycin, the cell populations from both wild type (Fig. 3.8B) and quadruple mutant (Fig. 3.8D) strains had shortened, similar to what was seen in a 24 hour culture of the quadruple mutant in the absence of moenomycin (Fig. 3.3E).

Structural analysis of vegetative PG from wild type and Class A PBP mutant strains. Atrih et al (9) found that PG from exponentially growing wild type *B. subtilis* cells was cross-linked by 29% of the peptide side chains and that cross-linking decreased in strains lacking PBP1. Muropeptides are separated using reversed phase-high pressure liquid chromatography (RP-HPLC) (Fig. 3.9) and have been previously identified (Table 3.3) by Atrih (9). Our analysis of PG from our exponentially growing wild type strain demonstrated that 26% of the muramic acid residues had peptides involved in cross-linking (Table 3.4). This percentage decreased to 24% in strains lacking at least PBP1 and 22% in all strains lacking at least PBPs 1 and 4 including both quadruple mutant strains (Table 3.4).

***In vitro* glycosyl transferase activity of the PBP1$^-$, 2c$^-$, 2d$^-$, 4$^-$ strain.** An *in vitro* glycosyl transferase assay was used to demonstrate this activity in protoplasts of the wild type, PBP1$^-$, PBP1$^-$ 4$^-$, and all triple and quadruple mutant strains. As observed previously, we were unable to detect GT activity in purified *B. subtilis* membrane preparations (97). Protoplasts, prepared in an isotonic sucrose solution, were mixed with

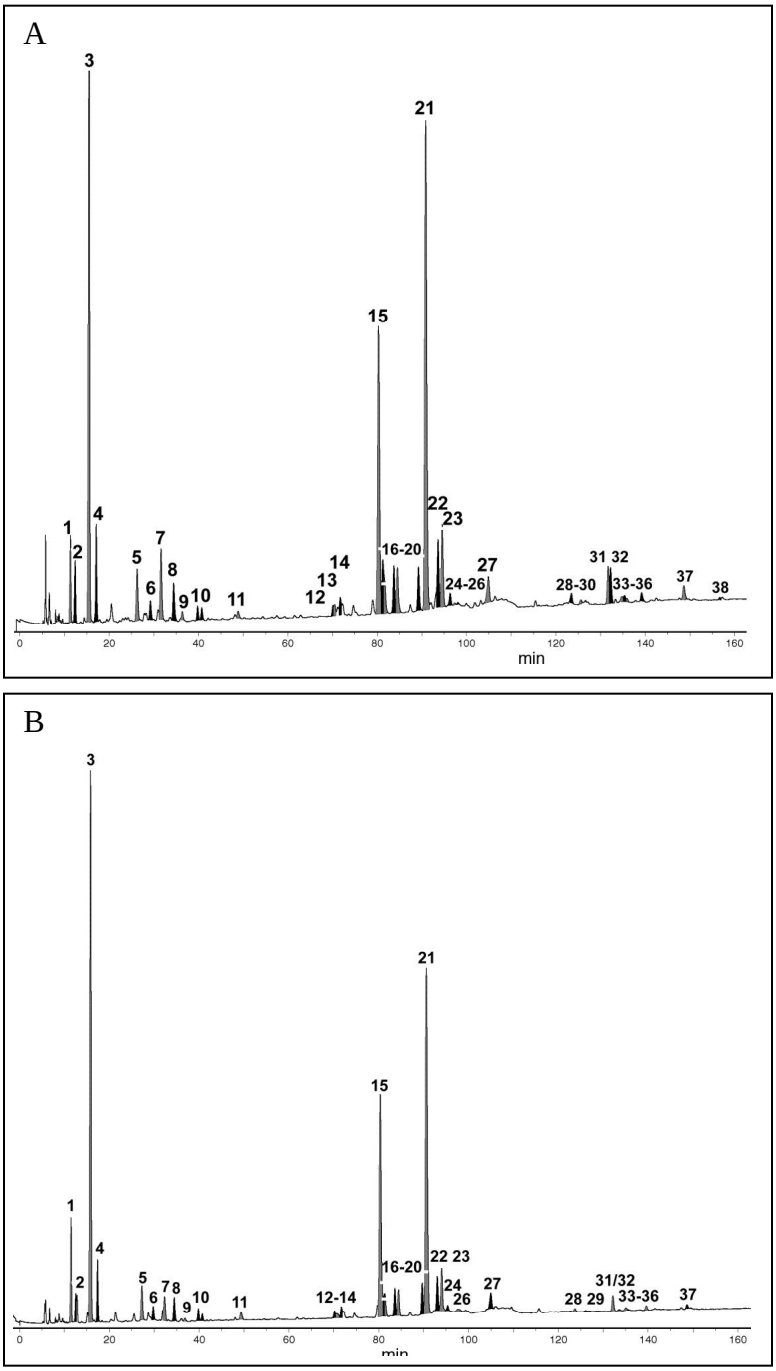

Figure 3.9. PG structure of a *B. subtilis* mutant lacking Class A PBPs. Muropeptides were prepared from vegetative cell PG of wild type (A) and PBP1$^-$, 2c$^-$, 2d$^-$, 4$^-$ (B) strains and separated by HPLC. Peaks are numbered as previously described (9) and are identified in Table 3.3.

Table 3.3: Muropeptide identities from peptidoglycan of *B. subtilis* PS832 and DPVB87

Muro-peptide*	Identity
1	Disaccharide tripeptide
2	Disaccharide tripeptide w/ 1 amidation and 1 phosphate
3	Disaccharide tripeptide w/ 1 amidation
4	Disaccharide tripeptide w/ 1 amidation missing an acetyl group
5	Disaccharide dipeptide
6	Disaccharide tripeptide dipeptide w/ 1 amidation
7	Disaccharide tetrapeptide w/ 1 amidation
8	Disaccharide tripeptide dipeptide w/ 2 amidations
9	Disaccharide pentapeptide (Ala-4-Gly-5) w/ 1 amidation
10	Disaccharide tripeptide tetrapeptide w/ 2 amidations
11	Disaccharide pentapeptide (Ala-4-Ala-5) w/ 1 amidation
12	Disaccharide tripeptide disaccharide tetrapeptide missing a glucosamine
13	Disaccharide tripeptide disaccharide tetrapeptide w/ 1 phosphate and 1 amidation
14	Disaccharide tetrapeptide tetrapeptide w/ 2 amidations
15	Disaccharide tripeptide disaccharide tetrapeptide w/ 1 amidation
16	Disaccharide tripeptide disaccharide tetrapeptide w/ 1 amidation and 1 phosphate
17	Disaccharide tripeptide disaccharide tetrapeptide w/ 2 amidations and either 1 phosphate or missing a glucosamine
18	Disaccharide tripeptide disaccharide tetrapeptide w/ 1 amidation and missing an acetyl group
19	Disaccharide tripeptide disaccharide tetrapeptide w/ 1 amidation and missing an acetyl group
20	Disaccharide tripeptide disaccharide tetrapeptide w/ 1 amidation
21	Disaccharide tripeptide disaccharide tetrapeptide w/ 2 amidations
22	Disaccharide tripeptide disaccharide tetrapeptide w/ 2 amidations and missing an acetyl group
23	Disaccharide tripeptide disaccharide tetrapeptide w/ 2 amidations and missing an acetyl group
24	Disaccharide pentapeptide (Gly-5) disaccharide tetrapeptide
25	Disaccharide pentapeptide (Gly-5) disaccharide tetrapeptide w/ 2 amidations
26	Disaccharide tetrapeptide disaccharide tetrapeptide w/ 2 amidations
27	Disaccharide pentapeptide disaccharide tetrapeptide w/ 2 amidations
28	Disaccharide tripeptide disaccharide tetrapeptide disaccharide tetrapeptide w/ 2 amidations
29	Disaccharide tripeptide disaccharide tetrapeptide disaccharide tetrapeptide missing a glucosamine
30	Disaccharide tripeptide disaccharide tetrapeptide disaccharide tetrapeptide w/ 2 amidations
31	Disaccharide tripeptide disaccharide tetrapeptide disaccharide tetrapeptide w/ 3 amidations
32	Disaccharide tripeptide disaccharide tetrapeptide disaccharide tetrapeptide w/ 3 amidations and missing an acetyl group
33	Disaccharide tripeptide disaccharide tetrapeptide disaccharide tetrapeptide w/ 3 amidations and missing an acetyl group
34	Disaccharide pentapeptide (Gly-5) disaccharide tetrapeptide disacchearide tetrapeptide w/ 2 or 3 amidations
35	Disaccharide tripeptide disaccharide tetrapeptide disaccharide tetrapeptide disaccharide tetrapeptide w/ 2 or 3 amidations
36	Anhydrodisaccharide tripeptide disaccharide tetrapeptide w/ 2 amidations
37	Disaccharide tripeptide disaccharide tetrapeptide disaccharide tetrapeptide disaccharide tetrapeptide w/ 4 amidations
38	Anhydrodisaccharide tripeptide disaccharide tetrapeptide disaccharide tetrapeptide w/ 3 amidations

* Numbered as indicated in Figure 3.9

Table 3.4. Structural parameters of *B. subtilis* PG [a]

Strain	PBP's Missing	% NAM with x-linked peptide	% Muropeptide [b]				
			Monomer	Dimer	Trimer	Tetramer	1, 6 Anhydro-
PS832	Wild Type	26.4 ± 0.5	48.2 ± 0.9	49.0 ± 0.7	2.5 ± 0.3	0.3	0.2
PS1869	2c	25.6 ± 0.6	49.7 ± 1.0	47.5 ± 0.6	2.5 ± 0.3	0.3 ± 0.1	0.3 ± 0.1
DPVB45	2d	26.6 ± 1.1	47.9 ± 2.0	49.0 ± 1.6	2.7 ± 0.4	0.4	0.3 ± 0.1
DPVB56	2c, 2d	25.9 ± 0.9	49.3 ± 1.6	47.7 ± 1.3	2.7 ± 0.3	0.3	0.3 ± 0.1
DPVB42	4	25.4 ± 0.4	50.1 ± 0.9	47.5 ± 0.9	2.2 ± 0.02	0.2	0.3
DPVB46	2c, 4	25.3 ± 0.5	50.4 ± 1.0	47.1 ± 0.7	2.3 ± 0.3	0.3	0.3
DPVB57	2d, 4	25.3 ± 0.2	50.2 ± 0.3	47.1 ± 0.3	2.3 ± 0.1	0.3	0.3
DPVB49	2c, 2d, 4	25.5 ± 0.2	50.0 ± 0.3	47.4 ± 0.2	2.4 ± 0.1	0.3	0.2
PS2062	1	24.2 ± 0.5	52.4 ± 1.1	45.7 ± 1.1	1.6 ± 0.1	0.3 ± 0.1	0.4 ± 0.1
PS2251	1, 2c	23.4 ± 0.5	53.9 ± 1.0	44.3 ± 1.1	1.5 ± 0.1	0.3 ± 0.1	0.3 ± 0.1
DPVB61	1, 2d	22.5 ± 2.6	55.5 ± 5.0	42.8 ± 4.7	1.3 ± 0.4	0.3	0.4 ± 0.1
DPVB63	1, 2c, 2d	24.1 ± 0.1	52.6 ± 0.2	45.3 ± 0.2	1.8	0.3	0.3 ± 0.1
DPVB68	1, 4	21.7 ± 1.5	56.9 ± 3.0	42.3 ± 2.8	0.6 ± 0.1	0.1	0.2
DPVB69	1, 2c, 4	23.2 ± 1.1	54.1 ± 2.3	44.8 ± 2.4	0.9	0.2 ± 0.1	0.2 ± 0.1
DPVB62	1, 2d, 4	22.3 ± 0.8	55.7 ± 1.6	43.4 ± 1.5	0.8 ± 0.1	0.1	0.2
DPVB87	1, 2c, 2d, 4	21.7 ± 0.7	56.8 ± 1.5	42.2 ± 1.6	0.8	0.2 ± 0.1	0.2
DPVB88	1, 2c, 2d, 4	21.9 ± 0.1	56.5 ± 0.1	42.6 ± 0.1	0.8 ± 0.1	0.2	0.2

[a] Values are averages of at least two independent analyses with errors of one standard deviation. In cases where no error is indicated the values in the multiple analyses were identical.

[b] Percentage of total muropeptides identified as either uncross-linked monomers or cross-linked dimers, trimers, and tetramers and those muropeptides containing 1, 6-anhydrodisaccharide muropeptides.

labeled, nucleotide-linked PG precursors simultaneously with a 2-fold dilution of the sucrose. Disruption of the protoplasts during this dilution allowed access of the precursors to the enzymes involved in production of lipid II. Reaction substrates and products were separated by paper chromatography, where polymerized PG strands remain at the origin. Radioactivity incorporated into insoluble material by protoplasts of each mutant strain was quantified and expressed as a percentage of that of the wild type protoplasts (Table 3.5). In general, PG synthetic activity decreased with successive loss of Class A PBPs. Addition of lysozyme to reactions resulted in significant decreases, usually more than 50%, in radioactivity remaining at the origin, demonstrating this material was PG. Addition of moenomycin, a specific inhibitor of PG-synthetic GTs decreased radioactivity remaining at the origin 70-97%. Lysozyme-insensitive, ^{14}C-containing polymers could result from several phenomena. First, some ^{14}C could be incorporated into a product other than PG. Second, some lysed protoplasts may produce inside-out vesicles, which would not allow access of lysozyme to PG synthesized within the vesicle. Finally, synthesis of multiply cross-linked PG with disaccharides would produce trimers and tetramers of cross-linked disaccharide muropeptides upon lysozyme digestion. These multimers may remain at the origin during chromatography. The fact that in all cases the majority of incorporation of radioactivity was sensitive to moenomycin suggests that we are mostly observing PG synthesis and that the latter two possibilities are more likely. The fact that the fraction of lysozyme-resistant material increased in strains lacking multiple Class A PBPs suggests that PG synthetic activity is decreasing relative to synthesis of other compounds. However, even in the absence of

Table 3.5. Incorporation of ^{14}C-UDP-NAG into glycan by *B. subtilis* protoplasts

PBP phenotype	Incorporation of ^{14}C-UDP-NAG (%)[a]	% Lysozyme sensitive[b]	% Moenomycin sensitive[c]
Wild Type	100	56	97
PBP 1$^-$	59	74	96
PBPs 1$^-$, 4$^-$	20	65	91
PBPs 2c$^-$, 2d$^-$, 4$^-$	52	44	90
PBPs 1$^-$, 2c$^-$, 2d$^-$	51	77	92
PBPs 1$^-$, 2c$^-$, 4$^-$	19	39	68
PBPs 1$^-$, 2d$^-$, 4$^-$	40	68	79
PBPs 1$^-$, 2c$^-$, 2d$^-$, 4$^-$	31	51	79
PBPs 1$^-$, 2c$^-$, 2d$^-$, 4$^-$	17	38	72

[a] Radioactivity remaining at origin expressed as a percentage of that found for the wild type.

[b] Percentage of radioactivity remaining at origin, for each strain, that is lost upon addition of lysozyme.

[c] Percentage of radioactivity remaining at origin, for each strain, that is lost upon addition of moenomycin.

Class A PBPs, >70% of incorporation of radioactivity was moenomycin sensitive, suggesting that the majority of incorporation was into PG.

DISCUSSION

Studies in several species have shown that strains lacking one or more Class A high-molecular weight PBPs were viable suggesting that the multiple PBPs within a cell have somewhat redundant functions. However, removal of two specific Class A PBPs of the three present in either *E. coli* or *S. pneumoniae* is lethal (42, 78, 143) indicating that some Class A PBP function is essential. In the present study, we have demonstrated that a *B. subtilis* strain lacking all four Class A PBPs is viable, although its growth rate is diminished 3-fold. The viability of the quadruple mutant strain, as well as structural analysis of its PG, demonstrates that it can synthesize PG, indicating that an unidentified protein, or protein complex, is performing the required GT activity. We were able to demonstrate that this GT could synthesize PG *in vitro* and that this activity was sensitive to the GT inhibitor moenomycin.

In contrast to what was observed *in vitro*, the novel GT activity may be moenomycin insensitive *in vivo*. When strains containing PBP1 were exposed to moenomycin, the growth of the culture entered a lag phase and the cells became filamentous and bent, a morphology very similar to what was seen in the quadruple mutant during exponential growth. These cells eventually resumed growth with a morphology similar to that of the quadruple mutant. Cells lacking at least PBP1 were largely unaffected by exposure to moenomycin. These results suggest that in a wild type

strain PBP1 is the major GT and that the novel GT is either not expressed or not in position to take over the major role. In the absence of PBP1, in the absence of all Class A PBPs, or in the presence of moenomycin, the novel GT polymerizes PG in an environment that is inaccessible to moenomycin *in vivo*. Alternatively, we may have observed the activities of two different GTs, one observed *in vivo* that is moenomycin resistant and one *in vitro* that is moenomycin sensitive. The abilities of different strains and of individual cells to survive moenomycin exposure and the rate at which they can adapt and reinitiate growth may be a function of two factors, the percentage of their PG synthetic activity that is being carried out by Class A PBPs and the percentage of cells at a particular stage of the cell cycle that is inherently sensitive or resistant to moenomycin.

Structural analysis of PG from all Class A PBP mutant strains showed that the percentage of peptide side chains involved in cross-linking was ~24% in all strains that lacked PBP1 and ~22% in strains that lacked both PBPs 1 and 4, including the quadruple mutant. These are 9% and 15% decreases, respectively, from the 26% cross-linking found in the wild type. Atrih and Foster (9) found a larger decrease in cross-linked muropeptides in the PBP1$^-$ strain (22% decrease) compared to wild type. However, the PG they used for analyzing strain differences was prepared from late stationary phase cultures, whereas we compared PG from exponentially growing cultures. Decreases in cross-linking may be directly due to the loss of the transpeptidase activity of PBP1 or to the loss of PBP1-containing complexes that bring other PBPs or wall-modifying proteins to sites of PG incorporation.

In the absence of PBP1, the PG synthetic machinery produces variability in cell morphology, wall thickness, and septation (80, 95). The role PBP1 plays in the control of wall formation is apparently important, but how it interacts with other proteins or cell structures to determine cell morphology is currently unknown. Recent data showed the presence of helical filaments, made up of MreB and Mbl monomers, lying just underneath the cytoplasmic membrane of *B. subtilis* (51). These proteins play roles in determining cell morphology (1, 51), and the helical filaments have been suggested to potentially exert spatial control on the PG synthetic machinery (51). If PBP1 is part of the pathway through which these proteins exert their effect on maintenance of a straight rod shape with consistent diameter, then the other Class A PBPs and a novel GT must be able to at least partially fill this role. Furthermore, Pederson et al found that in 48% of cells lacking PBP1, FtsZ localization was disrupted (80), suggesting that there is interplay between the wall synthetic machinery containing PBP1 and the cell division apparatus involving FtsZ. The question of what protein-protein interactions might be occurring between PG synthesizing machinery (PBP1?), proteins that regulate placement of cell division septa (Fts proteins), and proteins required for maintenance of cell morphology (helical filaments and Class B PBPs) is an intriguing area for future studies. Presumably, all these systems can also interact to some degree with the novel GT in order to produce rod-shaped cells and septa, suggesting that even in the presence of PBP1 this novel GT may be part of the PG synthetic apparatus.

The identity of the novel GT polymerizing PG in a strain lacking all Class A PBPs is unknown. In the *B. subtilis* genome (56), we find no protein product containing

significant sequence homology to the five motifs that are consistently found in all GT enzymes involved in synthesizing PG (34), indicating the presence of a novel class of GT. It has been proposed (45), and refuted (2, 128), that Class B PBPs may possess a GT activity in their N-terminal domains. We found that the relative abundance of two Class B PBPs, 2a and 2b, increased in the absence of PBP1 and more so in cells lacking both PBPs 1 and 4. The possibility remains that these two proteins may be involved, alone or in complex with other proteins, in the novel GT activity. Other candidate GT proteins may be those of the SEDS family (shape, elongation, division, sporulation)(39) such as RodA, which was enriched (along with a Class B PBP) in a membrane preparation that exhibited high levels of GT activity (45, 47). In addition, the *B. subtilis* genome encodes several uncharacterized proteins with similarity to GTs involved in the polymerization of other polysaccharides (31). Identification of this novel GT in *B. subtilis* may prove helpful to those researching this activity as a potential antibiotic target site.

ACKNOWLEDGEMENTS

This work was supported by grant GM56695 from the National Institutes of Health (D.L.P) and by grants from Sigma Xi (Grants-in-Aid of Research) and the Virginia Tech Graduate Student Associations' Graduate Research Development Program (D.C.M.). We thank David Nelson and Kevin Young for advice on the use of ^{125}I-penicillin X, Kit Pogliano for advice on fluorescence microscopy, Jill Sible and Rich Walker for advice and use of their microscopes, Bob Grant for the gift of moenomycin, and Marita Seppanen Popham for editing of the manuscript.

Chapter 4

Identification of the Proteins Involved in the Novel Glycosyl Transferase Activity

Introduction

The survival of all organisms depends on their ability to perform certain enzymatic activities and the ability to construct certain structures. In bacteria, survival from osmotic stress is dependent upon construction of peptidoglycan (PG), the structural component of the bacterial cell wall. PG consists of glycan strands cross-linked by peptide side-chains thereby making a semi-rigid structure that prevents cell rupture from osmotic stress and also confers the inherent shape of the various bacterial genera (Reviewed in (8)). In PG, the glycan strands are made of repeating subunits of N-acetylglucosamine (NAG) and N-acetylmuramic acid (NAM) and are synthesized from lipid-linked disaccharide-pentapeptide precursors by a glycosyl transferase (GT) (34). The peptide side-chains are then utilized by a transpeptidase (TP) to cross-link adjacent glycan strands (32, 34).

The family of penicillin-binding proteins (PBPs) catalyzes the final reactions required for the synthesis of PG (32, 34). Both the Class A and Class B high-molecular weight PBPs perform the transpeptidase activity within their C-terminal domain but only the Class A PBPs have demonstrated a second function that is performed from their N-terminal domain. This second function is the GT activity required for the polymerization of the glycan strands, and the Class A PBPs and mono-functional GTs (MGTs) are the only proteins that have demonstrated this GT activity *in vitro* (27, 46, 49, 74, 118, 135). The N-terminal domain contains amino acid motifs that are conserved in all Class A PBPs and mono-functional GTs (MGTs) found throughout all PG-synthesizing

eubacteria. It was thought that the Class B PBPs could also perform the GT activity (45), however, this claim has not been substantiated in subsequent studies (2, 128).

The transpeptidase activity performed by both HMW classes of PBPs has been shown to be essential for cell viability because of the number of antibiotics that target this reaction (32). However, it is believed that the GT activity, performed by the Class A PBPs, is also essential. In *B. subtilis*, *E.coli*, and *S. pneumoniae* removal of any one of the Class A PBPs might result in phenotypic changes, but it is not lethal - indicating functional redundancy among the PBPs (26, 42, 65, 66, 78, 95, 143). However, removal of two specific Class A PBPs in either *E. coli* or *S. pneumoniae* is lethal (26, 42, 78, 143), suggesting that some function of the Class A PBPs is essential. This is contradicted in *B. subtilis*, which has recently been shown to be viable, synthesize PG, and perform GT activity *in vitro* in the absence of all four Class A PBPs (66).

According to the genome sequence of *B. subtilis*, there are only four Class A PBPs and no MGTs (56). Therefore, the viability of a strain lacking all Class A PBPs suggests the presence of another protein or complex of proteins capable of performing the PG-synthesizing GT activity. Since there are no other proteins that contain the conserved amino acid motifs of the Class A PBP N-terminus (34), the protein(s) must be performing this reaction through a novel GT mechanism.

In this communication, I began the initial attempts to identify proteins involved in this novel GT activity by identifying fast-growing suppressor strains of the Class A PBP null mutants and using those strains to construct genomic libraries. These libraries are being used to transform the original Class A PBP null mutants and recipients will be

examined for an increase in growth rate. This increased growth rate will suggest transformation with a segment of cloned genome that contains a gene(s) that encode proteins containing the suppressor mutation and that are potentially involved in the GT activity.

Furthermore, it was previously shown that two Class B PBPs, PBP2a and PBP2b, appear to increase in abundance in strains lacking PBPs1 and 4, including the Class A quadruple mutant (66, 95). This suggests that expression of these two Class B PBPs may increase in order to compensate for an activity lost with the removal of the Class A PBPs. That compensated activity may be the GT activity that is thought to only be performed by the Class A PBPs. Therefore, mutations in some Class B PBP encoding genes were combined with the Class A PBP null mutant to see if any combination would be lethal. In fact, the combination of mutations in the Class B-encoding gene *pbpA* with the Class A-encoding genes, *ponA* and *pbpD*, is lethal. This suggests that PBP2a, encoded by *pbpA*, could be involved in either the novel GT activity or that it may provide an essential transpeptidase activity in the absence of the two vegetative Class A PBPs. Construction of a temperature sensitive PBP2a will allow for the demonstration of the loss of transpeptidase activity using radio-labeled penicillin or loss of GT activity using the previously described GT assay.

Methods and Materials

Bacterial growth and transformation. All strains of *B. subtilis* listed in Table 4.1 were derivatives of strain 168. Natural transformation was performed as previously described (3). Transformants were selected and maintained with appropriate antibiotics as follows: spectinomycin (100 μg/ml), kanamycin (10 μg/ml), erythromycin (0.5 μg/ml) plus lincomycin (12.5 μg/ml, macrolide-lincosamide-streptogramin B resistance), tetracycline (10 μg/ml), and chloramphenicol (3 μg/ml). Cultures were grown with shaking at 37˚C in 2x SG medium (59) without antibiotics except where noted.

Isolation of *ponA pbpD pbpF pbpG* fast-growing suppressor strains. For DPVB87 and DPVB88, two 100 ml cultures of 2x SG medium were inoculated with a single, separate colony from each strain and were grown overnight at 37˚C with shaking in the absence of antibiotics. A 50 μl sample was then subcultured at a 100-fold dilution into fresh medium. Following each 9-12 hour period, samples were taken from each saturated culture, diluted, and plated on LB in the absence of antibiotics to obtain single colonies, which were incubated at 37˚C. Plates were examined for colonies that grew larger than the general population of quadruple mutant colonies, and these large colonies were subsequently streaked to fresh plates. Those colonies that were maintained the large phenotype were then screened for resistance to the antibiotic markers present in the mutated Class A PBP-encoding genes. Finally, the presence of each Class A PBP mutant allele was demonstrated using PCR as previously described (66).

Table 4.1. *B. subtilis* strains used

Strain	Genotype[a]	Transformation		Source of reference
		Donor	Recipient	
DPVB42	Δ*pbpD*	DPVB30	DPVB40	(65)
DPVB45	Δ*pbpG*::Kn	pDPV35	PS832	(65)
DPVB46	Δ*pbpD* Δ*pbpF*::Erm^r	PS1869	DPVB42	(65)
DPVB49	Δ*pbpD* Δ*pbpG*::Kn Δ*pbpF*::Erm^r	DPVB45	DPVB46	(65)
DPVB66	Sp downstream of and opposing *ponA*	pDPV43	PS832	(66)
DPVB67	Sp downstream of *ponA* and opposing *ypoC*	pDPV44	PS832	(66)
DPVB68	Δ*ponA*::Sp Δ*pbpD*	PS2062	DPVB42	(65)
DPVB69	Δ*ponA*::Sp Δ*pbpD* Δ*pbpF*::Erm^r	PS2062	DPVB46	(65)
DPVB87	Δ*ponA*::Sp Δ*pbpD* Δ*pbpF*::Erm^r Δ*pbpG*::Kn	PS2062	DPVB49	(66)
DPVB88	Δ*ponA*::Sp Δ*pbpD* Δ*pbpF*::Erm^r Δ*pbpG*::Kn	PS2062	DPVB49	(66)
DPVB207	*pbpA*::Erm^r Δ*pbpH*::Sp *xylAp-pbpH*::Cm	DPVB202	DPVB203	(140)
DPVB221	Δ*ponA*::Sp Δ*pbpD* Δ*pbpF*::Erm^r Δ*pbpG*::Kn		DPVB87	This work
DPVB222	Δ*ponA*::Sp Δ*pbpD* Δ*pbpF*::Erm^r Δ*pbpG*::Kn		DPVB87	This work
DPVB223	Δ*ponA*::Sp Δ*pbpD* Δ*pbpF*::Erm^r Δ*pbpG*::Kn		DPVB88	This work
DPVB224	Δ*ponA*::Sp Δ*pbpD* Δ*pbpF*::Erm^r Δ*pbpG*::Kn		DPVB88	This work
DPVB240	Δ*pbpD* Δ*pbpF*::Erm^r Δ*pbpG*::Kn *pbpC*::Cm	DPVB49	PS2352	This work
DPVB241	Δ*pbpD* Δ*pbpF*::Erm^r Δ*pbpG*::Kn *pbpA*::Cm	DPVB49	PS2465	This work
DPVB242	Δ*ponA*::Sp Δ*pbpD* Δ*pbpF*::Erm^r Δ*pbpG*::Kn *pbpC*::Cm	DPVB240	DPVB69	This work
DPVB253	Δ*pbpD pbpA*::Cm	DPVB42	PS2465	This work
DPVB254	Δ*pbpD pbpA*::Cm Δ*pbpF*::Erm^r	DPVB46	PS2465	This work
DPVB255	Δ*ponA*::Sp *pbpA*::Cm	PS2465	PS2062	This work
DPVB260	Δ*pbpF*::Erm^r *pbpA*::Cm	PS1869	PS2465	This work
DPVB261	Δ*pbpD* Δ*pbpG*::Kn *pbpA*::Cm	DPVB253	DPVB49	This work
DPVB262	*pbpA*::Erm^r Δ*pbpH*::Sp *xylAp-pbpH*::Tc	DPVB207	pCm::Tc	This work
DPVB266	*pbpH*::Tc	PS832	pDPV172	This work
DPVB267	Δ*pbpD pbpC*::Cm	DPVB42	PS2352	This work

DPVB268	Δ*pbpD pbpH*::Tc	DPVB42	DPVB266	This work
DPVB269	Δ*ponA*::Sp *pbpH*::Tc	DPVB266	PS2062	This work
DPVB270	Δ*pbpF*::Erm^r *pbpH*::Tc	DPVB266	PS1869	This work
DPVB271	Δ*pbpG*::Kn *pbpH*::Tc	DPVB266	DPVB45	This work
DPVB272	Δ*ponA*::Sp Δ*pbpD pbpC*::Cm	DPVB267	DPVB68	This work
DPVB273	Δ*pbpD* Δ*pbpF*::Erm^r *pbpC*::Cm	DPVB267	DPVB49	This work
DPVB274	Δ*pbpD* Δ*pbpG*::Kn *pbpC*::Cm	DPVB267	DPVB68	This work
DPVB275	Δ*pbpD* Δ*pbpF*::Erm^r Δ*pbpG*::Kn *pbpC*::Cm	DPVB267	DPVB68	This work
DPVB276	Δ*ponA*::Sp Δ*pbpD pbpH*::Tc	DPVB268	DPVB68	This work
DPVB277	Δ*pbpD* Δ*pbpF*::Erm^r *pbpH*::Tc	DPVB268	DPVB49	This work
DPVB278	Δ*pbpD* Δ*pbpG*::Kn *pbpH*::Tc	DPVB268	DPVB49	This work
DPVB279	Δ*pbpD* Δ*pbpF*::Erm^r Δ*pbpG*::Kn *pbpH*::Tc	DPVB268	DPVB49	This work
DPVB280	Δ*pbpD* Δ*pbpF*::Erm^r Δ*pbpG*::Kn *pbpC*::Cm *pbpH*::Tc	DPVB275	DPVB268	This work
DPVB281	Δ*ponA*::Sp Δ*pbpD* Δ*pbpF*::Erm^r Δ*pbpG*::Kn *pbpH*::Tc	DPVB279	DPVB68	This work
DPVB282	Δ*ponA*::Sp Δ*pbpD* Δ*pbpF*::Erm^r Δ*pbpG*::Kn *pbpC*::Cm *pbpH*::Tc	DPVB280	DPVB68	This work
PS832	Prototrophic revertant of strain 168			Laboratory stock
PS1869	Δ*pbpF*::Erm^r	pDPC89	PS832	(93)
PS2062	Δ*ponA*::Sp	pDPC197	PS832	(91)
PS2061	Δ*prfA*::Sp	pDPC195	PS832	(91)
PS2352	*pbpC*::Cm	PS832	pTMA5	(73)
PS2465	*pbpA*::Cm	PS832	pTMA4	(72)

[a] Abbreviations: Erm^r, resistance to erythromycin and lincomycin; Sp, resistance to spectinomycin; Kn, resistance to kanamycin; Cm, resistance to chloramphenicol; Tc, resistance to tetracycline.

Genomic library construction. Chromosomal DNA was prepared from overnight cultures of each fast-growing suppressor strain and PEG precipitated. Chromosomal DNA (5 μg) was digested using 0.5, 0.2, and 0.04 units of *Sau*3AI (Promega) at 37˚C for 1 hour followed by incubation at 70˚C for 15 minutes to heat inactivate *Sau*3AI. Each digest (2 μg) was gel electrophoresed to determine which digest produced the majority of fragments between 2 and 6 kbp. One μg of the appropriate digests were ligated with 100 ng pJH101 (29) that was previously digested to interrupt the tet^R gene using 10 units of *Bam*HI (Promega/New England Biolabs) at 37˚C for 1 - 2 hours followed by incubation with 2 units of shrimp alkaline phosphatase (Promega) at 37˚C for an additional 1 - 2 hours. Both enzymes were either heat inactivated at 70˚C (Promega *Bam*HI) for 15 minutes or removed using a QIAquick PCR purification kit (Qiagen) (New England Biolabs *Bam*HI). Ligations were used to transform JM109 *E. coli* cells (Promega) using either heat shock or electroporation to obtain >5,000 recipient colonies representing the majority of the *B. subtilis* chromosome. Approximately 10% of the transformant colonies were screened for tetracycline sensitivity to verify that ≤90% of the plasmid clones contained inserts of chromosomal DNA.

Class A/Class B multiple mutant strain construction. The combination of Class A PBP single and multiple mutations with Class B mutations was performed using natural transformation with selection for the appropriate antibiotics. Confirmation of the Δ*pbpD* allele was performed by PCR as previously described (65) whenever a recipient strain containing that allele was transformed with donor chromosomal DNA containing a

wild type *pbpD*. For *pbpA*, PCR was performed using primers pbpA1, complementary to a sequence 68 - 48 bp upstream of *pbpA*, and PBPA3, complementary to a sequence 137 - 159 bp downstream of *pbpA*, which amplified a 2.4 kbp wild type fragment or a 5.9 kbp fragment for the mutant allele.

To prevent the duplicate usage of antibiotic markers for selection, some antibiotic markers were replaced with other antibiotic markers. A 2,123 bp fragment containing the Sp^R antibiotic cassette from *Hin*dIII- and *Bam*HI-digested pDG1515 (37) was ligated into *Bam*HI- and *Hin*dIII-digested pDPV113 thereby changing the Δ*pbpH*::Sp^R to Δ*pbpH*::Tc^R to generate pDPV172. pDPV172 was used to transform PS832 and a double crossover was verified by PCR amplifying the region from 272 bp upstream of *pbpH* using primer *pbpH*1 to 302 bp downstream of *pbpH* using primer *pbpH*2 resulting in the expected fragment size of 3,923 bp (140).

Plasmid construction and *pbpA* mutagenesis. A 2,275 bp PCR fragment was amplified from 45 bp into *pbpA* using a primer containing an *Eco*RV site engineered into the 5' end to 159 bp downstream of *pbpA* using a primer containing a *Sal*I site engineered into the 5' end. This fragment was cloned into the pGEM-T vector (Promega), digested using the *Eco*RV and *Sal*I sites, and then cloned into the *Eco*RV - *Sal*I digested pJH101 vector to create pDPV179. pDPV179 was mutagenized using hydroxylamine as previously described (38, 106).

The Cm^R marker in *xylAp-pbpH*::Cm of DPVB207 was replaced with a Tc^R marker using the antibiotic switching vector, ECE75 (113), to construct DPVB262. Mutagenized pDPV179 was used to electroporate JM107 *E. coli* cells (Promega) and the

plasmids obtained were used to transform DPVB262. Recipients were selected by plating in the presence of appropriate antibiotics and in the absence of xylose to select for full length *pbpA* to encode a functional PBP2a at 30˚C. Recipient colonies were picked to two separate plates and the identification of temperature sensitive mutants of *pbpA* were identified by growth at 30˚C and no growth at 42˚C.

Sequencing of *pbpA*. *pbpA* was amplified from DPVB221 chromosomal DNA using primers *pbpA*1 and *pbpA*3 as mentioned above. This 2,375 bp fragment was used for sequencing using the following primers: *pbpA*1; *pbpA*440, located 419 - 439 bp into *pbpA*; *pbpA*880, located 857 - 877 bp into *pbpA*; *pbpA*1320, located 1,299 - 1,319 bp into *pbpA*; and *pbpA*3. The PCR sequencing reaction was performed according to the Virginia Bioinformatics Institute (VBI) using Applied Biosystems (ABI) Bigdye (version 3.0) Terminator chemistry and the reaction products were sequenced using either an ABI 377 automated DNA sequencer or an ABI 3100 capillary sequencer at VBI. The sequences obtained were compared to the published sequence for *pbpA* (http://genolist.pasteur.fr/SubtiList/ and (56)).

Results

Isolation of fast-growing suppressor strains of the quadruple Class A PBP mutants. Previous characterization of the Class A PBP quadruple mutant strains demonstrated that they have growth rates approximately three-fold slower than wild type and two-fold slower than any of the triple mutants that lack PBP1 (66). Due to these results, it was believed that suppressor mutations conferring a fast-growth rate would be

easily identifiable. Hence, fast-growing colonies, identified as large colonies, were streaked to fresh plates. Those colonies that remained fast-growing were then tested for resistance to the antibiotics used for each Class A PBP mutation. Two fast-growing colonies (strains DPVB221 - 224) from each original quadruple mutant strain that were resistant to all antibiotics were then tested for the presence of each mutant allele using PCR as previously described (66). Doubling times for each fast-growing suppressor strain were determined to be approximately 22 minutes, almost that of wild type (Table 4.2).

Chromosomal DNA from each fast-growing suppressor strain was isolated and partially digested using various concentrations of *Sau*3AI. A portion of each digest was then electrophoresed to determine the digest that resulted in the majority of fragment sizes between 2 and 6 kbp. These fragments were then ligated with the *Bam*HI digested pJH101 vector, which were subsequently used to transform *E. coli* JM109 cells by either heat shock or electroporation. By obtaining at least 5000 Tc^S recipient colonies, the full genome of each suppressor strain should be represented. Although these genomic libraries have been constructed, their use to transform DPVB87 and DPVB88 has not been performed.

Combination of the Class A PBP null mutant with various Class B PBP mutations. It has been theorized that the Class B PBPs could perform the GT activity of the Class A PBPs even though they lack the conserved motifs found in the GT domain of the Class A PBPs and MGTs. Therefore, if one or more of these proteins is involved in this activity in the absence of the Class A PBPs, then the combination of one, or some,

Table 4.2. Growth rates of Class A PBP mutant strains[a]

Strain	PBP Phenotype	Doubling time[b] (min)
PS832	Wild type	20
PS1869	PBP2c$^-$	20
DPVB42	PBP4$^-$	20
DPVB45	PBP2d$^-$	20
PS2062	PBP1$^-$	25
DPVB49	PDP2c$^-$, PBP2d$^-$, PBP4$^-$	21
DPVB63	PBP1$^-$, PBP2c$^-$, PBP2d$^-$	28
DPVB69	PBP1$^-$, PBP2c$^-$, PBP4$^-$	28
DPVB62	PBP1$^-$, PBP2d$^-$, PBP4$^-$	31
DPVB87	PBP1$^-$, PBP2c$^-$, PBP2d$^-$, PBP4$^-$	62
DPVB88	PBP1$^-$, PBP2c$^-$, PBP2d$^-$, PBP4$^-$	63
DPVB221	PBP1$^-$, PBP2c$^-$, PBP2d$^-$, PBP4$^-$	22
DPVB222	PBP1$^-$, PBP2c$^-$, PBP2d$^-$, PBP4$^-$	20
DPVB223	PBP1$^-$, PBP2c$^-$, PBP2d$^-$, PBP4$^-$	21
DPVB224	PBP1$^-$, PBP2c$^-$, PBP2d$^-$, PBP4$^-$	24

[a] Growth was in liquid 2xSG medium at 37˚C.

[b] Doubling times are averages from at least three separate experiments.

Class B PBP mutation(s) with the Class A PBP null mutant might be lethal. The combination of mutations in either *pbpC* or *pbpH* with the Class A PBP null mutant did not result in any obvious phenotypic change. Mutations in the Class B PBP encoding genes *pbpB, pbpI,* and *spoVD* were not combined with the Class A PBP mutations because *pbpI* and *spoVD* are expressed only during sporulation and the single *pbpB* mutation is lethal. However, the mutation in the Class B PBP-encoding gene *pbpA*, was lethal when introduced into the Class A PBP null mutant.

The transformation to introduce the *pbpA* mutation into the Class A PBP null mutant was attempted in a manner that allowed for determination of competency of the recipient strain as well as for the recovery of previously mutated PBPs. First, the slow growth rate resulting from the lack of PBP1 might decrease the competency of the recipient strain, therefore, the Δ*ponA*::sp^{R} allele was the final mutation added to the recipient strain that contained the *pbpA, pbpD, pbpF,* and *pbpG* mutations. Recombinants were selected by plating in the presence of spectinomycin, the antibiotic selectable marker for the *ponA* mutation. Not only did this select for the *ponA* mutation in the recipient strain, but it also allowed for the recovery of any of the previously mutated PBPs even though that would require a second, independent recombination event. This second recombination event would occur at the same frequency, but would only be observed when it occurred with the selected recombination in the same recipient. Thus, the observation of the second, independent recombination would occur at a low frequency within the single recombinant population and therefore the expected, predominant recombinant would be the *ponA, pbpA, pbpD, pbpF,* and *pbpG* quintuple

mutant. If a second, independent recombination event did occur, then any possible genotype combination might be expected, but all would have the *ponA* mutant allele.

If a second, independent recombination did occur, resulting in the recovery of a wild-type allele, then the recombinants might present with two colony types. Even though the *ponA* mutation is the only single mutation that results in a decreased growth rate when compared to the other Class A PBP single mutants, only a double mutant lacking *ponA* and *pbpD* causes a further decrease in that growth rate (65, 95). These phenotypes suggest the appearance of two colony types, one small and one large, as a result of a double recombination event where the large colonies would recover the *pbpD* gene and the small colonies would recover any of the other wild type alleles. Finally, the *pbpD* mutation does not contain any selectable markers (65), therefore the large colonies expected to recover the wild-type *pbpD* allele would still retain the resistance genes to all selectable markers. However, all the other mutations contain selectable antibiotic markers and recovery of any of these wild type alleles would result in small colony types that lose one of the selectable resistance genes and becoming sensitive to that respective antibiotic.

Transformants received upon performing this transformation presented with two colony types, small and large. Screening of each colony for resistance to the antibiotic selectable marker for each gene demonstrated resistance to both erythromycin/lincomycin and kanamycin, the selectable markers for the *pbpF* and *pbpG* mutations, respectfully. Because of these results, recovery of the wild type allele for either *pbpF* or *pbpG* was ruled out. However, every small colony transformant was now sensitive to

chloramphenicol, the antibiotic selectable marker for the *pbpA* mutation, suggesting that these recombinants had recovered the *pbpA* wild type allele. Furthermore, each large colony was still resistant to each antibiotic, suggesting recovery of wild type *pbpD*. PCR was performed on 10 isolates, 2 large and 8 small representing equal percentages of the respective colony types, and it was determined that all small, chloramphenicol sensitive colonies had recovered the wild type, *pbpA* allele and all the large, fully resistant colonies had recovered the wild type, *pbpD* allele.

By making all combinations of double, triple, and quadruple mutants lacking *pbpA* with each Class A PBP, it was discovered that the lethal combination of these PBP mutations is *ponA*, *pbpA*, and *pbpD*. This explains why neither *pbpF* nor *pbpG* wild type alleles were recovered from the original transformation. The explanation for this lethal combination depends on the activities of PBP2a, encoded by *pbpA*. First, Class B PBPs are predicted to perform transpeptidase activity and therefore PBP2a could be performing a transpeptidase activity that is essential in the absence of the two main vegetative Class A PBPs, PBP1 and PBP4. However, *B. subtilis* contains five other Class B PBPs (three that are expressed during vegetative growth) that could theoretically perform the transpeptidase activity in the absence of PBP2a. This is presumably the case because the combination of mutations in both *pbpA* and *pbpH*, another Class B PBP, is lethal (140) demonstrating the functional redundancy of these two enzymes. But if the belief that the essential enzymatic activity of the Class A PBPs is the GT activity, then the second explanation for this lethal combination is that PBP2a might be at least involved in the novel GT activity.

Sequencing of *pbpA* in a suppressor strain of the Class A PBP quadruple mutant. A group of proteins that are potential candidates for involvement in the novel GT activity are the Class B PBPs. Following the results that the combination of *ponA pbpA pbpD* was lethal, *pbpA* and its promoter region was subsequently sequenced from one of the suppressor strains, DPVB221, to determine if there were any changes in the nucleotide sequence. The results of this sequencing procedure produced no changes in sequence in the suppressor mutant compared to that of the published sequence.

Present and Future Research

Isolation of the fast-growing suppressor strains lacking all four Class A PBPs presents the possibility of using their genomic DNA to identify the gene containing the suppressor mutation. Libraries containing a large representation of the genome from each of the fast-growing suppressor strains will be moved into the original quadruple mutants by electroporation and plated in the presence of chloramphenicol, the antibiotic selection for recombination of the plasmid into the chromosome. The production of fast growing colonies should be an easily identifiable phenotype and the plasmid containing the genomic DNA conferring the fast growing phenotype will be isolated from these colonies. These library constructs will then be used to transform the original quadruple mutants again to verify that the suppressor phenotype is truly plasmid-associated.

The genomic DNA carrying the suppressor gene will be partially sequenced using primers that anneal to the vector and will allow for the identification of the region of chromosome containing the suppressor mutation. The genes located within this region will be examined to determine whether or not their gene products might be involved in

the novel GT activity. If they are identified as potential candidates, then the genes will be sequenced from both the original quadruple mutants and suppressor strains to identify any sequence changes and also cloned into an expression vector to examine their ability to perform the GT activity *in vitro*.

The identification of the lethal *ponA pbpA pbpD* combination is interesting because it suggests the possibility that PBP2a might be involved in performing the GT activity present in the absence of the Class A PBPs. PBP2a is a Class B PBP and these proteins have been theorized to be capable of performing GT activity (45), although several researchers have shown that this appears not to be the case (2, 128). Therefore, in order for this activity to be associated with PBP2a, the activity must be demonstrated in the presence of a functional PBP2a and lost in the presence of a non-functional PBP2a. This may be accomplished by utilizing a temperature sensitive PBP2a.

Identification of a PBP2a^{ts} requires the use of a strain that would only be viable in the presence of a functional PBP2a. Recently, a strain that lacks both PBP2a and PBPH, encoded by *pbpH*, has been found to be non-viable, but is viable when *pbpH* is placed under the control of an inducible promoter (DPVB262) (140). This strain can now be used to identify a PBP2a^{ts} following mutagenesis of pDPV179.

The possibility remains that there could be more than one protein performing this activity either alone or in concert with other proteins. Although PBP2a is a suspect to be involved in the novel GT activity, other proteins may certainly be involved. This may truly be the case because sequencing of *pbpA* from one of the fast-growing suppressor strains did not show any changes in nucleotide sequence from that of the published

sequence. This does not rule out the fact that the *pbpA* sequence may have changed in any of the other suppressor strains, but it supports the fact that other proteins may be involved in this activity. Some suspect proteins for this activity are members of the SEDS (Septation, Elongation, Division, Sporulation) family (39). One member of this family, RodA, was enriched with other proteins (Class B PBPs) in a membrane preparation that showed high levels of activity (45, 47). Furthermore, enzymes performing the polymerization of other polysaccharides and which also contain some sequence similarity to GTs are found within the genome of *B. subtilis* (31). These are some possible proteins that may only be identified through the suppressor strains, and it is therefore essential to identify those suppressor genes using the genomic libraries.

Chapter 5

Final Discussion

The bacterial cell wall plays an essential role for cell viability and the structural component of this wall is peptidoglycan. The essential nature of this structure is evident in the number of antibiotics that target the enzymes involved in its synthesis (4, 12, 32, 48, 115, 122, 129) as well as the enzymes that act to break down the structure itself (33). Both types of actions cause destabilization of the peptidoglycan structure inevitably resulting in cell rupture and death. It is interesting to note that many of these antibiotic compounds are synthesized by prokaryotic organisms (116, 129), presumably as a defense mechanism for limiting the number of other species competing for nutrients essential for cell growth.

A group of proteins that are targeted by some types of antibiotics, such as β-lactams and glycopeptides (12, 32), are known as penicillin-binding proteins (PBPs). These proteins perform the essential enzymatic activities needed to polymerize glycan strands and cross-link those strands together to form that final structure known as peptidoglycan (PG). This family of proteins is divided into three classes based on the molecular weight and the presence of specific motifs. These motifs are conserved not only within each class, but throughout all Gram-positive and Gram-negative PG synthesizing eubacteria. Furthermore, all eubacteria appear to contain multiple proteins within each of these classes (34).

The conserved motifs found in proteins from each class of PBPs suggests an important feature, the enzymatic activity of each protein is inherently the same. This allows proteins to compensate for each other in the event one or more become inactivated either by a spontaneous mutation or by the action of an antibiotic. This functional

redundancy has been previously demonstrated in all classes throughout several organisms and although these proteins can certainly compensate for the inactivation of some, there appear to be specific roles performed by several proteins that can not be compensated by others. The research discussed in this dissertation is focused on the roles and GT activity of the Class A high-molecular weight PBPs of *B. subtilis*.

In *B. subtilis*, the functional redundancy and role specificity of these proteins seen in previous reports (80, 95) is supported and further demonstrated in Chapter 2. PBP1 is believed to be the primary Class A PBP for vegetative growth because a strain lacking only this Class A PBP results in slower growth rate and changes in cell morphology. These morphological changes increase with the loss of other Class A PBPs, suggesting there is at least some partial compensation. But it is apparent that there are one or more aspects of the PBP1 protein that enable it to participate in the specific roles for cell development, such as cell division.

Cell division is an important stage during the growth of an individual cell. The division process involves many proteins that are needed for DNA replication and partitioning, localization of cell division proteins, as well as synthesizing the division septa. Although interaction among all these proteins is mostly hypothetical, this interaction is assumed and suggests a concerted effort between the different division stages to prevent a catastrophic event, such as the sectioning of the chromosome due to the inability to properly partition the chromosome away from the division site. This is a type of interaction that may be occurring between PBP1 and other cell division proteins. PBP1 localizes to the division site, strains lacking PBP1 have deformed and irregularly placed septa, and the Class B PBP, PBP2b, is required for septal PG synthesis. Also, a

protein expressed from the same operon as PBP1, known as PrfA, is required for proper chromosomal partitioning, suggesting its possible involvement in the checkpoint between partitioning and septum synthesis. An interaction among these proteins might be needed to ensure the proper placement and synthesis of division septa into areas of the cell that are clear of chromosomal material.

The other major vegetative Class A PBP, PBP4, is the most simple of these proteins because it only contains short amino acid sequences beyond the required signal sequence, glycosyl transferase, and transpeptidase domains. A strain lacking only this PBP does not appear to have any phenotypic changes, suggesting that PBP4 is involved in non-specific, generalized PG synthesis throughout the cell surface. However, the phenotypic changes seen in strains lacking only PBP1 are increased in strains lacking both PBPs 1 and 4, suggesting PBP4 is able to compensate to some degree for PBP1. But, because PBP4 may lack the interaction abilities of PBP1, it is not capable of efficiently compensating for the lack of PBP1 in septal and cylindrical wall synthesis.

The specific roles played by the other Class A PBPs are also apparent in Chapter 2. Expression of either PBP2c or PBP2d is required during sporulation, because a strain lacking both proteins is unable to produce fully mature endospores. A strain lacking these two PBPs is able to synthesize what appears to be a structurally correct germ cell wall, but is unable to synthesize a structurally and morphologically correct cortex. Electron micrographs from this strain show completely deformed forespores in late stage sporulation that have large structures located at the poles of the forespore, with other areas that contain no obvious PG. These structures are truly cortex PG because mutations in genes required for the degradation of cortex PG added to the double mutant

background stabilizes the structures so that they are not degraded and are present after twenty-four hours of sporulation. The conclusion from this study is that PBPs 2c and 2d play redundant and essential roles in the synthesis of a normal germ cell wall and that this germ cell wall serves as a template for the cortex to be built upon. However, the absence of these two PBPs results in an undetectable structural alteration within the germ cell wall that causes synthesis of an abnormal cortex. To add to the role specificity of these two PBPs, it was recently found that PBP4 could not complement the double mutant phenotype even when it was expressed specifically within the forespore (Dean, *et al.*, Unpublished Data).

Finally, the GT activity of the Class A PBPs is believed to be an essential reaction for the synthesis of PG and is believed to be only performed by the Class A PBPs and mono-functional GTs (MGTs). The only purified proteins that have demonstrated this activity *in vitro* are the Class A PBPs and MGTs and only these proteins contain conserved amino acid motifs found in all PG-synthesizing GT's throughout all prokaryotes. Previous research that shows both *E. coli* and *S. pneumoniae* are not viable when two specific Class A PBPs are removed, even in the presence of a third Class A PBP and an MGT, presents the theory that possibly the GT activity of the Class A PBPs is essential. These results gave reason to believe the viability of *B. subtilis* depended on the presence of at least one functional Class A PBP. However, a *B. subtilis* strain lacking all four Class A PBPs is viable and this strain contains no other proteins that have the conserved motifs of the Class A PBPs. Therefore, some other protein or complex of proteins must be capable of performing this activity through a novel GT mechanism.

The GT activity present in the Class A PBP null mutant has been characterized. This activity was demonstrated *in vitro* by using protoplasts of each strain incubated in the presence of ^{14}C-labeled UDP-N-acetylglucosamine and the GT activity demonstrated by each strain decreased as the number of missing PBPs increased. This suggests that the novel GT activity is not as efficient in the absence of the Class A PBPs and showed contradictory results using moenomycin, an antibiotic that specifically inhibits the GT activity of the Class A PBPs. Growth of this strain in the presence of high concentrations (80 μg/ml) of moenomycin caused no apparent decrease in growth rate, while growth of strains with a wild type PBP1 slowed. This suggests that the Class A PBP GT activity was sensitive (particularly that of PBP1), while the novel GT activity was resistant to the antibiotic *in vivo*. However, the novel GT activity appeared to be sensitive to the antibiotic *in vitro*. These results indicate that the proteins involved in the novel GT activity are effected to some degree when placed in an *in vitro* system, possibly changing their environment enough to make the active site more accessible to the antibiotic.

Several experimental methods are being incorporated in an effort to identify the proteins involved in the novel GT activity. The identification of genes that encode proteins possibly involved in providing a fast-growing suppressor phenotype is one area of exploration. Four suppressor strains have been identified, two from each of the quadruple mutants, and have demonstrated doubling times almost equal to that of the wild type strain. Genomic DNA from each of these suppressor strains has been used to construct libraries, which will be used to transform the original, slow-growing quadruple mutant strains. Once these recombinants are made they will be examined for fast-growing colonies. The plasmids from the fast-growing colonies will then be recovered

and a portion adjacent to the vector will be sequenced to determine the region of chromosome that was integrated. Once this region is determined, this information will be used to identify the genes that may be involved in the novel GT activity. These genes may then be sequenced from the suppressor strains to identify any sequence changes and then tested for their ability to demonstrate GT activity *in vitro*.

The second method is to examine the transpeptidase activity and potential GT activity of PBP2a^{ts} mutants. PBP2a was demonstrated to be essential in the absence of the vegetative Class A PBPs, PBP1 and PBP4 and the essential activity of this protein may lie in the inherent activity common to all Class B PBPs, that being the transpeptidase activity. The transpeptidase activity of PBP2 in *E. coli* is required to maintain the proper rod morphology of this organism because inactivation of this protein, specifically by the β-lactam antibiotic mecillinam, induces growth of spherical cells and leads to cell death (131). Therefore, the transpeptidase activity from PBP2a is also believed to be important because this protein is involved in maintaining the rod morphology of *B. subtilis* and is essential in the absence of another Class B PBP, PbpH. Since PbpH can presumably complement the loss of PBP2a transpeptidase activity, then the alternative theory for the lethal PBP1^{-}, PBP4^{-}, PBP2a^{-} combination is that PBP2a could be involved in performing the novel GT activity. The penicillin-binding and glycosyl transferase assays will be performed *in vitro* using either purified membranes or protoplasts, respectively, of each strain. By performing separate assays using PBP2a^{ts} variants, the demonstration of both enzymatic activities at the permissive temperature and loss of activities at the non-permissive temperature might implicate involvement of PBP2a in the novel GT activity.

It should be noted that sequencing of *pbpA* from one of the four fast-growing suppressor strains did not show any changes in nucleotide sequence. This does not rule out the possibility for involvement of PBP2a in the GT activity but suggests that there truly are other proteins involved. Furthermore, the other three fast-growing suppressor strains may contain nucleotide changes in *pbpA*. This supports the reason for isolating multiple fast-growing suppressor strains to increase the possibility of identifying as many genes as possible.

Other experimental methods that may be used to identify proteins involved in the novel GT activity require the use of the antibiotic moenomycin. Class A PBPs have been purified from moenomycin-affinity columns (114, 133). However this requires a large amount of purified antibiotic, which we have been unable to obtain. Furthermore, if this novel GT activity is performed through the interaction of two or more proteins, then solubilizing the membranes required prior to loading the sample on the column may result in dissociation of the proteins causing none to bind moenomycin.

Another method is to cross-link any proteins involved in the GT activity through the *in vitro* moenomycin interaction. This procedure will utilize a ^{125}I-labeled moenomycin photocross-linker. The *in vitro* interaction of the enzymatic complex and antibiotic places the proteins in close proximity to the antibiotic and through UV irradiation, the cross-linker will react with amines or carboxyl groups of the proteins. The potentially ^{125}I-labeled protein(s) will then be identified using mass spectrometry and the genes encoding these proteins can then be identified in the *B. subtilis* chromosome.

The fact that there are multiple proteins that may be involved in performing this activity may not allow for the identification of this enzyme complex. If this activity

requires an enzymatic complex, then each protein would need to be identified and the ability to demonstrate the activity *in vitro* from a purified protein would require the full complex. Therefore, if PBP2a is involved in a complex performing this activity, then demonstration of the loss of activity at the restrictive temperature will only indicate that PBP2a plays a role. However, through the utilization of either the genomic libraries constructed from the suppressor mutants or the identification of enzymes that interact with moenomycin, the possibility of identifying each protein involved in the activity is more likely. Still, the requirement to demonstrate the GT activity *in vitro* may not be possible with such a complex and could leave the question as to whether these proteins truly are involved.

The presence of the conserved motifs found in the Class A PBPs and MGTs definitely suggests their requirement for the GT activity. Furthermore, only purified Class A PBPs and MGTs have demonstrated this activity *in vitro*. These data, plus results showing at least one of two Class A PBPs is required for cell viability in *E. coli* and *S. pneumoniae*, suggests that the GT activity of the Class A PBPs is essential for cell viability. However, the research in *B. subtilis* showing GT activity in the absence of such proteins indicates other proteins that lack these conserved motifs are certainly capable of performing the activity. Therefore, there must be some other component specific to those Class A PBPs of *E. coli* and *S. pneumoniae* that makes them essential for cell viability. This component could very well be required for the specific roles these proteins play in cell development. One possible role may be involved in the formation of the presently hypothetical, PG synthesizing complexes formed between these and other proteins, a role that neither the remaining Class A PBP nor MGT is able to conduct - resulting in cell

lysis. This is certainly demonstrated in the Class B PBPs and suggests that even with the innate redundancy of function found in each class, the role specificity of the individual protein is required for proper cell development.

The identification of an enzyme or enzymatic complex involved in the novel GT activity is important for antibiotic research. With the rise in antibiotic resistance among many pathogenic microorganisms, the search for antibiotic targets becomes more and more urgent. The GT activity has been the focus of antibiotic research for several years and the suggestion that other proteins with no sequence similarity to the known GTs are capable of performing the activity might cause researchers to conclude this would not be a viable target. Better yet, this target site could be strengthened if it is found to contain a similar glycosyl transferase mechanism. In either case, the study of protein interactions and protein role specificity using these proteins as models will lead to a better understanding of the various complex synthetic machinery involved in other metabolic processes within the cell.

References Cited

1. **Abhayawardhane, Y., and G. C. Stewart.** 1995. *Bacillus subtilis* possesses a second determinant with extensive sequence similarity to the *Escherichia coli mreB* morphogene. J Bacteriol **177:**765-73.

2. **Adam, M., C. Fraipont, N. Rhazi, M. Nguyen-Disteche, B. Lakaye, J. M. Frere, B. Devreese, J. Van Beeumen, Y. van Heijenoort, J. van Heijenoort, and J. M. Ghuysen.** 1997. The bimodular G57-V577 polypeptide chain of the class B penicillin- binding protein 3 of *Escherichia coli* catalyzes peptide bond formation from thiolesters and does not catalyze glycan chain polymerization from the lipid II intermediate. J Bacteriol **179:**6005-9.

3. **Anagnostopoulos, C., and J. Spizizen.** 1961. Requirements for transformation in *Bacillus subtilis*. J. Bacteriol. **81:**74-76.

4. **Anderson, J. S., M. Matsuhashi, M. A. Haskin, and J. L. Strominger.** 1967. Biosythesis of the peptidoglycan of bacterial cell walls. II. Phospholipid carriers in the reaction sequence. J Biol Chem **242:**3180-90.

5. **Anderson, J. S., P. M. Meadow, M. A. Haskin, and J. L. Strominger.** 1966. Biosynthesis of the peptidoglycan of bacterial cell walls. I. Utilization of uridine diphosphate acetylmuramyl pentapeptide and uridine diphosphate acetylglucosamine for peptidoglycan synthesis by particulate enzymes from *Staphylococcus aureus* and *Micrococcus lysodeikticus*. Arch Biochem Biophys **116:**487-515.

6. **Anderson, J. S., and J. L. Strominger.** 1965. Isolation and utilization of phospholipid intermediates in cell wall glycopeptide synthesis. Biochem Biophys Res Commun **21:**516-21.

7. **Archibald, A. R., J. J. Armstrong, J. Baddiley, and J. B. Hay.** 1961. Teichoic acids and the structure of bacterial cell walls. Nature **191:**570-572.

8. **Archibald, A. R., I. C. Hancock, and C. R. Harwood.** 1993. Cell Wall Structure, Synthesis, and Turnover, p. 381-410. *In* A. L. Sonenshein, J. A. Hoch, and R. Losick (ed.), *Bacillus subtilis* and Other Gram-Positive Bacteria. American Society for Microbiology, Washington, D.C.

9. **Atrih, A., G. Bacher, G. Allmaier, M. P. Williamson, and S. J. Foster.** 1999. Analysis of peptidoglycan structure from vegetative cells of *Bacillus subtilis* 168 and role of PBP 5 in peptidoglycan maturation. J. Bacteriol. **181:**3956-3966.

10. **Atrih, A., P. Zollner, G. Allmaier, and S. J. Foster.** 1996. Structural analysis of *Bacillus subtilis* 168 endospore peptidoglycan and its role during differentiation. J. Bacteriol. **178:**6173-6183.

11. **Atrih, A., P. Zollner, G. Allmaier, M. P. Williamson, and S. J. Foster.** 1998. Peptidoglycan structural dynamics during germination of *Bacillus subtilis* 168 endospores. J. Bacteriol. **180:**4603-4612.

12. **Barna, J. C., and D. H. Williams.** 1984. The structure and mode of action of glycopeptide antibiotics of the vancomycin group. Annu Rev Microbiol **38:**339-57.

13. **Blumberg, P. M., and J. L. Strominger.** 1972. Five penicillin-binding components occur in *Bacillus subtilis* membranes. J. Biol. Chem. **247:**8107-8113.

14. **Blumberg, P. M., and J. L. Strominger.** 1972. Isolation by covalent affinity chromatography of the penicillin-binding components from membranes of *Bacillus subtilis*. Proc Natl Acad Sci U S A **69:**3751-5.

15. **Boland, F. M., A. Atrih, H. Chirakkal, S. J. Foster, and A. Moir.** 2000. Complete spore-cortex hydrolysis during germination of *Bacillus subtilis* 168 requires SleB and YpeB. Microbiology **146:**57-64.

16. **Botta, G. A., and J. T. Park.** 1981. Evidence for Involvement of Penicillin-Binding Protein 3 in Murein Synthesis During septation but not During Cell Elongation. J. Bacteriol **145:**333-340.

17. **Buchanan, C. E., and A. Gustafson.** 1992. Mutagenesis and mapping of the gene for a sporulation-specific penicillin-binding protein in *Bacillus subtilis*. J. Bacteriol. **174:**5430-5435.

18. **Buchanan, C. E., and M.-L. Ling.** 1992. Isolation and sequence analysis of *dacB*, which encodes a sporulation-specific penicillin-binding protein in *Bacillus subtilis*. J. Bacteriol. **174:**1717-1725.

19. **Catalano, F. A., J. Meador-Parton, D. L. Popham, and A. Driks.** 2001. Amino acids in the *Bacillus subtilis* morphogenetic protein SpoIVA with roles in spore coat and cortex formation. J Bacteriol **183:**1645-54.

20. **Coote, J. G.** 1972. Sporulation in *Bacillus subtlis*. Characterization of oligosporogenous mutants and comparison of their phenotypes with those of asporogenous mutants. J. Gen. Microbiol. **71:**1-15.

21. **Cutting, S., A. Driks, R. Schmidt, B. Kunkel, and R. Losick.** 1991. Forespore-specific transcription of a gene in the signal transduction pathway that governs pro-σ^K processing in *Bacillus subtilis*. Genes & Dev. **5:**456-466.

22. **Cutting, S., S. Panzer, and R. Losick.** 1989. Regulatory studies on the promoter for a gene governing synthesis and assembly of the spore coat in *Bacillus subtilis*. J. Mol. Biol. **207:**393-404.

23. **Daniel, R. A., S. Drake, C. E. Buchanan, R. Scholle, and J. Errington.** 1994. The *Bacillus subtilis spoVD* gene encodes a mother-cell-specific penicillin-binding protein required for spore morphogenesis. J. Mol. Biol. **235:**209-220.

24. **Daniel, R. A., E. J. Harry, and J. Errington.** 2000. Role of penicillin-binding protein PBP 2B in assembly and functioning of the division machinery of *Bacillus subtilis*. Mol Microbiol **35:**299-311.

25. **Daniel, R. A., A. M. Williams, and J. Errington.** 1996. A complex four-gene operon containing essential cell division gene *pbpB* in *Bacillus subtilis*. J Bacteriol **178:**2343-50.

26. **Denome, S. A., P. K. Elf, T. A. Henderson, D. E. Nelson, and K. D. Young.** 1999. *Escherichia coli* mutants lacking all possible combinations of eight penicillin binding proteins: viability, characteristics, and implications for peptidoglycan synthesis. J Bacteriol **181:**3981-93.

27. **Di Berardino, M., A. Dijkstra, D. Stuber, W. Keck, and M. Gubler.** 1996. The monofunctional glycosyltransferase of *Escherichia coli* is a member of a new class of peptidoglycan-synthesising enzymes. FEBS Lett **392:**184-8.

28. **Errington, J.** 1993. *Bacillus subtilis* sporulation: Regulation of gene expression and control of morphogenesis. Microbiol. Rev. **57:**1-33.

29. **Ferrari, F. A., A. Nguyen, D. Lang, and J. A. Hoch.** 1983. Construction and properties of an integrable plasmid for *Bacillus subtilis*. J. Bacteriol. **154:**1513-1515.

30. **Foster, S. J.** 1994. The role and regulation of cell wall structural dynamics during differentiation of endospore-forming bacteria. J. Appl. Bacteriol. Symposium Suppl. **76:**25S-39S.

31. **Foster, S. J., and D. L. Popham.** 2001. Structure and synthesis of cell wall, spore cortex, teichoic acids, S-layers, and capsules, p. 21-41. *In* A. L. Sonenshein, J. A. Hoch, and R. Losick (ed.), *Bacillus subtilis* and Its Close Relatives: From Genes to Cells. American Society for Microbiology, Washington, D.C.

32. **Ghuysen, J.-M.** 1991. Serine β-lactamases and penicillin-binding proteins. Annu. Rev. Microbiol. **45:**37-67.

33. **Ghuysen, J.-M., D. J. Tipper, and J. L. Strominger.** 1966. Enzymes that degrade bacterial cell walls. Meth. Enzym. **8:**685-699.

34. **Goffin, C., and J. M. Ghuysen.** 1998. Multimodular penicillin-binding proteins: an enigmatic family of orthologs and paralogs. Microbiol. Mol. Biol. Rev. **62:**1079-1093.

35. **Gomez, M., S. Cutting, and P. Stragier.** 1995. Transcription of *spoIVB* is the only role of sigma G that is essential for pro-sigma K processing during spore formation in *Bacillus subtilis*. J Bacteriol **177:**4825-7.

36. **González-Castro, M. J., J. López-Hernández, J. Simal-Lozano, and M. J. Oruña-Concha.** 1997. Determination of amino acids in green beans by derivitization with phenylisothiocyanate and high-performance liquid chromatography with ultraviolet detection. J. Chrom. Sci. **35:**181-185.

37. **Guérout-Fleury, A.-M., K. Shazand, N. Frandsen, and P. Stragier.** 1995. Antibiotic-resistance cassettes for *Bacillus subtilis*. Gene **167:**335-337.

38. **Hanzelka, B. L., A. M. Stevens, M. R. Parsek, T. J. Crone, and E. P. Greenberg.** 1997. Mutational analysis of the *Vibrio fischeri* LuxI polypeptide: critical regions of an autoinducer synthase. J Bacteriol **179:**4882-7.

39. **Henriques, A. O., P. Glaser, P. J. Piggot, and C. P. Moran, Jr.** 1998. Control of cell shape and elongation by the *rodA* gene in *Bacillus subtilis*. Mol Microbiol **28:**235-47.

40. **Higashi, Y., J. L. Strominger, and C. C. Sweeley.** 1967. Structure of a lipid intermediate in cell wall peptidoglycan synthesis: a derivative of a C55 isoprenoid alcohol. Proc Natl Acad Sci U S A **57:**1878-84.

41. **Holtje, J. V.** 1998. Growth of the stress-bearing and shape-maintaining murein sacculus of *Escherichia coli*. Microbiol Mol Biol Rev **62:**181-203.

42. **Hoskins, J., P. Matsushima, D. L. Mullen, J. Tang, G. Zhao, T. I. Meier, T. I. Nicas, and S. R. Jaskunas.** 1999. Gene disruption studies of penicillin-binding proteins 1a, 1b, and 2a in *Streptococcus pneumoniae*. J Bacteriol **181:**6552-6555.

43. **Huber, G., and G. Nesemann.** 1968. Moenomycin, an inhibitor of cell wall synthesis. Biochem Biophys Res Commun **30:**7-13.

44. **Ishikawa, S., K. Yamane, and J. Sekiguchi.** 1998. Regulation and characterization of a newly deduced cell wall hydrolase gene (*cwlJ*) which affects germination of *Bacillus subtilis* spores. J Bacteriol **180:**1375-1380.

45. **Ishino, F., and M. Matsuhashi.** 1981. Peptidoglycan synthetic enzyme activities of highly purified penicillin-binding protein 3 in *Echerichia coli*: a septum-forming reaction sequence. Biochem. Biophys. Res. Commun. **101:**905-911.

46. **Ishino, F., K. Mitsui, S. Tamaki, and M. Matsuhashi.** 1980. Dual enzyme activities of cell wall peptidoglycan synthesis, peptidoglycan transglycosylase and penicillin-sensitive transpeptidase, in purified preparations of *Escherichia coli* penicillin-binding protein 1A. Biochem. Biophys. Res. Commun. **97:**287-293.

47. **Ishino, F., W. Park, S. Tomioka, S. Tamaki, I. Takase, K. Kunugita, H. Matsuzawa, S. Asoh, T. Ohta, B. G. Spratt, and M. Matsuhashi.** 1986. Peptidoglycan synthetic activities in membranes of *Escherichia coli* caused by overproduction of penicillin-binding protein 2 and RodA protein. J. Biol. Chem. **261:**7024-7031.

48. **Izaki, K., M. Matsuhashi, and J. L. Strominger.** 1968. Biosynthesis of the peptidoglycan of bacterial cell walls. 8. Peptidoglycan transpeptidase and D-alanine carboxypeptidase: penicillin-sensitive enzymatic reaction in strains of *Escherichia coli*. J Biol Chem **243:**3180-92.

49. **Jackson, G. E., and J. L. Strominger.** 1984. Synthesis of peptidoglycan by high molecular weight penicillin-binding proteins of *Bacillus subtilis* and *Bacillus stearothermophilus*. J Biol Chem **259:**1483-90.

50. **Jacoby, G. H., and K. D. Young.** 1988. Unequal distribution of penicillin-binding proteins among inner membrane vesicles of *Escherichia coli*. J Bacteriol **170:**3660-7.

51. **Jones, L. J., R. Carballido-Lopez, and J. Errington.** 2001. Control of cell shape in bacteria: helical, actin-like filaments in *Bacillus subtilis*. Cell **104:**913-22.

52. **Karmazyn-Campelli, C., C. Bonamy, B. Savelli, and P. Stragier.** 1989. Tandem genes encoding σ-factors for consecutive steps of development in *Bacillus subtilis*. Genes & Dev. **3:**150-157.

53. **Kleppe, G., and J. L. Strominger.** 1979. Studies of the high molecular weight penicillin-binding proteins of *Bacillus subtilis*. J. Biol. Chem. **254:**4856-4862.

54. **Kleppe, G., W. Yu, and J. L. Strominger.** 1982. Penicillin-binding proteins in *Bacillus subtilis* mutants. Antimicrob. Agents and Chemother. **21:**979-983.

55. **Kroos, L., B. Zhang, H. Ichikawa, and Y. T. Yu.** 1999. Control of sigma factor activity during *Bacillus subtilis* sporulation. Mol Microbiol **31:**1285-94.

56. **Kunst, F., N. Ogasawara, I. Moszer, A. M. Albertini, G. Alloni, V. Azevedo, M. G. Bertero, P. Bessieres, A. Bolotin, S. Borchert, R. Borriss, L. Boursier, A. Brans, M. Braun, S. C. Brignell, S. Bron, S. Brouillet, C. V. Bruschi, B. Caldwell, V. Capuano, N. M. Carter, S. K. Choi, J. J. Codani, I. F. Connerton, A. Danchin, and et al.** 1997. The complete genome sequence of the gram-positive bacterium *Bacillus subtilis*. Nature **390:**249-256.

57. **Kurz, M., W. Guba, and L. Vertesy.** 1998. Three-dimensional structure of moenomycin A--a potent inhibitor of penicillin-binding protein 1b. Eur J Biochem **252:**500-7.

58. **Lakaye, B., C. Damblon, M. Jamin, M. Galleni, S. Lepage, B. Joris, J. Marchand-Brynaert, C. Frydrych, and J.-M. Frere.** 1994. Synthesis, purification and kinetic properties of fluorescein-labelled penicillins. Biochem. J. **300:**141-145.

59. **Leighton, T. J., and R. H. Doi.** 1971. The stability of messenger ribonucleic acid during sporulation in *Bacillus subtilis*. J. Biol. Chem. **254:**3189-3195.

60. **Lowry, O. H., N. J. Rosebrough, A. L. Farr, and R. J. Randall.** 1951. Protein measurement with the Folin phenol reagent. J. Biol. Chem. **193:**265-275.

61. **Lugtenberg, E. J., A. v Schijndel-van Dam, and T. H. van Bellegem.** 1971. *In vivo* and *in vitro* action of new antibiotics interfering with the utilization of N-acetyl-glucosamine-N-acetyl-muramyl-pentapeptide. J Bacteriol **108:**20-9.

62. **Mason, J. M., R. H. Hackett, and P. Setlow.** 1988. Regulation of expression of genes coding for small, acid-soluble proteins of *Bacillus subtilis* spores: studies using *lacZ* gene fusions. J. Bacteriol. **170:**239-244.

63. **Masson, J. M., and R. Labia.** 1983. Synthesis of a ^{125}I-radiolabeled penicillin for penicillin-binding proteins studies. Anal Biochem **128:**164-8.

64. **Matsuhashi, M., M. Wachi, and F. Ishino.** 1990. Machinery for cell growth and division: penicillin-binding proteins and other proteins. Res Microbiol **141:**89-103.

65. **McPherson, D. C., A. Driks, and D. L. Popham.** 2001. Two class A high-molecular-weight penicillin-binding proteins of *Bacillus subtilis* play redundant roles in sporulation. J Bacteriol **183:**6046-53.

66. **McPherson, D. C., and D. L. Popham.** 2003. Peptidoglycan synthesis in the absence of Class A penicillin-binding proteins in *Bacillus subtilis*. J Bacteriol **185:**1423-31.

67. **Meador-Parton, J., and D. L. Popham.** 2000. Structural analysis of *Bacillus subtilis* spore peptidoglycan during sporulation. J. Bacteriol. **182:**4491-4499.

68. **Meadow, P. M., J. S. Anderson, and J. L. Strominger.** 1964. Enzymatic polymerization of UDP-acetylmuramyl.L-ala.D-glu.L-lys.D-ala.D-ala and UDP-acetylglucosamine by a particulate enzyme from *Staphylococcus aureus* and its inhibition by antibiotics. Biochem Biophys Res Commun **14:**382-7.

69. **Mercer, K. L., and D. S. Weiss.** 2002. The *Escherichia coli* cell division protein FtsW is required to recruit its cognate transpeptidase, FtsI (PBP3), to the division site. J Bacteriol **184:**904-12.

70. **Moriyama, R., A. Hattori, S. Miyata, S. Kudoh, and S. Makino.** 1996. A gene (*sleB*) encoding a spore cortex-lytic enzyme from *Bacillus subtilis* and response of the enzyme to L-alanine-mediated germination. J Bacteriol **178:**6059-6063.

71. **Murray, T., D. L. Popham, C. B. Pearson, A. R. Hand, and P. Setlow.** 1998. Analysis of outgrowth of *Bacillus subtilis* spores lacking penicillin- binding protein 2a. J. Bacteriol. **180:**6493-6502.

72. **Murray, T., D. L. Popham, and P. Setlow.** 1997. Identification and characterization of *pbpA* encoding *Bacillus subtilis* penicillin-binding protein 2A. J. Bacteriol. **179:**3021-3029.

73. **Murray, T., D. L. Popham, and P. Setlow.** 1996. Identification and characterization of *pbpC*, the gene encoding *Bacillus subtilis* penicillin-binding protein 3. J. Bacteriol. **178:**6001-6005.

74. **Nakagawa, J., S. Tamaki, S. Tomioka, and M. Matsuhashi.** 1984. Functional biosynthesis of cell wall peptidoglycan by polymorphic bifunctional polypeptides. J. Biol. Chem. **259:**13937-13946.

75. **Nicholson, W. L., and P. Setlow.** 1990. Sporulation, germination, and outgrowth., p. 391-450. *In* C. R. Harwood and S. M. Cutting (ed.), Molecular biological methods for *Bacillus*. John Wiley & Sons Ltd., Chichester, England.

76. **Oke, V., M. Shchepetov, and S. Cutting.** 1997. SpoIVB has two distinct functions during spore formation in *Bacillus subtilis*. Mol. Microbiol. **23:**223-230.

77. **Paidhungat, M., K. Ragkousi, and P. Setlow.** 2001. Genetic requirements for induction of germination of spores of *Bacillus subtilis* by Ca(2+)-dipicolinate. J Bacteriol **183:**4886-93.

78. **Paik, J., I. Kern, R. Lurz, and R. Hakenbeck.** 1999. Mutational analysis of the *Streptococcus pneumoniae* bimodular class A penicillin-binding proteins. J Bacteriol **181:**3852-3856.

79. **Park, J. T., and A. N. Chatterjee.** 1954. Membrane associated reactions involved in bacterial cell wall mucopeptide synthesis. Fed. Proc **13:**466-472.

80. **Pedersen, L. B., E. R. Angert, and P. Setlow.** 1999. Septal localization of penicillin-binding protein 1 in *Bacillus subtilis*. J Bacteriol **181:**3201-3211.

81. **Pedersen, L. B., T. Murray, D. L. Popham, and P. Setlow.** 1998. Characterization of *dacC*, which encodes a new low-molecular-weight penicillin-binding protein in *Bacillus subtilis*. J. Bacteriol. **180:**4967-4973.

82. **Pedersen, L. B., K. Ragkousi, T. J. Cammett, E. Melly, A. Sekowska, E. Schopick, T. Murray, and P. Setlow.** 2000. Characterization of *ywhE*, which encodes a putative high-molecular-weight class A penicillin-binding protein in *Bacillus subtilis*. Gene **246:**187-196.

83. **Pedersen, L. B., and P. Setlow.** 2000. Penicillin-binding protein-related factor A is required for proper chromosome segregation in *Bacillus subtilis*. J Bacteriol **182:**1650-1658.

84. **Pogliano, J., N. Osborne, M. D. Sharp, A. Abanes-De Mello, A. Perez, Y. L. Sun, and K. Pogliano.** 1999. A vital stain for studying membrane dynamics in bacteria: a novel mechanism controlling septation during *Bacillus subtilis* sporulation. Mol Microbiol **31:**1149-59.

85. **Popham, D. L.** 2002. Specialized peptidoglycan of the bacterial endospore: the inner wall of the lockbox. Cell Mol Life Sci **59:**426-33.

86. **Popham, D. L., M. E. Gilmore, and P. Setlow.** 1999. Roles of low-molecular-weight penicillin-binding proteins in *Bacillus subtilis* spore peptidoglycan synthesis and spore properties. J. Bacteriol. **181:**126-132.

87. **Popham, D. L., J. Helin, C. E. Costello, and P. Setlow.** 1996. Analysis of the peptidoglycan structure of *Bacillus subtilis* endospores. J. Bacteriol. **178:**6451-6458.

88. **Popham, D. L., J. Helin, C. E. Costello, and P. Setlow.** 1996. Muramic lactam in peptidoglycan of *Bacillus subtilis* spores is required for spore outgrowth but not

for spore dehydration or heat resistance. Proc. Natl. Acad. Sci. U S A **93:**15405-15410.

89. **Popham, D. L., B. Illades-Aguiar, and P. Setlow.** 1995. The *Bacillus subtilis dacB* gene, encoding penicillin-binding protein 5*, is part of a three-gene operon required for proper spore cortex synthesis and spore core dehydration. J. Bacteriol. **177:**4721-4729.

90. **Popham, D. L., J. Meador-Parton, C. E. Costello, and P. Setlow.** 1999. Spore peptidoglycan structure in a *cwlD dacB* double mutant of *Bacillus subtilis*. J. Bacteriol. **181:**6205-6209.

91. **Popham, D. L., and P. Setlow.** 1995. Cloning, nucleotide sequence, and mutagenesis of the *Bacillus subtilis ponA* operon, which codes for penicillin-binding protein (PBP) 1 and a PBP-related factor. J. Bacteriol. **177:**326-335.

92. **Popham, D. L., and P. Setlow.** 1993. Cloning, nucleotide sequence, and regulation of the *Bacillus subtilis pbpE* operon, which codes for penicillin-binding protein 4* and an apparent amino acid racemase. J. Bacteriol. **175:**2917-2925.

93. **Popham, D. L., and P. Setlow.** 1993. Cloning, nucleotide sequence, and regulation of the *Bacillus subtilis pbpF* gene, which codes for a putative class A high-molecular-weight penicillin-binding protein. J. Bacteriol. **175:**4870-4876.

94. **Popham, D. L., and P. Setlow.** 1994. Cloning, nucleotide sequence, mutagenesis, and mapping of the *Bacillus subtilis pbpD* gene, which codes for penicillin-binding protein 4. J. Bacteriol. **176:**7197-7205.

95. **Popham, D. L., and P. Setlow.** 1996. Phenotypes of *Bacillus subtilis* mutants lacking multiple class A high-molecular-weight penicillin-binding proteins. J Bacteriol **178:**2079-2085.

96. **Priest, F. G.** 1993. Systematics and Ecology of *Bacillus*, p. 3 - 16. *In* J. A. a. L. Hoch, R. (ed.), *Bacillus subtilis* and Other Gram-Positive Bacteria. American Society for Microbiology, Washington D. C.

97. **Reynolds, P. E.** 1971. Peptidoglycan synthesis in bacilli. I. Effect of temperature on the in vitro system from *Bacillus megaterium* and *Bacillus stearothermophilus*. Biochim Biophys Acta **237:**239-54.

98. **Rogers, H. J., H. R. Perkins, and J. B. Ward.** 1980. Microbial cell walls and membranes. Chapman and Hall, London.

99. **Romeis, T., and J. V. Holtje.** 1994. Specific interaction of penicillin-binding proteins 3 and 7/8 with soluble lytic transglycosylase in *Escherichia coli*. J Biol Chem **269:**21603-21607.

100. **Schaller, K., J. V. Holtje, and V. Braun.** 1982. Colicin M is an inhibitor of murein biosynthesis. J Bacteriol **152:**994-1000.

101. **Schleifer, K. H., and O. Kandler.** 1972. Peptidoglycan types of bacterial cell walls and their taxonomic implications. Bacteriol. Rev. **36:**407-477.

102. **Sekiguchi, J., K. Akeo, H. Yamamoto, F. K. Khasanov, J. C. Alonso, and A. Kuroda.** 1995. Nucleotide sequence and regulation of a new putative cell wall hydrolase gene, *cwlD*, which effects germination in *Bacillus subtilis*. J. Bacteriol. **177:**5582-5589.

103. **Setlow, P.** 1994. Mechanisms which contribute to the long-term survival of spores of *Bacillus* species. J. Appl. Bacteriol. Sympos. Suppl. **76:**49S-60S.

104. **Severin, A., C. Schuster, R. Hakenbeck, and A. Tomasz.** 1992. Altered murein composition in a DD-carboxypeptidase mutant of *Streptococcus pneumoniae*. J. Bacteriol. **174:**5152-5155.

105. **Simpson, E. B., T. W. Hancock, and C. E. Buchanan.** 1994. Transcriptional control of *dacB*, which encodes a major sporulation-specific penicillin-binding protein. J. Bacteriol. **176:**7767-7769.

106. **Slock, J., D. VanRiet, D. Kolibachuk, and E. P. Greenberg.** 1990. Critical regions of the *Vibrio fischeri* luxR protein defined by mutational analysis. J Bacteriol **172:**3974-9.

107. **Southern, E. M.** 1975. Detection of specific sequences among DNA fragments separated by gel electrophoresis. J. Mol. Biol. **98:**503-517.

108. **Spratt, B. G.** 1975. Distinct penicillin-binding proteins involved in the division, elongation, and shape of *Escherichia coli* K12. Proc. Natl. Acad. Sci. USA **72:**2999-3003.

109. **Spratt, B. G.** 1977. Temperature-sensitive cell division mutants of *Escherichia coli* with thermolabile penicillin-binding proteins. J. Bacteriol. **131:**293-305.

110. **Spratt, B. G., V. Jobanputra, and U. Schwarz.** 1977. Mutants of *Escherichia coli* which lack a component of penicillin-binding protein 1 are viable. FEBS Lett. **79:**374-378.

111. **Spratt, B. G., and A. B. Pardee.** 1975. Penicillin-binding proteins and cell shape in E. coli. Nature **254:**516-7.

112. **Spratt, B. G., J. Zhou, M. Taylor, and M. J. Merrick.** 1996. Monofunctional biosynthetic peptidoglycan transglycosylases [letter]. Mol Microbiol **19:**639-40.

113. **Steinmetz, M., and R. Richter.** 1994. Plasmids designed to alter the antibiotic resistance expressed by insertion mutations in *Bacillus subtilis*, through in vivo recombination. Gene **142:**79-83.

114. **Stembera, K., A. Buchynskyy, S. Vogel, D. Knoll, A. A. Osman, J. A. Ayala, and P. Welzel.** 2002. Moenomycin-mediated affinity purification of penicillin-binding protein 1b. Chembiochem **3:**332-40.

115. **Stewert, G., and J. L. Strominger.** 1967. Bacitracin, an Inhibitor of the Dephosphoylation of Lipidpyrophosphate. PNAS **57:**767-773.

116. **Stover, A. G., and A. Driks.** 1999. Secretion, localization, and antibacterial activity of TasA, a *Bacillus subtilis* spore-associated protein. J Bacteriol **181:**1664-72.

117. **Stragier, P., and R. Losick.** 1996. Molecular genetics of sporulation in *Bacillus subtilis*. Annu Rev Genet **30:**297-341.

118. **Suzuki, H., Y. V. Heijenoort, T. Tamura, J. Mizoguchi, Y. Hirota, and J. V. Heijenoort.** 1980. In vitro peptidoglycan polymerization catalysed by penicillin binding protein 1b of *Escherichia coli* K-12. FEBS Lett. **110:**245-249.

119. **Suzuki, H., Y. Nishimura, and Y. Hirota.** 1978. On the process of cellular division in *Escherichia coli*: a series of mutants of *E. coli* altered in the penicillin-binding proteins. Proc. Natl. Acad. Sci. USA **75:**664-668.

120. **Taku, A., and D. P. Fan.** 1979. Dissociation and reconstitution of membranes synthesizing the peptidoglycan of *Bacillus megaterium*. A protein factor for the polymerization step. J Biol Chem **254:**3991-9.

121. **Tamaki, S., S. Nakajima, and M. Matsuhashi.** 1977. Thermosensitive mutation in *Escherichia coli* simultaneously causing defects in penicillin-binding protein-1Bs and in enzyme activity for peptidoglycan synthesis in vitro. Proc Natl Acad Sci U S A **74:**5472-6.

122. **Tamura, G., T. Sasaki, M. Matsuhashi, A. Takatsuki, and M. Yamasaki.** 1976. Tunicamycin Inhibits the Formation of Lipid Intermediate in Cell-Free Peptidoglycan Synthesis of Bacteria. Agric. Biol. Chem. **40:**447-449.

123. **Tipper, D. J., and J. J. Gauthier.** 1972. Structure of the bacterial endospore, p. 3-12. *In* H. O. Halvorson, R. Hanson, and L. L. Campbell (ed.), Spores V. American Society for Microbiology, Washington, D.C.

124. **Tipper, D. J., and P. E. Linnet.** 1976. Distribution of peptidoglycan synthetase activities between sporangia and forespores in sporulating cells of *Bacillus sphaericus*. J. Bacteriol. **126:**213-221.

125. **Todd, J. A., E. J. Bone, and D. J. Ellar.** 1985. The sporulation-specific penicillin-binding protein 5a from *Bacillus subtilis* is a DD-carboxypeptidase *in vitro*. Biochem. J. **230:**825-828.

126. **Todd, J. A., A. N. Roberts, K. Johnstone, P. J. Piggot, G. Winter, and D. J. Ellar.** 1986. Reduced heat resistance of mutant spores after cloning and mutagenesis of the *Bacillus subtilis* gene encoding penicillin-binding protein 5. J. Bacteriol. **167:**257-264.

127. **Van Heijenoort, Y., M. Derrien, and J. Van Heijenoort.** 1978. Polymerization by transglycosylation in the biosynthesis of the peptidoglycan of *Escherichia coli* K 12 and its inhibition by antibiotics. FEBS Lett **89:**141-4.

128. **van Heijenoort, Y., M. Gomez, M. Derrien, J. Ayala, and J. van Heijenoort.** 1992. Membrane intermediates in the peptidoglycan metabolism of *Escherichia coli*: possible roles of PBP 1b and PBP 3. J Bacteriol **174:**3549-57.

129. **van Heijenoort, Y., M. Leduc, H. Singer, and J. van Heijenoort.** 1987. Effects of moenomycin on *Escherichia coli*. J Gen Microbiol **133 (Pt 3):**667-74.

130. **Vicente, M., and J. Errington.** 1996. Structure, function and controls in microbial division. Mol Microbiol **20:**1-7.

131. **Vinella, D., D. Joseleau-Petit, D. Thevenet, P. Bouloc, and R. D'Ari.** 1993. Penicillin-binding protein 2 inactivation in *Escherichia coli* results in cell division inhibition, which is relieved by FtsZ overexpression. J Bacteriol **175:**6704-10.

132. **Vollmer, W., and J. V. Holtje.** 2000. A simple screen for murein transglycosylase inhibitors. Antimicrob Agents Chemother **44:**1181-5.

133. **von Rechenberg, M., and J. V. Holtje.** 2000. Two-step procedure for purification and separation of the essential penicillin-binding proteins PBP 1A and 1Bs of *Escherichia coli*. FEMS Microbiol Lett **189:**201-4.

134. **von Rechenberg, M., A. Ursinus, and J. V. Holtje.** 1996. Affinity chromatography as a means to study multienzyme complexes involved in murein synthesis. Microb Drug Resist **2:**155-7.

135. **Wang, Q. M., R. B. Peery, R. B. Johnson, W. E. Alborn, W. K. Yeh, and P. L. Skatrud.** 2001. Identification and characterization of a monofunctional glycosyltransferase from *Staphylococcus aureus*. J Bacteriol **183:**4779-85.

136. **Ward, J. B.** 1973. The chain length of the glycans in bacterial cell walls. Biochem. J. **133:**395-398.

137. **Warth, A. D., and J. L. Strominger.** 1972. Structure of the peptidoglycan from spores of *Bacillus subtilis*. Biochemistry **11:**1389-1396.

138. **Warth, A. D., and J. L. Strominger.** 1971. Structure of the peptidoglycan from vegetative cell walls of *Bacillus subtilis*. Biochemistry **10:**4349-4358.

139. **Warth, A. D., and J. L. Strominger.** 1969. Structure of the peptidoglycan of bacterial spores: occurrence of the lactam of muramic acid. Proc. Natl. Acad. Sci. USA **64:**528-535.

140. **Wei, Y., T. Havesy, D. C. McPherson, and D. L. Popham.** 2003. Rod-shaped Determination by the *Bacillus subtilis* Class B Penicillin-Binding proteins Encoded by *pbpA* and *pbpH*. J. Bacteriol **Submitted for publication**.

141. **Wu, J.-J., R. Schuch, and P. J. Piggot.** 1992. Characterization of a *Bacillus subtilis* operon that includes genes for an RNA polymerase σ factor and for a putative DD-carboxypeptidase. J. Bacteriol. **174:**4885-4892.

142. **Yanouri, A., R. A. Daniel, J. Errington, and C. E. Buchanan.** 1993. Cloning and sequencing of the cell division gene *pbpB*, which encodes penicillin-binding protein 2B in *Bacillus subtilis*. J. Bacteriol. **175:**7604-7616.

143. **Yousif, S. Y., J. K. Broome-Smith, and B. G. Spratt.** 1985. Lysis of *Escherichia coli* by beta-lactam antibiotics: deletion analysis of the role of penicillin-binding proteins 1A and 1B. J Gen Microbiol **131:**2839-45.

144. **Zheng, L., and R. Losick.** 1990. Cascade regulation of spore coat gene expression in *Bacillus subtilis*. J. Mol. Biol. **212:**645-660.

Derrell C. McPherson
Virginia Polytechnic Institute and State University
Department of Biology
2119 Derring Hall MC 0406
Blacksburg, Virginia 24061
e-mail: demcpher@vt.edu
(H) 540-381-8988 (W) 540-231-5137

EDUCATION

Doctorate of Philosophy, Biology - May, 2003
Virginia Polytechnic Institute and State University, Blacksburg, VA
Department of Biology

Research Topic: Studies of the Class A High Molecular Weight Penicillin-Binding Proteins in *Bacillus subtilis*.

Project includes: Bacterial genetics, protein overexpression and purification, small molecule purification, high pressure liquid chromatography and mass spectrometry for peptidoglycan structural analysis, transmission electron microscopy, epifluorescence microscopy, Southern and western blots, gene manipulation, chemical mutagenesis, non-radioactive chemifluorescence and radioactive detection systems.

Major Professor: David L. Popham, Ph.D.
Associate Professor of Microbiology

Master of Science, Biology, May 1998
Hampton University, Hampton, VA
Department of Biological Sciences

Thesis: Lead Resistant Bacterial Isolate from Composted Sludge

Major Professor: Abiodun Adibi, Ph.D.
Associate Professor of Microbiology

Bachelor of Science, Biology, May 1992
Christopher Newport College, Newport News, VA

PROFESSIONAL EXPERIENCE

Teaching

Graduate Teaching Assistant: Laboratory Instructor,
Department of Biology
Virginia Polytechnic Institute and State University, Blacksburg, VA
Taught laboratory sections in Pathogenic Microbiology
August 1999 – December 1999
Taught laboratory sections in General Microbiology
August 1998 – December 1998

PRESENTATIONS

Studies into the Identification of the Novel Glycosyl Transferase Activity Present in *Bacillus subtilis* in the Absence of Class A PBPs
Washington, D. C.
American Society for Microbiology National Conference, May 21, 2003

Peptidoglycan Synthesis in the Absence of Class A High-Molecular-Weight Penicillin-Binding Proteins in *Bacillus subtilis* (Poster Presentation)
Salt Lake City, Utah
American Society for Microbiology National Conference, May 20, 2002

Peptidoglycan Synthesis in *Bacillus subtilis* in the Absence of Class A Penicillin-Binding Proteins
Virginia Biotechnology Research Park, Richmond, Virginia
Regional meeting of the Virginia Branch American Society for Microbiology, November 2-3, 2001

The Role of Forespore Specific Class A PBPs in Spore Peptidoglycan Synthesis
Harvard University, Boston, Massachusetts
New England Spores Conference, April 22, 2001

Genetic Analysis of the Four Class A High-Molecular-Weight Penicillin-Binding Proteins of *Bacillus subtilis* (Poster Presentation)
Los Angeles, California
American Society for Microbiology National Conference, May 23, 2000

Studies of Class A High Molecular-Weight Penicillin-Binding Proteins in *Bacillus subtilis*
Virginia/Maryland Regional College of Veterinary Medicine, Blacksburg, Virginia
Regional meeting of the Virginia Branch American Society for Microbiology, November 5, 1999

PUBLICATIONS

Wei, Yuping, Teresa Havasy, Derrell C. McPherson, and David L. Popham. Rod Shape Determination by the *Bacillus subtilis* Class B Penicillin-Binding Proteins Encoded by *pbpA* and *pbpH*. Submitted for publication.

McPherson, Derrell C. and David L. Popham. 2003. Peptidoglycan Synthesis in the Absence of Class A Penicillin-Binding Proteins in *Bacillus subtilis*. J. Bacteriol. **185**(4): 1423-1431.

McPherson, Derrell C., Adam Driks, and David L. Popham. 2001. Two Class A High-Molecular Weight Penicillin-Binding Proteins of *Bacillus subtilis* Play Redundant and Essential Roles in Sporulation. J. Bacteriol. **183:**6046-6053.

GRANTS and AWARDS

2003 John L. Johnson Memorial Scholarship
2003 Graduate Student Assembly, Travel Fund
2003 American Society for Microbiology, Corporate Partner Travel Grant Award
2001 Graduate Student Assembly, Graduate Research Development Project
2000 Sigma Xi, Grants-in-Aid of Research
2000 Graduate Student Assembly, Travel Fund

PROFESSIONAL MEMBERSHIPS

American Society for Microbiology
Toastmasters International, Christiansburg Chapter
Offices held: President (Aug., 2002 - present)
Treasurer (Aug., 2001 - July, 2002)